5-1-2019

A functional analysis of the defense response of Glycine max as it relates to parasitism by the plant parasitic nematode Heterodera glycines

Prakash Mani Niraula

A functional analysis of the defense response of *Glycine max* as it relates to parasitism by the plant parasitic nematode *Heterodera glycines*

By

Prakash Mani Niraula

A Dissertation
Submitted to the Faculty of
Mississippi State University
in Partial Fulfillment of the Requirements
for the Degree of Doctor of Philosophy
in Biological Sciences
in the Department of Biological Sciences

Mississippi State, Mississippi

May 2019

A functional analysis of the defense response of *Glycine max* as it relates to parasitism by the plant parasitic nematode *Heterodera glycines*

By

Prakash Mani Niraula

Approved:

_____

Vincent Klink
(Major Professor)

_____

Gary W. Lawrence
(Committee Member)

_____

Dragica Jeremic
(Committee Member)

_____

Ying Wang
(Committee Member)

_____

Mark E. Welch
(Graduate Coordinator)

_____

Rick Travis
Dean
College of Arts & Sciences

Name: Prakash Mani Niraula

Date of Degree: May 3, 2019

Institution: Mississippi State University

Major Field: Biological Sciences

Major Professor: Vincent Klink

Title of Study: A functional analysis of the defense response of *Glycine max* as it relates to parasitism by the plant parasitic nematode *Heterodera glycines*

Pages in Study 159

Candidate for Degree of Doctor of Philosophy

The soybean cyst nematode (SCN), *Heterodera glycines*, a plant parasitic pest, causes severe yield losses of soybean (*Glycine max*). Although a number of studies have identified various genes that function in defense, including a role for the vesicular transport machinery acting against *H. glycines* in infected roots, a regulatory mechanism occurring behind the transcriptional engagement of the vesicular transport system and delivery of the transported cargo proteins is not fully understood. The main goal of the current study is to determine the functional effect of genetically engineering the circadian clock gene, *CIRCADIAN CLOCK ASSOCIATED 1* (*CCA1*) in *G. max* to examine a role on *H. glycines* parasitism. The outcome of the study has determined the functional effect of main clock component CCA1-1 along with other oscillator genes such as *TIMING OF CAB 1* (*TOC1-1*), *GIGANTEA* (*GI-1*) and *CONSTANS* (*CO-4*) to enhance resistance against *H. glycines* parasitism. Further, the reduced level of the expression of *Gm-CCA1-1* in infected roots, in comparison to uninfected roots, has demonstrated that clock components might have arrested and altered its expression during the nematode infection process. The study has also investigated the role of *XYLOGLUCAN ENDO-*

TRANSGLYCOSYLASE /HYDROLASE (*XTH*), *Gm*-XTH43, during the resistance process soybean has to *H. glycines*. The results have demonstrated higher xyloglucan (XyG) amounts to be synthesized in the *Gm*-XTH43 overexpressing (OE) lines. In contrast, there is less XyG in the *Gm*-XTH43 RNA interference (RNAi) lines that have a negatively regulated XTH gene. These observations have led to elucidating the role in the potential cell wall rearrangement and the underlying metabolic processes required for the generation of the proper XyG architecture required for defense occurring outside of the plant cell. Furthermore, the observed result of lower level of weight average molecular weight (WAMW) of XyG in *Gm*-XTH43-OE and higher MW of XyG in *Gm*-XTH43-RNAi than respective control roots have demonstrated a key role in, presumably, changing the cell wall by the remodeling of the XyG chain as it relates to the cell wall architecture.

DEDICATION

This dissertation is dedicated to my mother the late Sushila Niraula, who always encouraged and inspired me for better education.

ACKNOWLEDGEMENTS

I would like to thank first and foremost my supervisor Dr. Vincent Klink for his years of mentorship throughout my Ph.D. program. I am very much obliged for his persistent and strict guidance, but very valuable suggestions and co-operation in my process of learning all the techniques conducting research and scientific writing.

I would like to express my sincere appreciation to Dr. Gary W. Lawrence for all the help regarding greenhouse experiments. Without his expertise and guidance on crops and nematodes, I could not have succeeded this far. I am very much grateful To Dr. Lawrence for providing excellent facilities, encouragement, continuous support, discussions, and guidance throughout the research project. I would like to extend my gratitude to my committee member, Dr. Dragica Jeremic, for providing the opportunity to conduct the cell wall analysis study under her supervision. I am thankful to her for giving me time and space to learn and conduct biochemical studies, including the HPLC analysis. Similarly, I would like to thank Dr. Ying Wang, committee member, for giving constructive advice and encouragement that went toward the completion of my work.

Research is a team effort from the start to the completion. Without support of my friends, it would have been much more difficult. Especially, I would like to acknowledge Dr. Xuefeng Zhang, Dr. Shankar Pant, Dr. Brant McNeece, Dr. Keshav Sharma, Dr. Bisho Ram Lawaju, Jillian Harris, Jian Jiang, Dr. Weasam A.R. Aljaafri, Ismail Khan, Rishi Khatri, Mandeep Adhikari, Hallie Troell and Tineka Burkhead for being there to

support me technically and morally. I am also very thankful to Yi Xiu Pinnix (Jan) for all the help during the time related to the greenhouse research. I am also grateful to all the undergraduate student workers and volunteers for their assistance during my active greenhouse experiments as well as the molecular work.

I am always grateful for my family for their love and support. I want to thank all of my teachers from elementary school to the university level for all of their knowledge and inspiration, guiding me to pursuing higher studies. My sincere gratitude is extended to the Department of Biological Sciences and Department of Sustainable Bioproducts for providing great laboratory resources for this research. Last but not the least, thanks to all my friends at MSU, faculty and staff in Department of Biological Sciences. The Teaching Assistantships that have been provided to me over the years during the school year and summers by the Department of Biological Sciences have made this work possible.

TABLE OF CONTENTS

LIST OF TABLES

LIST OF FIGURES

CHAPTER I

INTRODUCTION

Heterodera glycines (soybean cyst nematode [SCN]) infection

Heterodera glycines (soybean cyst nematode [SCN]), a major obligate biotrophic pathogen of *Glycine max* (soybean), is known to be a major soybean yield reducing pathogen, causing more agricultural loss than the rest of the pathogens combined (Wrather et al. 2006). The *H. glycines* is a sedentary endoparasite as it completes life cycle inside a living plant root. The *H. glycines* has a life cycle of about 30-35 days (Lauritis et al., 1983).

The *H. glycines* life cycle consists of four juvenile stages and an adult stage resulting from successive molts. The first stage juveniles (J1s) hatch and the first molt occurs inside the cyst. Then, J1s develop into the second stage juveniles (J2s). The J2s move through the soil, toward the plant. Eventually, the *H. glycines* engages with and infects the plant root by burrowing into it. The location of the J2 infection of soybean normally is behind the root tip where a lateral root formation is still in progress (Sobczak & Golinowski, 2009). The J2s that are successfully reside in the roots are classified based on the stage of infection, while the J2s which do not find the feeding location eventually die. The first feeding stage is the pre-infective juveniles (pi-J2). The *H. glycines* organ used to sense the location of the root and leading to the penetration of the roots are the amphids and stylet. As pi-J2s burrow into the roots, they are regarded as infective J2s (i-

J2). Typically, the stylet consists of three parts; stylet cone, stylet shaft and stylet knobs. The three stylet knobs are supported by muscle layers. The nematodes move through the cells by repeated penetration of adjacent cells with their stylet until the perforation weakens the cell enough to allow the nematode to pass through. The i-J2 burrows into the root and when encountering a root pericycle or nearby cell pierces the cell with its stylet, a straw-like mouth part that injects substances into the root cell with the goal of creating a feeding cell from which it nurses. After penetrating the target cell, i-J2s inject substances synthesized in esophageal and/or sub-ventral glands that alter major physiological and biochemical changes in the root cell. The nurse cells (syncytia) that the *H. glycines* feeds from are initially induced to be formed by *H. glycines*. The syncytium is an amalgamation of several hundred root cells sharing a common cytoplasm with their accompanying nuclei. The syncytium provides nutrients needed for the completion of the *H. glycines* life cycle (Hussey, 1989; Jones, 2018). The J2s that eventually will become female increase further in size and undergo J3 and J4 molts, resulting in its lemon shape. For these parasitizing nematodes, the cephalic region remains embedded in the root while the posterior erupts out of root boundary. The J2s that eventually become males feed and remain sedentary and then stop feeding. These nematodes subsequently molt twice into vermiform J4 males which exit the roots and search for females as it prepares for mating. After copulation, the fertilized eggs develop in the egg mass inside the female body. When the female dies, her body serves as a cyst to protect the eggs enclosed within the structure in the soil (Jones and Northcote, 1972; Lauritis et al., 1983; Niblack, 2005). The cysts, which protect the eggs against unfavorable conditions, varies considerably in size ranging about 200 to 1,000 μm (Mulvey, 1972). After successful copulation, a female can

produce 200-600 viable eggs. Some eggs are exuded into the gelatinous matrix that can hatch quickly, while the majority are retained in the cyst after the death of the female. Depending on temperature, soil moisture, soil types and host species, eggs encased within the cysts can survive for several years (Noel, 1986). It has been reported that eggs within a cyst can survive in temperatures of -40º C for several months (Hu et al., 2016). The presence of favorable temperatures (22-26º C), moisture and root exudates are believed to play crucial roles in the hatching of eggs into the J2-juvenile stage (Tefft et al., 1982; Melton et al., 1986) .

Features of the susceptible and resistance response to *H. glycines*

When *H. glycines* encounters a root, two major types of root responses can occur. These responses include a susceptible or a resistant reaction. It is possible for plants to also be tolerant to infection which may be a form of a susceptible interaction since the *H. glycines* successfully completes their life cycle while the seed yield and growth habit remain unaffected. During the earlier phases of the susceptible and resistant reactions, the interaction between *H. glycines* and the root are about the same. During these periods, the nematode commences burrowing into the root at about the same rates leading up to when it selects the pericycle or nearby cell for feeding site establishment. Consequently, earlier parasitism phases are expected to be similar between susceptible and resistant responses. At this phase of root infection, parasite development in both of susceptible and resistant cultivars of soybean are essentially indistinguishable. These observations are supported by their nearly identical transcriptomic profiles while cytological and ultrastructural observations of roots suggest infected cells undergo similar biochemical and

physiological events in order to cope with pathogenic invasion (de Almeida Engler, 1999; Hermsmeier et al., 1998; Davis et al., 2004).

In a susceptible response to *H. glycines*, after an initial developmental stage, elaboration of the feeding site takes place with a large uptake of solutes. The large multinucleated feeding structure, the syncytium, is formed by cell wall degradation and fusion of the adjoining protoplasts (Jones & Northcote, 1972). Several plant proteins and enzymes comprise biochemical pathways that are functioning during syncytium development, providing a rich food source for nematode development (reviewed by Sobczak & Golinowski, 2011). Different pools of nematode effectors such as cell wall modifying enzymes are essential to suppress host defenses. Cyst nematodes produce a peptide similar to plant CLAVATA3 (CLE) protein, manipulating the clavata signaling pathway, important in feeding site induction (Wang et al., 2005). Some nematode effectors interact directly with the auxin influx protein PIN FORMED1 (PIN1) and PIN3, preventing the transport of auxin away from feeding structure (Lee et al., 2011). This role of the effector leads to a local increase of the hormone, allowing for the radial expansion of the syncytium (Ithal et al., 2007).

In all resistant cultivars of soybean, the i-J2s are capable of penetrating and inducing syncytia formation. However, the syncytia become necrotic soon after its establishment, leading to nematode death (Mahalingam & Skorupska, 1996). The timing of necrosis and degeneration of syncytia varies among resistant cultivars (Mahalingam & Skorupska, 1996; Ithal et al., 2007; Kandoth et al., 2011). The earlier defense response to infection involves basal defenses activated by the detection of pathogen-associated molecular pattern (PAMPs) by extracellular pattern recognition receptors (Schwessinger

& Zipfel, 2008). The later phase of the defense response involves basal as well as resistance (R) gene mediated effector-triggered immune (ETI) responses, suppressing the pathogen directly or indirectly. The various effectors trigger different plant defense genes while accumulating proteins and phytohormones, leading to extensive hypersensitive reactions (HR) and systemic acquired resistance (SAR) (Takahashi et al., 2004; Ithal et al., 2007; Klink et al. 2007; Hosseini, et al., 2010).

The genetics of *H. glycines* resistance

The USDA (United States Department of Agriculture) has been collecting and maintaining natural accessions of *G. max* that have been made in its native range in Asia. Thousands of accessions have been tested for their ability to resist *H. glycines* infection with the earliest being *G. max*$_{[\text{Peking/PI 548402}]}$ that has shown a resistant reaction occurring at the site of parasitism (Ross & Brim, 1957; Ross, 1958). Subsequent mapping efforts have resulted in the identification of *H. glycines* resistance quantitative trait loci (QTLs) from different soybean germplasm (reviewed in Concibido et al., 2004). Three major recessive resistance loci *rhg1*, *rhg2* and *rhg3* and two major dominant resistant loci *Rhg4* and *Rhg5* have been identified through these genetic analyses (Caldwell et al., 1960; Matson & Williams, 1965; Rao-Arelli, 1994).

To facilitate resistance gene identification, laser capture microdissection (LCM) has been employed for extraction of the syncytia from the rest of the uninfected root cells which would allow for the isolation of mRNA from those cells for gene expression studies. The earlier gene expression studies have relied on cDNA library construction and microarray analysis, identifying differentially expressed genes relating to the resistant reactions (Klink et al., 2005, 2007a, 2009a, b; 2010a,b, 2011). Using this technique

Matsye et al. (2011) has identified 1,787 genes that are expressed specifically within the cells undergoing a defense response. The analysis has examined genes that are expressed within the *rhg1* locus (Matsye et al. 2011). The experiments have led to the demonstration that alpha soluble NSF attachment protein (α-SNAP), as a part of the *rhg1* locus, had been among only two genes expressed within the locus (Matsye et al., 2011). Functional analyses have demonstrated α-SNAP is the *rhg1* gene, proving the examination of the 1,787 expressed genes would be a useful approach to understanding the defense process (Matsye et al., 2012).

Several studies have been carried out in both susceptible and resistant cultivars of soybean, showing the involvement of other defense related genes acting in response to *H. glycines* infection (Alkharouf et al., 2006; Klink et al., 2005, 2007b; Matsye et al., 2012). Pant et al. (2014) has identified the elevated level of expression of defense genes including homologs of *PATHOGENESIS RELATED 1* (*PR1*) and *NONEXPRESSOR OF PR1* (*NPR1*), *XYLOGLUCAN ENDO-TRANSGLYCOSYLASE/HYDROLASE* (*XTH*), *ENHANCED DISEASE SUSCEPTIBILITY* (*EDS1*) and the *Arabidopsis thaliana* R gene *BOTRYTIS INDUCED KINASE1* (*BIK1*). A number of studies have demonstrated the role of the vesicular transport machinery in the formation of cell wall appositions (CWAs) in the defense response against *H. glycines* infected roots (Matsye et al., 2012; Pant et al., 2014, 2015; Sharma et al., 2016). However, the regulatory mechanism behind the vesicle transport machinery and CWA development and how they accomplish plant defense to pathogens like *H. glycines* had not become fully understood. More recent studies have implicated the mitogen activated protein kinase (MAPK) signaling cascade functioning downstream of these signaling processes. Consequently, by proving so, the work has

provided an important link between receptor signaling and transcription (McNeece et al., 2019).

Justification of the *G. max-H. glycines* pathosystem as an experimental model

A great deal of studies have been carried out using the genetic model *A. thaliana* on various plant defense mechanisms. However, the nature of its growth (small with very little root mass) does not make *A. thaliana* an ideal model to understand the pathogenic process occurring in root systems. An alternative model, *G. max*, has proven to be ideal for understanding plant interactions to root obligate pathogens like *H. glycines*. Factors making *G. max* a useful model include that its genome is sequenced (Schmutz et al., 2010). Furthermore, there are many plant introductions (PIs) available for the study of compatible and incompatible interactions, while in contrast, the generation of susceptible and resistant reactions can be accomplished even in the same genotype (Niblack et al., 2006; Klink et al. 2007b; Matsye et al., 2011, 2012; Cook et al., 2012). *H. glycines*, a biotrophic pathogen of *G. max*, creates a very well-defined infection site that it parasitizes while it maintains that interaction in the root for a comparatively long time. The events occurring during this process are well characterized in which a pericycle cell undergoes a reaction that leads to the eventual formation of a syncytium. These features allow for the collection of the various relevant cells at important time points occurring during the course of the susceptible and resistant reactions. Furthermore, *G. max* has a duplicated genome, thus, serving as a model crop for most of the crop plants that have duplicated genomes (Doyle et al., 1999). Furthermore, gene cassettes can easily be engineered into the roots of plants, allowing for the overexpressing or silencing of genes to be performed quite easily. The basic genetic knowledge derived from the gene

expression experiments can be implemented into *G. max- H. glycines* pathosystem, consequently improving agriculture in applied manner. The expression of genes in timed events along with functional assays allows for an understanding of the defense process that *G. max* has towards *H. glycines* which will certainly be impactful for research in root biology and the development or enhancement of resistance in breeding programs.

Aim of the research project

The aim of this dissertation is to determine the functional effect of genetically engineered candidate resistance genes, identified to be expressed within syncytia in *G. max* undergoing its respective defense reaction *H. glycines* parasitism, has on parasitism. The genetic analyses are focused in on determining gene expression levels and patterns present during the respective susceptible and resistant reactions with the objective of determining the cellular events that relate to the defense process. Prior work has identified and demonstrated a pool of genes that are expressed to a higher level during defense response in *G. max* as it combats *H. glycines* infection (Matsye et al., 2011, 2012). In this dissertation, selected genes expressed specifically in the cell undergoing the resistant reaction are overexpressed in the susceptible soybean genotype *G. max*$_{[\text{Williams 82/PI 518671}]}$ to determine if the experimentally induced expression leads to an engineered resistant reaction. In contrast, RNAi of that same target gene in the resistant soybean genotype *G. max*$_{[\text{Peking/PI 548402}]}$ is done to determine if the experimentally decreased expression leads to an engineered susceptible reaction. (Klink et al., 2010; Matsye et al., 2011, 2012; Pant et al. 2014). The combination of these two opposing outcomes has been used to demonstrate that the gene functions in the defense process (Pant et al., 2014). The proposed study presented in this dissertation on additional genes that comprise the 1,787

candidate defense genes identified by Matsye et al. (2011) interconnects to previous work and expands the knowledge on the mechanism of resistance against the development of *H. glycines* in soybean.

Specifically, the study is aimed to determine the expression pattern of circadian rhythm genes in soybean as it relates to the central circadian clock oscillators with other clock associated genes that function in defense. This dissertation is directed to determine the role of main clock component and other clock associated genes in defense against *H. glycines*. Further, defense genes responsible for cell wall appositions (CWAs) including XyG remodeling, the vesicular transport machinery, and their relation to circadian clock genes. By performing these studies, a genetic link will be made between already identified membrane receptors, MAPK signaling and transcription factors that are central to metabolic processes that lead to output responses like hemicellulose modification which would occur through the action of XTH. Consequently, the intended genetic expression and biochemical analysis would provide the first molecular and structural data regarding the actual cell wall modification as an actual part of the defense process that *G. max* has toward *H. glycines*.

Dissertation outline

The introduction provided in the previous section has highlighted the plant-nematode interaction, specifically in *G. max-H. glycines* pathosystem, in terms of susceptible and resistant responses. Meanwhile, the defense activation and implementation in the plant is intrinsic, combating pathogenic attack as well as further responses that occur after infection. However, the knowledge in the overall mechanism of

innate immunity through the circadian clock and molecular, and structural output of defense response is still limited.

CCA1 is the main circadian clock oscillator, first identified in *A. thaliana*. My dissertation focuses on the expression level of a soybean *CCA1*, *Gm*-CCA1-1, among uninfected and infected soybean plants along with the respective controls. In Chapter 2, my dissertation analyzes the difference in expression of the main clock component genes in soybean roots against the *H. glycines* infection. Further in this chapter, the functional effects of the genetic manipulation of the clock components in relation to *H. glycines* infection has been determined.

In Chapter 3, I analyze the role of XyG as it relates to the soybean defense response to *H. glycines*. From extracted polysaccharides from *Gm*-XTH43-OE and *Gm*-XTH43-RNAi transgenic lines, along with respective controls, XyGs have been quantified and determined. The experiments have determined the molecular weight of XyGs as it directly relates to polysaccharide chain length occurring in cell walls.

In Chapter 4, the expression of clock components has been cross checked for in relation to the expression of a panel of other already proven defense genes cDNA library through qPCR. The genes relate to the central clock oscillator. The genes are also shown to exhibit defense functions.

In Chapter 5, I provide a summary that develops a conclusion of all the results in respect to the plant-parasitic interaction and immune responses. In addition, it discusses the future directions and recommendation for significance of actual biochemical study along with molecular gene expression studies. The summary provides an overarching synthesis of the presented work.

References

Alkharouf, N. W., Klink, V. P., Hunter, C., Margaret, S. B., Meyer, S., Knap, H. T., & Khan, R. (2006). Timecourse microarray analyses reveal global changes in gene expression of susceptible *Glycine max* (soybean) roots during infection by *Heterodera glycines* (soybean cyst nematode), 838–852. https://doi.org/10.1007/s00425-006-0270-8

Allen, T. W., Bradley, C. A., Sisson, A. J., Byamukama, E., Chilvers, M. I., Coker, C. M., … Wrather, J. A. (2017). Soybean Yield Loss Estimates Due to Diseases in the United States and Ontario, Canada, from 2010 to 2014. *Plant Health Progress*, *18*(1), 19–27. https://doi.org/10.1094/PHP-RS-16-0066

Caldwell, B. E., Brim, C. A., & Ross, J. P. (1960). Inheritance of Resistance of Soybeans to the Cyst Nematode, *Heterodera Glycines*1. *Agronomy Journal*, *52*, 635–636. https://doi.org/10.2134/agronj1960.00021962005200110007x

Concibido, V. C., Diers, B. W., & Arelli, P. R. (2004). A Decade of QTL Mapping for Cyst Nematode Resistance in Soybean. *Crop Sci*, *44*(July 2003), 1121–1131. https://doi.org/10.2135/cropsci2004.1121

Cook, D. E., Lee, T. G., Guo, X., Melito, S., Wang, K., Bayless, A. M., … Bent, A. F. (2012). Copy Number Variation of Multiple Genes at Rhg1 Mediates Nematode Resistance in Soybean.

Davis, E. L., Hussey, R. S., & Baum, T. J. (2004). Getting to the roots of parasitism by nematodes. *Trends in Parasitology*, *20*(3), 134–141. https://doi.org/10.1016/j.pt.2004.01.005

de Almeida Engler, J. (1999). Molecular Markers and Cell Cycle Inhibitors Show the Importance of Cell Cycle Progression in Nematode-Induced Galls and Syncytia. *The Plant Cell Online*, *11*(5), 793–808. https://doi.org/10.1105/tpc.11.5.793

Doyle, J., Doyle, L., & Brown, A. (1999). Origins , colonization , and lineage recombination in a widespread perennial soybean polyploid complex, *96*(September), 10741–10745.

Hermsmeier, D., Mazarei, M., & Baum, T. J. (1998). Differential Display Analysis of the Early Compatible Interaction Between Soybean and the Soybean Cyst Nematode. *MPMI\r*, *11*(12), 1258–1263. https://doi.org/10.1094/MPMI.1998.11.12.1258

Hu, W., Chen, S., & Liu, X. (2016). Effect of temperature treatment on survival of and its associated fungi and bacteria. *Nematology*, *18*(7), 845–855. https://doi.org/https://doi.org/10.1163/15685411-00003000

Hussey, R. S. (1989). Disease-Inducing Secretions of Plant-Parasitic Nematodes. *Annual Review of Phytopathology*, *27*(1), 123–141. https://doi.org/10.1146/annurev.py.27.090189.001011

Ithal, N., Recknor, J., Nettleton, D., Maier, T., Baum, T. J., & Mitchum, M. G. (2007). Developmental Transcript Profiling of Cyst Nematode Feeding Cells in Soybean Roots. *Molecular Plant-Microbe Interactions*, *20*(5), 510–525. https://doi.org/10.1094/MPMI-20-5-0510

Jones, M. G. K. (2018). Host cell responses to endoparasitic nematode attack: structure and function of giant cells and syncytia*. *Annals of Applied Biology*, *97*(3), 353–372. https://doi.org/10.1111/j.1744-7348.1981.tb05122.x

Jones, M. G. K., & Northcote, D. H. (1972). Nematode-induced syncytium--a multinucleate transfer cell, (June).

Kandoth, P. K., Ithal, N., Recknor, J., Maier, T., Nettleton, D., Baum, T. J., & Mitchum, M. G. (2011). The soybean Rhg1 locus for resistance to the soybean cyst nematode Heterodera glycines regulates expression of a large number of stress- and defense-related genes in degenerating feeding cells. *Plant Physiology*. Retrieved from http://www.plantphysiol.org/content/early/2011/02/18/pp.110.167536.abstract

Klink, V. P., Alkharouf, N., MacDonald, M., & Matthews, B. (2005). Laser Capture Microdissection (LCM) and expression analyses of *Glycine max* (soybean) syncytium containing root regions formed by the plant pathogen *Heterodera glycines* (soybean cyst nematode). *Plant Molecular Biology*, *59*(6), 965–979. https://doi.org/10.1007/s11103-005-2416-7

Klink, V. P., Hosseini, P., Matsye, P., Alkharouf, N. W., & Matthews, B. F. (2009). *A gene expression analysis of syncytia laser microdissected from the roots of the Glycine max (soybean) genotype PI 548402 (Peking) undergoing a resistant reaction after infection by Heterodera glycines (soybean cyst nematode)*. *Plant Molecular Biology* (Vol. 71). https://doi.org/10.1007/s11103-009-9539-1

Klink, V. P., Hosseini, P., Matsye, P. D., Alkharouf, N. W., & Matthews, B. F. (2010). Syncytium gene expression in *Glycine max*[PI 88788]roots undergoing a resistant reaction to the parasitic nematode *Heterodera glycines*. *Plant Physiology and Biochemistry*, *48*(2–3), 176–193. https://doi.org/10.1016/j.plaphy.2009.12.003

Klink, V. P., Overall, C. C., Alkharouf, N. W., MacDonald, M. H., & Matthews, B. F. (2007). A time-course comparative microarray analysis of an incompatible and compatible response by *Glycine max* (soybean) to *Heterodera glycines* (soybean cyst nematode) infection. *Planta*, *226*(6), 1423–1447. https://doi.org/10.1007/s00425-007-0581-4

Klink, V. P., Overall, C. C., Alkharouf, N. W., MacDonald, M. H., & Matthews, B. F. (2010). Microarray detection call methodology as a means to identify and compare transcripts expressed within syncytial cells from soybean (*Glycine max*) roots undergoing resistant and susceptible reactions to the soybean cyst nematode (*Heterodera glycines*). *Journal of Biomedicine and Biotechnology*, *2010*(Dcm). https://doi.org/10.1155/2010/491217

Klink, V.P., Hosseini, P., Matsye, P.D., Alkharouf, N.W., Matthews, B.F. 2011. Differences in gene expression amplitude overlie a conserved transcriptomic program occurring between the rapid and potent localized resistant reaction at the syncytium of the *Glycine max* genotype Peking (PI 548402) as compared to the prolonged and potent resistant reaction of PI 88788. Plant Molecular Biology 75:141-165.Koenning, S., & Wrather, A. (2010). Soybean Pathology White Paper. *Crop Science*, *103*(2), /PHP-2010-1122-01-RS. https://doi.org/10.1094/PHP-2010-1122-01-RS.Abstract

Lauritis, J. A., Rebois, R. V, & Graney, S. (1983). Development of *Heterodera glycines* Ichinohe on Soybean , Glycine max (L .) Merr ., under Gnotobiotic Conditions ~. *Journal of Nematology*, *3*(Scn 3), 272–281.

Lee, C., Chronis, D., Kenning, C., Peret, B., Hewezi, T., Davis, E. L., … Mitchum, M. G. (2011). The Novel Cyst Nematode Effector Protein 19C07 Interacts with the *Arabidopsis* Auxin Influx Transporter LAX3 to Control Feeding Site Development. *Plant Physiology*, *155*(2), 866–880. https://doi.org/10.1104/pp.110.167197

Mahalingam, R., & Skorupska, H. T. (1996). Cytological expression of early response to infection by *Heterodera glycines* lchinohe in resistant PI 437654 soybean, *998*, 986–998.

Matson, A. L., & Williams, L. F. (1965). Evidence of a Fourt Gene for Resistance to the Soybean Cyst Nematodde 1. *Crop Science*, *5*(5), 477.

Matsye, P. D., Kumar, R., Hosseini, P., Jones, C. M., Tremblay, A., Alkharouf, N. W., … Klink, V. P. (2011). Mapping cell fate decisions that occur during soybean defense responses. *Plant Molecular Biology*, *77*(4–5), 513–528. https://doi.org/10.1007/s11103-011-9828-3

Matsye, P. D., Lawrence, G. W., Youssef, R. M., Kim, K. H., Lawrence, K. S., Matthews, B. F., & Klink, V. P. (2012). The expression of a naturally occurring, truncated allele of an α-SNAP gene suppresses plant parasitic nematode infection. *Plant Molecular Biology*, *80*(2), 131–155. https://doi.org/10.1007/s11103-012-9932-z

McNeece, B., Sharma, K., Lawrence, G. W., Lawrence, K. S., & Klink, V. P. (2019). The mitogen activated protein kinase (MAPK) gene family functions as a cohort during the Glycine max defense response to Heterodera glycines. *Plant Physiology and Biochemistry*, 1–19. https://doi.org/https://doi.org/10.1016/j.plaphy.2019.01.018

Melton, T. A., Jacobsen, B. J., & Noel, G. R. (1986). Effects of Temperature on Development of *Heterodera glycines* on *Glycine max* and *Phaseolus vulgaris* 1. *Journal of Nematology*, *18*(4), 468–474.

Mulvey, R. H. (1972). Identification of Heterodera cysts by terminal and cone top structures. *Canadian Journal of Zoology*, *50*(10), 1277–1292. https://doi.org/10.1139/z72-173

Niblack, T. (2005). *Soybean Cyst Nematode Life Cycle*. *Plant Disease* (Vol. 89).

Niblack, T. L., Lambert, K. N., & Tylka, G. L. (2006). A Model Plant Pathogen from the Kingdom Animalia: *Heterodera glycines*, the Soybean Cyst Nematode. *Annual Review of Phytopathology*, *44*(1), 283–303. https://doi.org/10.1146/annurev.phyto.43.040204.140218

Noel, G. R. (1986). The Soybean Cyst Nematode BT - Cyst Nematodes. In F. Lamberti & C. E. Taylor (Eds.) (pp. 257–268). Boston, MA: Springer US. https://doi.org/10.1007/978-1-4613-2251-1_17

Pant, S. R., Krishnavajhala, A., Mcneece, B. T., Lawrence, G. W., Klink, V. P., Pant, S. R., … Klink, V. P. (2015). SIMULATING DISEASE1 (LSD1), functions in Glycine glycines The syntaxin 31-induced gene , LESION SIMULATING DISEASE1 (LSD1), functions in *Glycine max* defense to the root parasite *Heterodera glycines*, *2324*. https://doi.org/10.4161/15592324.2014.977737

Pant, S. R., Matsye, P. D., McNeece, B. T., Sharma, K., Krishnavajhala, A., Lawrence, G. W., & Klink, V. P. (2014). Syntaxin 31 functions in *Glycine max* resistance to the plant parasitic nematode *Heterodera glycines*. *Plant Molecular Biology*, *85*(1–2), 107–121. https://doi.org/10.1007/s11103-014-0172-2

Rao-Arelli, A. P. (1994). Inheritance of resistance to *Heterodera glycines* race 3 in soybean accessions. *Plant Disease (USA)*.

Rincker, K., Cary, T., & Diers, B. W. (2017). Impact of Soybean Cyst Nematode Resistance on Soybean Yield. *Crop Science*, *57*, 1373–1382. https://doi.org/10.2135/cropsci2016.07.0628

Ross, J., & Brim, C. (1957). Resistance of soybean to the soybean-cyst nematode as determined by a double-row method. *Plant Dis. Rep.*, *41*, 923–924. Retrieved from https://ci.nii.ac.jp/naid/10030433670/en/

Ross, J. P. (1958). Host-parasite relationship of the soybean cyst nematode in resistant soybean roots. *Phytopathology*, *48*(10), 578–579.

Schmutz, J., Cannon, S. B., Schlueter, J., Ma, J., Mitros, T., Nelson, W., … Jackson, S. A. (2010). Genome sequence of the palaeopolyploid soybean. *Nature*, *463*(7278), 178–183. https://doi.org/10.1038/nature08670

Schwessinger, B., & Zipfel, C. (2008). News from the frontline: recent insights into PAMP-triggered immunity in plants. *Current Opinion in Plant Biology*, *11*(4), 389–395. https://doi.org/10.1016/j.pbi.2008.06.001

Sharma, K., Pant, S. R., Mcneece, B. T., Lawrence, G. W., Klink, V. P., Sharma, K., … Lawrence, G. W. (2016). Co-regulation of the *Glycine max* soluble N-ethylmaleimide-sensitive fusion protein attachment protein receptor (SNARE) - containing regulon occurs during defense to a root pathogen, *9145*. https://doi.org/10.1080/17429145.2016.1195891

Sobczak, M., & Golinowski, W. (2009). Structure of Cyst Nematode Feeding Sites BT - Cell Biology of Plant Nematode Parasitism. In R. H. Berg & C. G. Taylor (Eds.) (pp. 153–187). Berlin, Heidelberg: Springer Berlin Heidelberg. https://doi.org/10.1007/978-3-540-85215-5_6

Sobczak, M., & Golinowski, W. (2011). Cyst Nematodes and Syncytia BT - Genomics and Molecular Genetics of Plant-Nematode Interactions. In J. Jones, G. Gheysen, & C. Fenoll (Eds.) (pp. 61–82). Dordrecht: Springer Netherlands. https://doi.org/10.1007/978-94-007-0434-3_4

Takahashi, H., Kanayama, Y., Zheng, M. S., Kusano, T., Hase, S., Ikegami, M., & Shah, J. (2004). Antagonistic interactions between the SA and JA signaling pathways in *Arabidopsis* modulate expression of defense genes and gene-for-gene resistance to cucumber mosaic virus. *Plant and Cell Physiology*, *45*(6), 803–809. https://doi.org/10.1093/pcp/pch085

Tefft, P. M., Rende, J. F., & Bone, L. W. (1982). Factors Influencing Egg Hatching of the Soybean Cyst Nematode *Heterodera glycines* Race 3. *Proc. Helminthol. Soc. Wash*, *49*(2), 258–265.

Wang, X., Mitchum, M. G., Gao, B., Li, C., Diab, H., Baum, T. J., … Davis, E. L. (2005). A parasitism gene from a plant-parasitic nematode with function similar to CLAVATA3/ESR (CLE) of *Arabidopsis thaliana*. *Molecular Plant Pathology*, *6*(2), 187–191. https://doi.org/10.1111/J.1364-3703.2005.00270.X

Wrather, J. a., Anderson, T. R., Arsyad, D. M., Gai, J., Ploper, L. D., Porta-Puglia, a., … Yorinori, J. T. (1997). Soybean Disease Loss Estimates for the Top 10 Soybean Producing Countries in 1994. *Plant Disease*, *81*(1), 107–110. https://doi.org/10.1094/PDIS.1997.81.1.107

Wrather, J. A., & Koenning, S. R. (2006). Estimates of disease effects on soybean yields in the United States 2003 to 2005. *Journal of Nematology*, *38*(2), 173–180. https://doi.org/10.1094/PHP-2009-0401-01-RS

Ye, W. (2017). Soybean Cyst Nematode (*Heterodera glycines*) Distribution in North Carolina, U.S.A. *Plant Health Progress*, *18*(4), 230–232. https://doi.org/10.1094/PHP-08-17-0050-BR

CHAPTER II

A ROLE OF THE CENTRAL CIRCADIAN REGULATOR IN THE DEFENSE OF *GLYCINE MAX* TO THE ROOT PARASITE *HETERODERA GLYCINES*

Abstract

Besides stomatal activity in leaves, the role of CCA1 along with other central oscillator components including *TIMING OF CAB1* (*TOC1*), *GIGANEA* (*GI*) and *CONSTANS* (*CO*) have been well established in signaling pathways in various adverse conditions and even cross-talk with defense genes during pathogen attack. The functional effect of *Gm*-CCA1-1 and other clock oscillator genes including *Gm*-TOC1-1, *Gm*-GI-1 and *Gm*-CO-4 against root nematodes have demonstrated their role in the defense process against *H. glycines*. The levels of mRNA of *Gm*-CCA1-1 in both OE and RNAi lines cycled through light (day)-dark (night) cycles, peaks late in the day. Notably, the amplitude and average expression level of *Gm*-CCA1-1 has been observed to be reduced in infected plants among OE lines with no significant change among RNAi lines, but it is still much higher than control and RNAi lines. Decreased levels of *Gm*-CCA1-1 mRNA among infected plant roots clearly shows clock components might have been arrested and altered in their expression during infection. However, a decreased circadian rhythm might be a greater consequence in global transcript regulation during infection than clock components regulating defense genes.

Introduction

Plant circadian rhythms

The rhythmic changes occurring in various metabolic and physiological process and rhythmic patterns of transcriptional/translational expression cycle alternately through high-activity and low-activity phases with a regular periodicity of about 24 hours. This periodicity is referred to as the circadian rhythm. Persistence of the rhythm in the absence of an external controlling factor suggests an endogenous nature of the circadian rhythm that is governed by an internal pacemaker called the oscillator that is insensitive to temperature, as shown by temperature compensation (McClung, 2001). The circadian rhythm synchronizes with a strong modulator such as light, termed as 'entrainment'. Such endogenous time keeping that anticipates environmental cycles, change and synchronizing the time of environmental conditions, and other activities increases the efficiency of metabolic and physiological process of biological entity including plants (Genoud et al., 2002; Zeier et al., 2004; Roden & Ingle, 2009).

The plant circadian oscillator consists of an interlocking feedback loop. The morning loop comprises, *CCA1* and *LATE ELONGATED HYPOCOTYL* (*LHY*), which activates two *PSEUDORESPONSE REGULATOR* (*PRR*) genes, *PRR7* and *PRR9*, functioning as negative feedback inhibition of *CCA1* and *LHY* (Young, 1998; Dunlap, 1999; Iwasaki & Kondo, 2000). At the same time, CCA1 and LHY repress the expression of *TOC1*/*PRR1* expression and evening complex (EC), a trimeric protein assembly composed of PHYTOCLOCK 1 (LUX1), EARLY FLOWERING (ELF3) and EARLY FLOWERING (ELF4) (Park et al., 1999; Doyle et al., 2002; Mizoguchi et al., 2002; Hazen et al., 2005). Another feedback is active in the evening, EC switches off the

expression of *PRR7* and *PRR9* and as a result, *CCA1* and *LHY* transcription resumes (Ferre et al., 2005; Rawat et al., 2011). TOC1 is a key transcription factor functioning within the loop that activates the expression of *CCA1* and *LHY*. Another component, GI, activity reinforces *TOC1* gene expression (Dixon et al., 2011; Helfer et al., 2011; Huang et al., 2012).

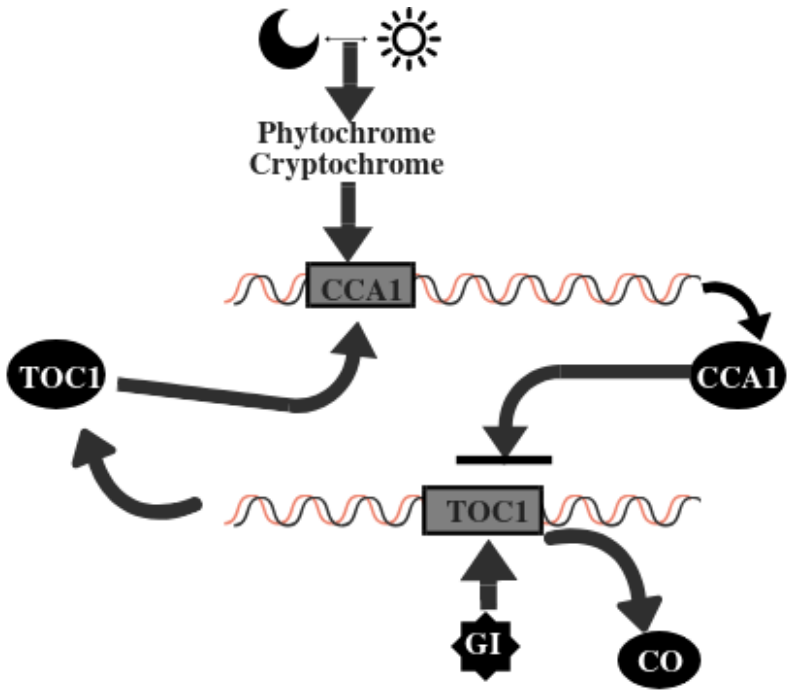

Figure 2.01 *A. thaliana* simplified molecular model of circadian clock.

Note: The input light signal is perceived by phytochromes and cryptochromes. Two main components of central oscillator are CCA1 and TOC1. CCA1 is a negative regulator of *TOC1* gene while TOC1 is a positive regulator of the *CCA1* gene. CO, itself a product of oscillator is homologous to TOC1, which initiates the flowering process. GI activates expression of *CCA1* in association with TOC1.

Importance of circadian rhythm in plant

The circadian system orchestrates plant physiological and biochemical processes and behavior which serves to optimally align metabolic functions of the plant with changes in the environmental cycle of light and dark phases. The circadian system works in three units. The input pathway ensures synchrony of the core clockwork with the day/light on receiving change in external stimuli such as light. The core clockwork is made up by an auto-regulatory loop-work of clock proteins that maintains a 24-hour rhythm of expression. Lastly, there are output pathways that drive the expression of genes that are regulated by the circadian core clock (Covington et al., 2008; Hazen et al., 2009). A regulatory relationship of gene expression occurring within the core oscillator in the plant influences a wide range of metabolic and signaling pathways. Plant regulatory genes functioning in photosynthesis, flowering and stomatal conductance have all been shown to be expressed more effectively in anticipation of the dark/light transition in circadian rhythmic wild type than circadian arrhythmic plant (Green et al., 2002). Another concept to consider is diel, defined as a 24 hour period irrespective of day/night. Plants anticipate diel environmental changes through the endogenously driven regulatory system affecting growth and development of the plant (Lu et al., 2005; Covington et al., 2008; Fukushima et al., 2009; Graf et al., 2010). The relative growth rate (RGR) of leaves and the root system has been found to be reduced significantly in circadian main regulator (CCA1) overexpressed than control plants (Ruts et al., 2012). The growth of every photosynthetic plant is directly associated with the rate of assimilation of starch. This assimilation is adjusted by the circadian rhythm in that CCA1, being a major component of the central oscillator, alternates carbohydrate assimilation and adjustment

with the exogenous day-light condition (Gibon et al., 2004; Dodd et al., 2005; Graf et al., 2010). Besides, the circadian oscillator and associated genes play a master role in maintaining homeostasis during biotic/abiotic stresses and anticipation of likely pathogen attack, even cross-talk with the defense genes (Wang et al., 2011; Lai et al., 2012; Yoshida et al., 2014; Zhang et al., 2013).

In nature, plants are constantly being exposed to biotic and abiotic stresses. Experiments have shown that the innate immune system is controlled by circadian rhythm in order to provide immunity (Zhang et al., 2013). A biological circadian clock is a diurnal regulation that controls all aspects of behavior and physiology to optimize them with the frame work for the solar day (Brown, 2014). Light is primarily required for photosynthesis. Besides this role, there is increasing evidence showing that light is also the mediator that links the circadian clock to the regulation of the innate immune response (Genoud et al., 2002; Zeier et al., 2004; Chandra-Shekara et al., 2006; Roden & Ingle, 2009). Plants are known to adapt to day-night cycles by a highly specialized circadian machinery. Under light signals, plants undergo massive molecular gene expression cascades. Those molecules regulate and control the level of metabolism and, consequently, the behavior of the plants. The interplay between the pathogen, susceptible host and favorable environmental conditions together are required for a successful infection of a disease. However, the vulnerability of the host to the pathogen is variable, sensitive to different developmental stages and different times of the day (Roden & Ingle, 2009). Furthermore, entrainment of the circadian clock by light is mediated by phytochromes and cryptochromes that translocate to the nucleus in response to light where they regulate gene expression. Additionally, regulatory element promoters have

been identified that are responsive to both light and pathogen derived signals (Evrard et al., 2009).

The circadian clock allows plants to anticipate predictable daily changes in abiotic and biotic stimuli reinforcing the immune system (Lai et al., 2012; Yoshida et al., 2014). The plant defense response in an anticipation of likely pathogen attack triggers both basal and R-gene mediated resistance and even cross-talk with other defense gene products signifies the importance of circadian rhythm and associated genes (Wang et al., 2011; Zhang et al., 2013). Plants, as they lack an adaptive immune response have to solely depend on innate immune responses. The rhythmic regulation of the defense genes involved in both R-gene specific programmed cell death (PCD) and general basal resistance is controlled positively and/or negatively by main clock component CCA1, encoding a MY-b related transcription factor (Wang & Tobin, 1998; Harmer et al., 2000; Wang et al., 2011). The expression pattern of defense R-genes overlap with the expression pattern of CCA1 in wild type. Further, the rhythmic co-expression of defense genes with CCA1 in the absence of the pathogen indicates an anticipation of infection according to the circadian clock (Wang et al., 2011). Important defense genes found to be regulated by CCA1 are *ATP-BINDING CASSEETTE* (*ABC*) transporters, *BRASSINOSTEROID INSENSITIVE-ASSOCIATED KINASES1/SOMATIC EMBRYOGENESIS RECEPTOR-LIKE KINASES3* (*BAK1*/*SERK3*), *NON-EXPRESSOR PR PROTEIN 1* (*NPR1*), RESISTANCE/RECOGNITION TO *PERONOSPORA PARASITICA* (*RPP4*) (Wang et al., 2011). The plasma membrane localized ABC-G type transporter protein has been shown to function as a resistance protein during race specific defense reaction in different pathogens including in *G. max* to *H. glycines* (Humphry et

al., 2010; Johansson et al., 2014; Sharma et al. 2016). BAK1/SERK3, receptor like kinases that function in defense through BIK1 by recognizing a bacterial PAMP, plays roles in diverse processes such as pathogen response as receptor of a PAMP, brassinosteroid hormone signaling, recognition of rhizobial nodulation factor (NF) that induces immune or symbiotic responses (Roux et al., 2011). NPR1 and RPP4 are likely to be involved in transcriptional regulation, as they are key regulators of salicylic acid (SA)-dependent defense responses (Cao et al., 1994; Van et al., 2002; Pant et al., 2016).

There is cross-talk occurring between the clock and defense activation. The *A. thaliana* glycine-rich RNA binding protein (AtGRP7), which performs roles in floral transition, development and stress tolerance and plant defense, as slave constituent of the oscillator, has been found to be affected in arrhythmic *CCA1* mutants (*cca1-1*) while *CCA1*-OE plants have a shortened circadian period (Zhang et al., 2013). In contrast, infection of both virulent and avirulent (in higher dose) *Pseudomonas syringae* strains shortens the circadian period and similar feedback regulation recapitulated with treatment with a 22-amino-acid synthetic peptide known as flagellin 22 (flg22) PAMP, suggesting pathogen triggered immunity (PTI) induced by flg22 feedbacks to regulate the clock activity. Since flg22 activates PTI, effector triggered immunity (ETI) and callose deposition and genes involved in flg22 signal transduction are shown to be under the influence of the circadian clock (Bhardwaj et al., 2011). Consequently, such cross-talk between the clock and defense confers advantages for plants fitness which is intricately connected with the plant growth and innate immunity.

Study objectives

There is an agreement in large extent that the role of the circadian rhythm and the main constituent of circadian clock oscillator (CCA1) goes beyond regulating metabolic and physiological events in plants. Recent studies have shown roles in plant defense against abiotic and biotic stresses in a diel cycle as CCA1 and related proteins involved in signal transduction conferring both basal and R-gene mediated immunity to the plant. Ruts et al. (2012), have demonstrated the involvement of the circadian clock in the regulation of diel whole plant growth. In which, a defective clock affected carbon allocation and metabolism thereby reducing growth. Graf et al. (2010) confirmed the role of the circadian clock gene in an adjustment and anticipation of light/dark cycle for the normal control of carbohydrate partitioning and utilization. According to Lai et al. (2012), the circadian clock is involved in regulating ROS homeostasis and maintaining permissive levels. Similarly, Both Wang et al. (2011) and Zhang et al. (2013) have elucidated the defense role of clock component against biotrophic (bacterial and fungal) pathogens such that clock defective transgenic plants are shown to have compromised resistance as compared to the wild type. Interestingly, Wang et al. (2011) have demonstrated the involvement of clock components with other defense genes in R-gene mediated defense involving SA-signaling. Zhang et al. (2013) have demonstrated a cross-talk between defense genes and CCA1 that defense activation also serves as an input signal to regulate clock activity. In defense against plant pathogen, the cytoplasmic receptor-like kinase BOTRYTIS INDUCED KINSE1 (BIK1) plays an important role in mediating flagellin-like signaling (flg22) from BAK1/FLS2 receptor complex (Veronese et al., 2006). A *Gm*-BIK1 has been shown to act as a component in plant defense

conferring SA induced, vesicle transport mediated defense as PAMP-triggered immune PTI response or ETI (effector-triggered immune response) to *H. glycines*. (Pant et al., 2014; McNeece et al., 2019).

Since, our experimental system consists of *H. glycines*, a biotrophic pathogen to a compatible and incompatible soybean accession *G. max*$_{[\text{William 82/PI 518671}]}$ and *G. max*$_{[\text{Peking/PI 548402}]}$, we tend to observe whether a role of circadian clock component CCA1 and other clock associated genes functions in a defense against *H. glycines*. Further, we aimed to interconnect between circadian rhythm and plant defense response produced by soybean. It is hypothesized that circadian clock components (CCA1 and related genes), normally expressed rhythmically in order to maintain and anticipate change in external stimuli, are also involved in regulating defense gene products providing an innate immunity to *H. glycines*.

Materials and Methods

Gene cloning and genetic transformation

The DNA sequence of the candidate *G. max* genes have been obtained at Phytozome (http://www.phytozome.net/). The primers have been designed according to the features of the destination vector that would be used in, with the CACC nucleotide sequence added to the 5' end of the forward primer for introduction into the pENTER entry vector (Invitrogen®). Amplicons have been generated by PCR and visualized in 1% agarose gel then purified by Wizard® SV Gel and PCR Clean-Up System (Promega®). Amplicons have then been ligated into the directional pENTER/D-TOPO vector and transformed into a chemically competent *E. coli* strain (One shot TOP10) and colonies have been chemically selected on LB-kanamycin (5µg/ml) agar plates based on protocol

(Invitrogen®). Upon plasmid extraction and confirming the DNA sequencing result to the original Genbank accession, the amplicons have been shuttled into the pRAP15 (OE) and pRAP17 (RNAi) destination vectors. Agar plates containing LB-tetracycline (5µg/ml) have been used to select for bacteria containing the vectors that are successful in transformation. Upon extraction of the plasmid, the amplicon-containing destination vectors have been transformed to chemically competent *Agrobacterium rhizogenes* strain K599 (K599) and again, transformed colonies have been selected on LB-tetracycline (5µg/ml). An overnight incubation at 28° C has been performed to genetically transform soybean, leading to the production of new, transgenic roots.

Soybean roots transformation

Six day old soybean plants have been used for genetic transformation according to Matsye et al. (2012). For K599 transformed with pRAP15 OE vectors, the bacteria have been used to transform the candidate resistance gene into *G. max*$_{[\text{Williams 82/PI 548402}]}$ of the *rhg1*$^{-/-}$ genetic background that is susceptible to *H. glycines*. For K599 transformed with the pRAP17 RNAi vectors, the genetic cassette has been transformed into *G. max*$_{[\text{Peking/PI548402}]}$ of the *rhg1*$^{+/+}$ genetic background that presents a resistance response to *H. glycines*. K599 which contains the applicable pRAP15 or pRAP17 empty vector has been regarded as the control. The successfully-made transgenic plant roots have been identified by fluorescence of the enhanced green fluorescent protein (eGFP) reporter using an eGFP Dark Reader Spot Lamp ® (ClareChemicals®), (Klink et al. 2009).

Infection and sample collection

The *H. glycines*[NL1-Rhg/HG-type 7/race 3] which accomplishes a susceptible reaction in *G. max*[Williams 82/PI 548402] and resistant reaction in *G. max*[Peking/PI548402] has been used for the infection of the transgenic soybean plant to ascertain its influence on parasitism (Klink et al., 2005; Pant et al., 2014). Eggs have been released from the females with a 150 µM aperture sieve and washed into a 25µM aperture sieve. Inoculum has been prepared by suspending J2 (juvenile) SCN at a concentration of 2,000 J2s/ml (Colgrove & Niblack, 2008; Matsye et al., 2012). Each soybean plant has been inoculated with 2,000 J2s/ml making the inoculum holes in the soil near the base of the root system. The holes had been covered once the inoculum has soaked in to prevent expulsion from watering. For the confirmation of infection, the acid-fuchsin staining procedure of Byrd et al. (1983) has been performed at 0, 3 and 6 dpi.

For the *Gm*-CCA1-1-OE and *Gm*-CCA1-1-RNAi time course studies, in a growth chamber setting of 12 hours day/12 hours dark, 25°C, 80% humidity, the identified transgenic and control plants had first been kept for a week to acclimate to the chamber conditions. Then, the transgenic plants had been infected with prepared (2,000 J2s/ml) inoculum of *H. glycines*. Along with control root samples, both infected and non-infected transformed root samples had been collected for 6 consecutive days at 4-hour intervals. For a day equaling 24 hours, sample collection began at 4 AM then subsequently at an interval of every 4 hours. As soon as the root samples had been taken, liquid nitrogen had been used to immerse the sample to preserve it, prevent RNA degradation. Samples have then been kept at -80°C in a freezer.

Cyst extraction

After 30 days of inoculation, cyst extraction from soybean roots had been performed. The technique had involved massaging the root in a bucket full of water. The procedure has led to the release of the cysts from the soil/root system, followed by stirring to suspend the soil per cyst mixture. The suspension had been poured through 20-mesh sieves followed by 100-mesh sieve to collect cysts (Klink et al., 2009; Matsye et al., 2012). Subsequently, cyst count, and root weights had been documented for each plant for future data analysis.

Female index calculation and data analysis

The female index (FI) has been calculated for each plant using formula given by Golden et al. (1970). The FI has been calculated as FI= (Nx/ Ns)*100, where Nx is the average number of females on the test cultivar (pRAP15 or pRAP17 lines containing the candidate resistance gene under study) and Ns is the average number of females on the control (standard susceptible or resistant) cultivar (Golden et al., 1970; Schmitt & Shannon, 1992; Matsye et al., 2012; Matthews et al., 2013; Pant et al., 2014). The FI has been calculated as a function of root mass, tested statistically using Mann-Whitney-Wilcoxon (MWW) Rank-Sum Test, $p < 0.05$ (Matsye et al., 2012). Each plant had been considered a replicate, and three experimental replicates, with at least 10 individual replicates have been considered to calculate FI.

Quantitative real-time PCR (qPCR)

Regarding the time series, the consecutive RNA samples have been collected for 6 days post infection at 4 hour intervals and used for construction of cDNA. The root

samples have been processed with an RNA isolation protocol (RNeasy Mini Kit, Qiagen®) and a cDNA construction protocol (Invitrogen®). After normalization of cDNA to 100 µg/µl, the level of expression of circadian clock regulator genes in the transgenic roots have been confirmed by qPCR, with the ribosomal protein gene S21 taken as the control (Klink et al., 2005; Matsye et al., 2012; Pant et al., 2014). Other expression patterns of genes of interest, particularly pathogenesis related genes have also been tested in response to the engineered clock regulator genes expression in order to establish the relationship among them. A probe (Taqman 6 carboxyfluorescein-6-FAM) with Black Hole Quencher (BHQ1) (MWG Operon®) have been used for qPCR reaction. The reaction contains 20 µl Taqman Gene Expression Master Mix (Applied Biosystems®), 0.9µl of 100µM forward primer, 0.9 µl of 100µM reverse primer, 2 µl of 2.5 µM 6-FAM (MWG Operon®) probe and 9.0 µl of template cDNA. The qPCR reaction is accomplished by pre-incubation of 50° C for 2 min, followed by 95° C for 10min. Proceeding from this step is alternating 95° C for 15 seconds then, 60° C for 1 min for 40 cycles. The $2^{-\Delta\Delta C}{}_{t}$ method has been used for statistical analysis to calculate relative changes in gene expression and has been followed according to the derived formula presented in Livak & Schmittgen, (2001).

Results

Transgenic root identification and infection

Successful transgenic experiments have been obtained by observing the eGFP reporter. The successfully-made transgenic plants with the respective clock genes in pRAP15 and pRAP17 vectors along with respective controls have been identified as transgenic lines as revealed by fluorescence (Figure 2.2).

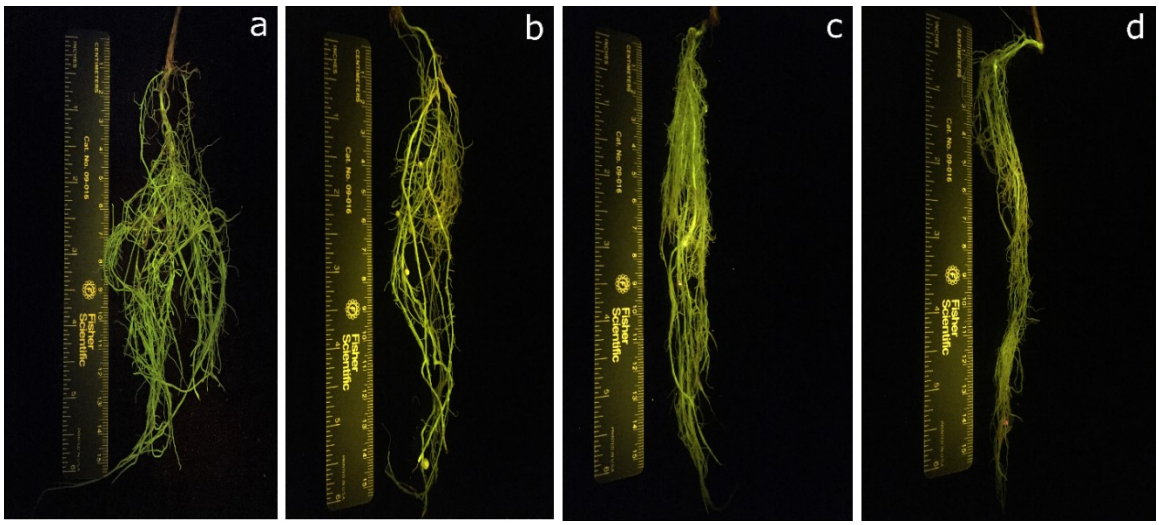

Figure 2.02 Genetically engineered roots of *G. max* roots. a. Control (pRAP15 vector), b. *Gm*-CCA1-1-OE; c. Control (pRAP17 vector), d. *Gm*-CCA1-1-RNAi.

The expression of *Gm*-CCA1-1 occurs with periodicity in uninfected roots.

To demonstrate that *Gm*-CCA1-1 is expressed with periodicity, *Gm*-CCA1-1-OE, *Gm*-CCA1-1-RNAi, and their respective controls have been grown in the growth chamber. The expression of the genes has been compared to their respective 0 dpi time point levels. The expression of the clock genes has been confirmed by qPCR. The results show that *Gm*-CCA1-1-OE has led to its overexpression, but with a rhythmic periodicity that is much greater than its control (Figure 2.3). In contrast, the results also show that the *Gm*-CCA1-1-RNAi has led to its decrease in expression, but with a rhythmic periodicity that is much greater than its pRAP17control (Figure 2.4).

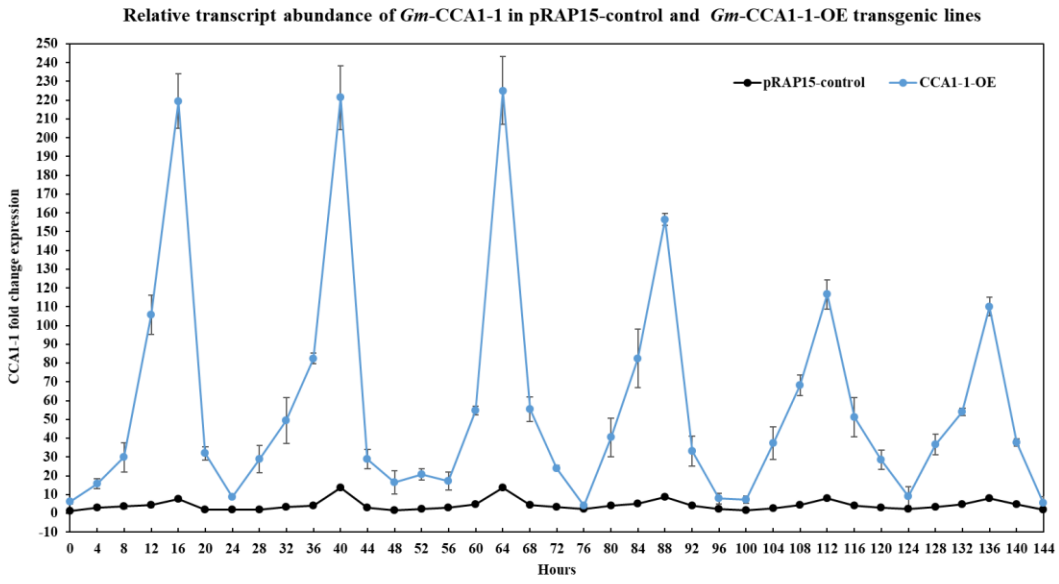

Figure 2.03 Quantitative PCR for the *Gm*-CCA1-1 gene in OE and pRAP15-control lines

Note: The y-axis depicts the relative fold change in expression as compared to 0 dpi control. The x-axis depicts the different time points RNA samples has been taken for six days (0 hours[h] up to 144h). Bars are standard error.

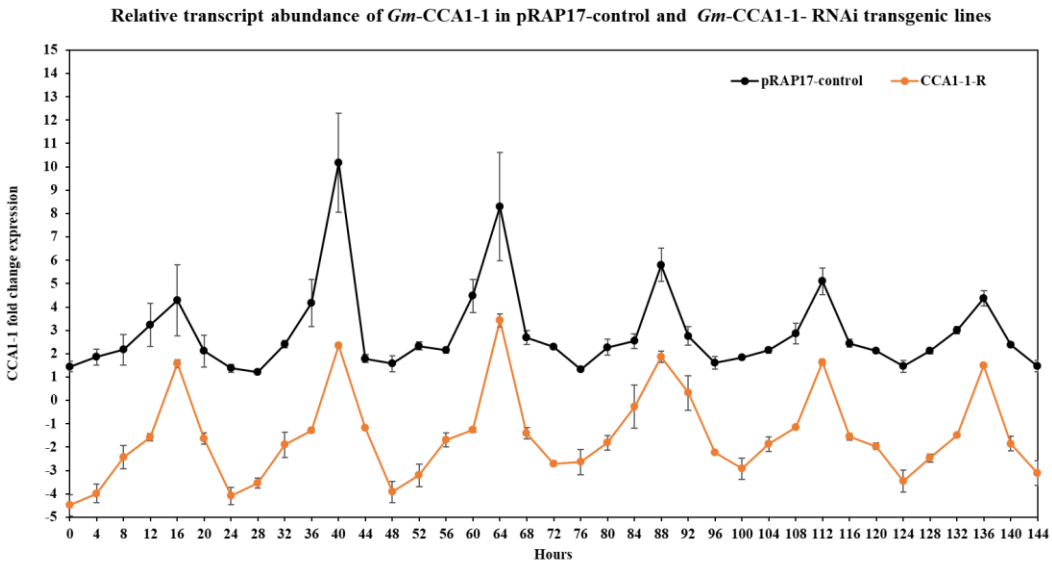

Figure 2.04 Quantitative PCR for the *Gm*-CCA1-1 gene in RNAi and pRAP17-control lines

Note: The y-axis depicts the relative fold change in expression as compared to 0 dpi control. The x-axis depicts the different time points RNA samples has been taken for six days (0 hours[h] up to 144h). Bars are standard error.

Performance of *H. glycines* in *Gm*-CCA1-1-OE and RNAi transgenic plants

The transgenic soybean plants had then been infected with *H. glycines*[NL1-Rhg/HG-type7/race3]. Transgenic plants had then been infected and kept in the greenhouse for 30 days for functional studies and for rhythmic gene expression analyses as root samples had been collected into liquid nitrogen and kept at -80°C. Acid-fuchsin staining of representative roots have been performed over a series of 6 consecutive, uninterrupted days. The experiment has confirmed the infection stages of *H. glycines* to soybean roots (Figure 2.5).

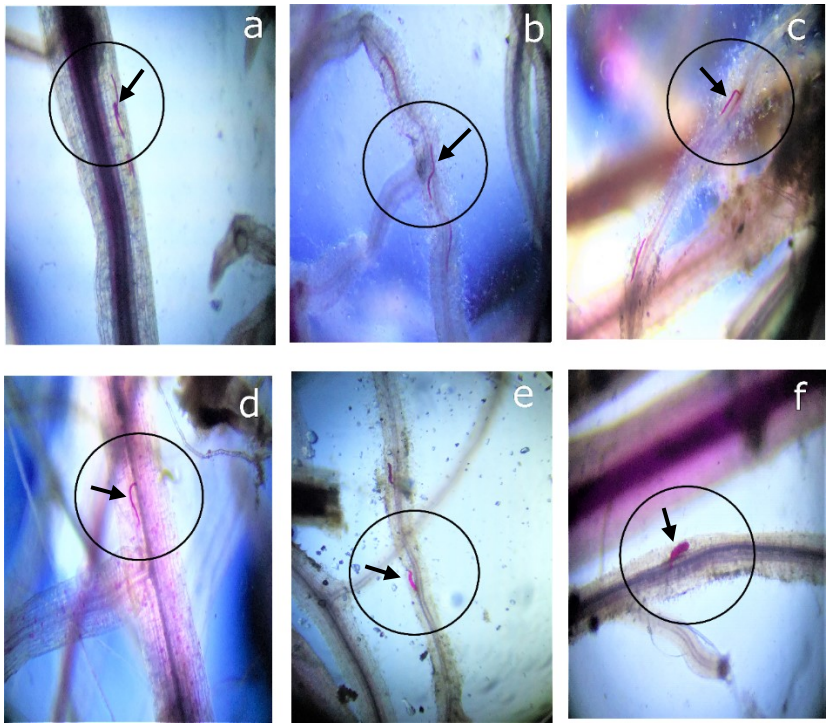

Figure 2.05 *H. glycines* developmental stages in days post infection (dpi), stained with acid fuchsin. a. 1 dpi; b. 2 dpi; c. 3 dpi; d. 4 dpi; e. 5 dpi; f. 6 dpi.

Note: [The pinkish red-colored objects pointed by arrow head (inside the black circles) are acid fuchsin-stained *H. glycines* infecting soybean roots]

The level of effect that *Gm*-CCA1-1 overexpression and RNAi has on *H. glycines* parasitism in *G. max*

The roots of *G. max*$_{[\text{Williams 82/PI 518671}]}$ that are overexpressing the central clock component gene *Gm*-CCA1-1 have shown suppression of parasitism in the susceptible cultivar as measured by the FI. In a complimentary approach an RNAi construct of *Gm*-CCA1-1 engineered into the root of resistant cultivar *G. max*$_{[\text{Peking/PI548402}]}$ is shown to have increased the number of females as measured by the FI. The FI analysis has demonstrated that *Gm*-CCA1-1-OE in *G. max*$_{[\text{William 82/PI 518671}]}$ has reduced the FI significantly compared to control population in *G. max*$_{[\text{Williams 82/PI 518671}]}$ (Figure 2.6).

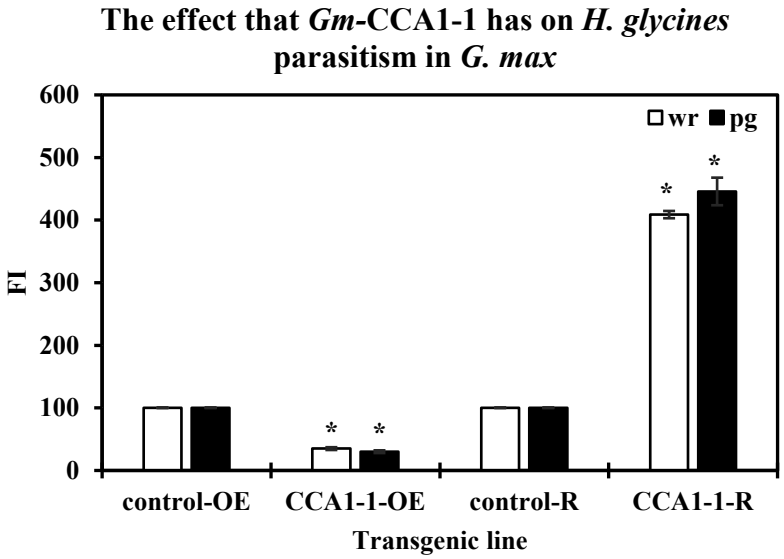

Figure 2.06 The effect on *H. glycines* parasitism of *Gm*-CCA1-1-OE and *Gm*-CCA1-1-RNAi.

Note: The calculated FI for the cysts per whole root (wr) and cyst per gram (pg). (*) denotes $p < 0.05$, statistically significant using Mann-Whitney-Wilcoxon Rank Sum Test. The experimental error represented by bar is standard error.

The RNAi approach has been used in the resistant cultivar *G. max*[Peking/PI 548402]. Similar to the *Gm*-CCA1-1-OE plants, RNAi plants have been selected with the eGFP reporter. Upon 30 days of infection, cysts have been extracted and analyzed for the effect *Gm*-CCA1-1-RNAi suppression had on parasitism through the FI analysis. The *G. max*[Peking/PI 548402] undergoing RNAi for *Gm*-CCA1-1 has resulted in an increase in the FI by two-fold in whole root (wr) as well as per gram (pg) of root compared to control plants (Figure 2.6).

The expression of *Gm*-CCA1-1 in uninfected and infected OE lines as compared to control

Entrained in a 12 hours light and 12 hours dark photoperiod (LD 12:12), the levels of *Gm*-CCA1-1 mRNA have been measured. Figure 2.4 shows that *Gm*-CCA1-1 is

expressed rhythmically, with peak levels occurring around 4 hours after dusk (at around 8:00 PM) of each day. The difference in the expression pattern of *Gm*-CCA1-1 among infected and non-infected OE lines shows that the peaks for the *Gm*-CCA1-1 are slightly lower in infected than non-infected plants (Figure 2.7). However, they are still much higher than the pRAP15-control plants as shown in earlier Figure 2.3.

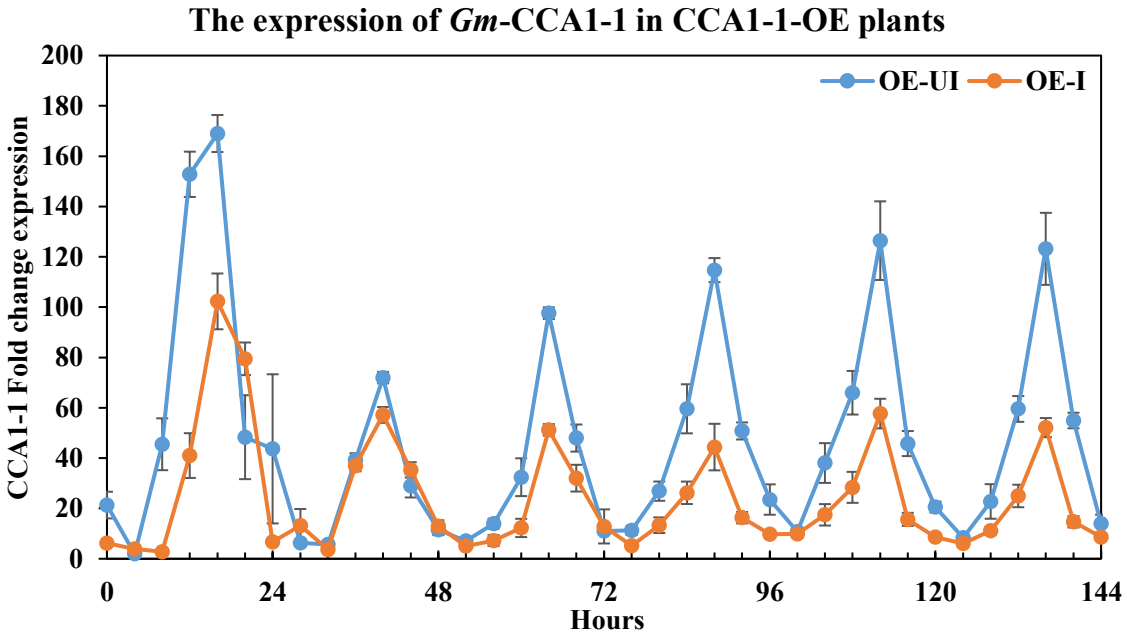

Figure 2.07 Quantitative PCR for the *Gm*-CCA1-1 gene in OE lines. The x-axis depicts the time point that the RNA samples have been isolated from genetically engineered root tissue. The y-axis depicts the relative fold change in expression as compared to a control. *Gm*-CCA1-1-OE lines uninfected (OE-UI), *Gm*-CCA1-1-OE lines infected (OE-I). Bars are standard error.

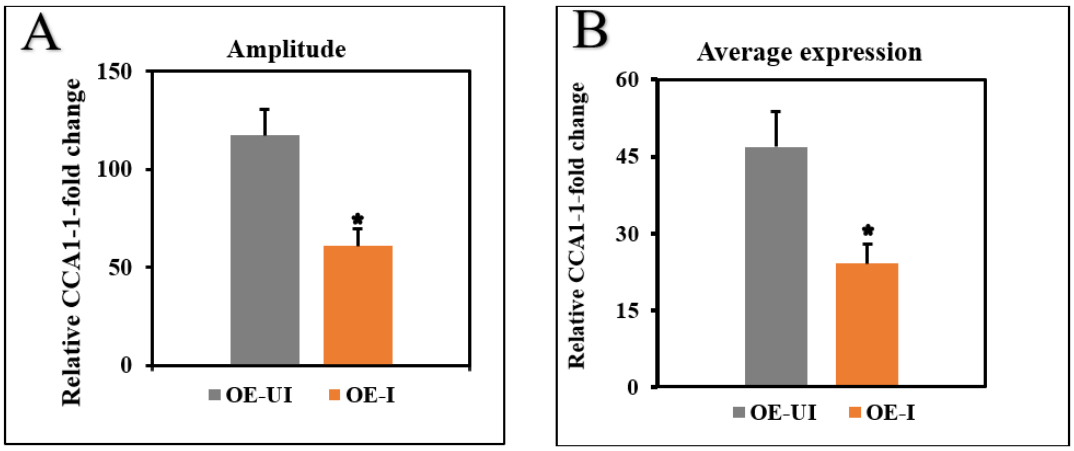

Figure 2.08 The amplitude (A) and average expression (B) of relative *Gm*-CCA1-1 fold change is lower in *Gm*-CCA1-1-OE line infected (OE-I) than *Gm*-CCA1-1-OE line uninfected (OE-UI).

Note: Bars are standard error, (*) represents statistically significant $p<0.05$, determined using student t-test. This experiment has been repeated three times with similar results.

The overexpression of *Gm*-CCA1-1, that has been carried out in *G. max*[William 82/PI 518671], has shown that the *Gm*-CCA1-1 expression pattern as rhythms up to the conclusion of the experiment at 144 hours in both uninfected and infected plant roots. In Figure 2.8 (A) and 2.8 (B), bar graphs represent the estimates of amplitude and average expression of *Gm*-CCA1-1 among SCN *Gm*-CCA1-1-OE-I and *Gm*-CCA1-1-OE-UI lines, respectively.

Expression of *Gm*-CCA1-1 in uninfected and infected RNAi lines as compared to control

The endogenous *Gm*-CCA1-1 gene expression has been analyzed in *Gm*-CCA1-1-RNAi plants grown in LD 12:12 photoperiod cycles. The expression of the *Gm*-CCA1-1 gene had remained consistently lower in *Gm*-CCA1-1-RNAi plants. A slight increase in *Gm*-CCA1-1 transcript levels have been observed among infected roots in comparison to the non-infected *Gm*-CCA1-1 RNAi soybean plants (Figure 2.9).

The reduced levels of *Gm*-CCA1-1 gene expression among the infected, in comparison to the non-infected *Gm*-CCA1-1-OE lines, suggests that the expression of the endogenous *Gm*-CCA1-1 gene is being repressed in infected plants. This outcome could be due to the possibility that it functions in a negative autoregulatory feedback loop governing the expression of *Gm*-CCA1-1 gene (Wang & Tobin, 1998).

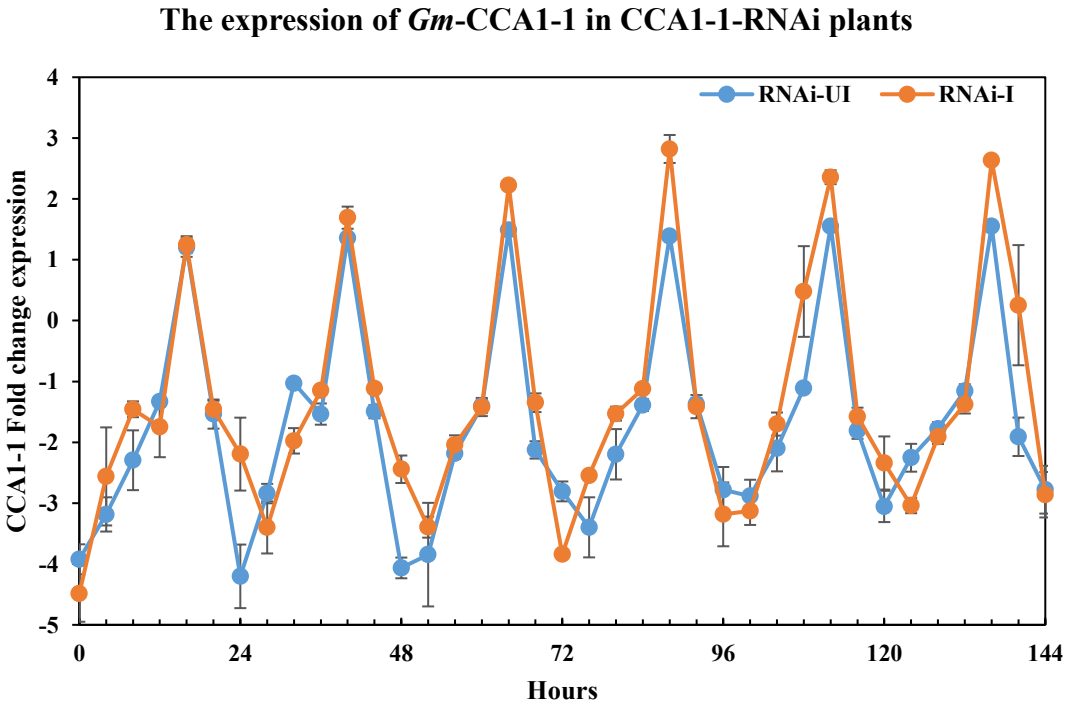

Figure 2.09 Quantitative PCR for *Gm*-CCA1-1 gene in the RNAi lines. The x-axis depicts the time point that the RNA samples have been isolated from the genetically engineered root tissue. The y-axis depicts the relative fold change in expression as compared to a control. *Gm*-CCA1-1-RNAi lines uninfected (RNAi-UI), *Gm*-CCA1-1-RNAi lines infected (RNAi-I). Bars are standard error.

Similar to the results found in the Gm-CCA1-1-OE plants, the difference in the expression pattern of *Gm*-CCA1-1 among infected and non-infected RNAi lines shows

that the peaks for the *Gm*-CCA1-1 are slightly more leveled off in infected than non-infected plants. However, they are still lower than the pRAP17-control plants as shown in earlier Figure 2.4.

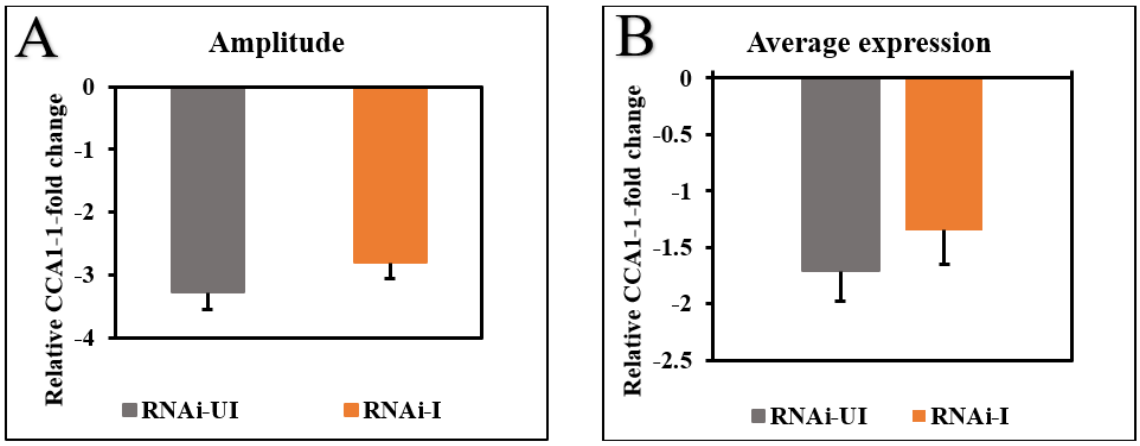

Figure 2.10 The amplitude (A) and average expression (B) of relative *Gm*-CCA1-1-fold change are relatively higher in *Gm*-CCA1-1-RNAi line infected (RNAi-I) than *Gm*-CCA1-1-RNAi line uninfected (RNAi-UI).

Note: Bars are standard error, (*) represents statistically significant $p<0.05$, determined using student t-test. This experiment has been repeated three times with similar results.

The RNAi method of gene silencing has been used with the pRAP17 construct of *Gm*-CCA1-1 in the *G. max*[Peking/PI 548402] cultivar. In Figure 2.10 (A) and 2.10 (B), bar graphs represent the estimates of amplitude and average expression of *Gm*-CCA1-1 among *H. glycines* infected RNAi (RNAi-I) and uninfected RNAi line (RNAi-UI) lines, respectively. Both the amplitude and average expression of *Gm*-CCA1 have been found to be slightly less suppressed in infected than uninfected plant roots, but not to a statistically significant level. The results indicate that *H. glycines* infection has decreased the periodicity of *Gm*-CCA1-1 expression with the consequence of an increased FI.

The effect that the other clock component genes have on *H. glycines* parasitism in *G. max*

In order to analyze the effect of other core component of clock oscillator genes on parasitism, the engineered plants have been allowed to undergo the process of infection for 35 days. The cysts have been extracted and analyzed for the FI as presented earlier for *Gm*-CCA1-1 (Figure 2.6). The control in each OE experiment has more than 10 plants engineered with the empty pRAP15 vector in *G. max*$_{[\text{Williams 82/PI 518671}]}$. In contrast, the control for RNAi of each clock gene has been *G. max*$_{[\text{Peking/PI 548402}]}$ expressing the empty pRAP17 vector construct. The FI analysis demonstrates that *Gm*-TOC1-1-OE, *Gm*- GI-1-OE and *Gm*-CO-4-OE in *G. max*$_{[\text{William 82/PI518671}]}$ has reduced the FI significantly in both the whole root count as well as per gram of root (Figure 2.11), (Figure 2.12) and (Figure 2.13) compared to control population in *G. max*$_{[\text{William 82/PI518671}]}$.

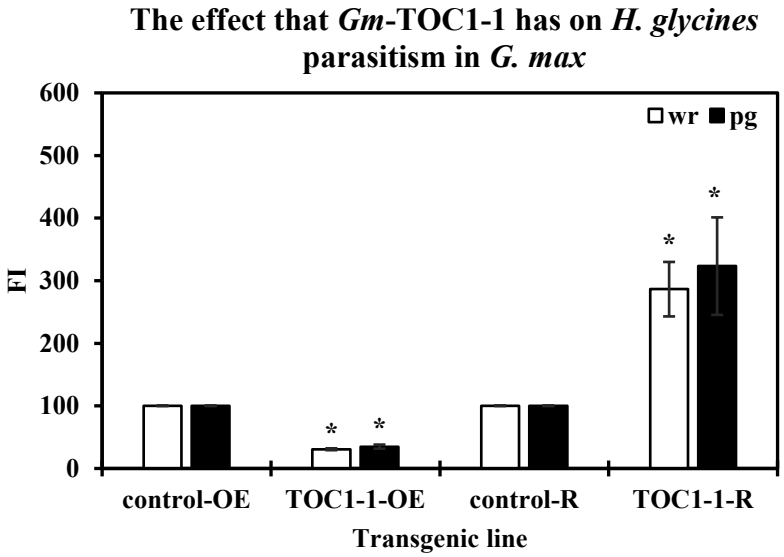

Figure 2.11 The TOC1-1 functions in defense to *H. glycines* as calculated by the FI for *Gm*-TOC1-1-OE and *Gm*-TOC1-1-RNAi lines as compared to the controls.

Note: The controls is set to a FI of 100. The calculated FI for the cysts per whole root (wr) and cyst per gram (pg). (*) denotes $p < 0.05$, statistically significant using Mann-Whitney-Wilcoxon Rank Sum Test. The experimental error represented by bar is standard error.

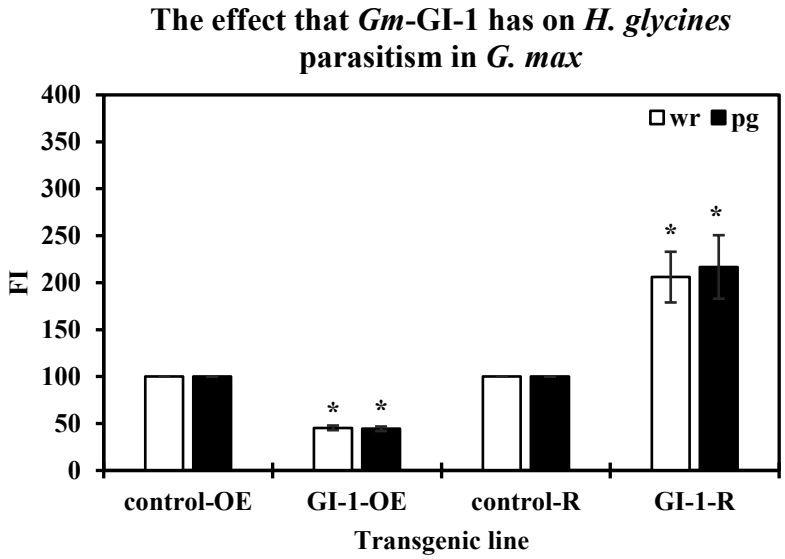

Figure 2.12 The GI-1 functions in defense to *H. glycines* as calculated by the FI for *Gm*-GI-1-OE and *Gm*-GI-1-RNAi lines as compared to the controls.

Note: The controls is set to a FI of 100. The calculated FI for the cysts per whole root (wr) and cyst per gram (pg). (*) denotes $p < 0.05$, statistically significant using Mann-Whitney-Wilcoxon Rank Sum Test. The experimental error represented by bar is standard error.

The RNAi constructs of other clock components have led to an increase in the FI (Figure 2.11, 2.12, 2.13). In these experiments, cysts have been extracted and analyzed for the effect that RNAi has on parasitism through FI analysis. The *G. max*$_{[Peking/PI\ 548402]}$ undergoing RNAi for *Gm*-TOC1-1 has resulted in an increased FI by 2.8 fold in whole root (wr) and 3.2 fold across per gram of the roots (pg) as compared to control plants (Figure 2.11). Similarly, the RNAi of *Gm*-GI-1 and *Gm*-CO-4 in *G. max*$_{[Peking/PI\ 548402]}$ has shown an increase in FI of 2.0 fold (wr), 2.1 fold (pg) (Figure 2.12) and 2.6 fold (wr) and 3.4 fold (pg) (Figure 2.13), respectively, as compared to the controls.

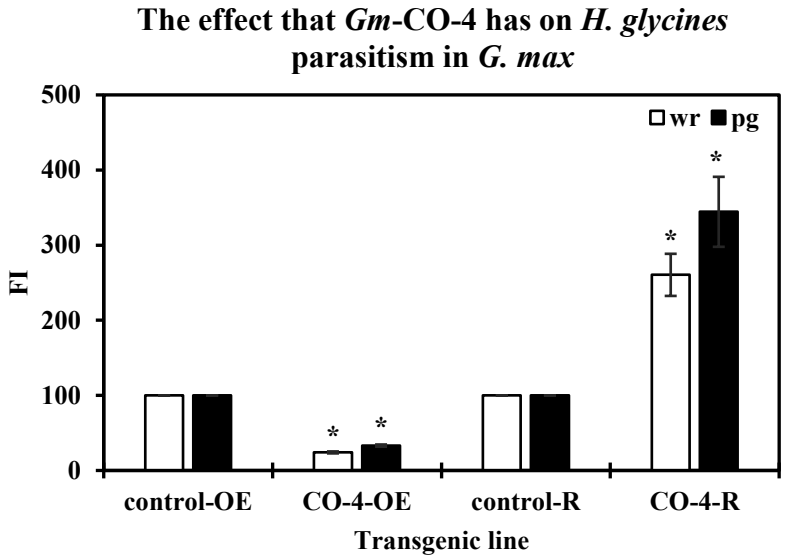

Figure 2.13 The *Gm*-CO-4 functions in defense to *H. glycines* calculated by the FI for *Gm*-CO-4-OE and *Gm*-CO-4-RNAi lines as compared to the controls.

Note: The controls is set to a FI of 100. The calculated FI for the cysts per whole root (wr) and cyst per gram (pg). (*) denotes $p < 0.05$, statistically significant using Mann-Whitney-Wilcoxon Rank Sum Test. The experimental error represented by bar is standard error.

Discussion

Multiple positive and negative factors comprise the circadian networks that interlock in an autoregulatory organization (Bell-Pedersen et al., 2005; Wijnen & Young, 2006). In *A. thaliana*, there is reciprocal regulation between the MYB transcription factor CCA1 and TOC1 (Alabadí et al., 2001). Along with other oscillators, these main circadian components regulate different metabolic, physiological and signaling pathways, anticipating environmental changes such as adjustments with exogenous day-light condition, biotic/abiotic stresses and even cross-talk with defense genes during likely pathogen attack (Suarez-Lopez et al., 2001; Dixon et al., 2011; Helfer et al., 2011; Sawa

& Kay, 2011; Wang et al., 2011; Lai et al., 2012; Zhang et al., 2013; Yoshida et al., 2014).

The role of CCA1 and other central oscillator components, such as TOC1, ELF3, GI, CO and CCA1 HIKING EXPEDITION (CHE) have been well established in their defense roles affecting stomatal activity in leaves (Suarez-Lopez et al., 2001; Legnaioli et al., 2009; Bhardwaj et al., 2011; Sawa & Kay, 2011). There might be the involvement of these components in the stomatal-independent immunity conferring resistance capability to other plant body organs such as the shoot and root systems as systematic immune responses. Our results of the functional effect of clock oscillator genes against root nematodes suggest that, collectively, clock oscillator enhances the resistance against biotrophic pathogen such as *H. glycines* in the root system as well.

CCA1 also acts as a positive integrator that interconnects clock and defense pathways against biotrophic pathogens (Griebel & Zeier, 2008; Wang et al., 2011). CHE, a central component of circadian clock, has been found to be involved in inducing isochorismate synthase 1 (ICS1) and SA synthesis associated genes *PHYTOALEXIN-DEFICIENT 4* (*PAD4*) and *ENHANCED DISEASE SUSCEPTIBILITY 1* (*EDS1*) (Zheng et al., 2015). Because SA induces production of NPR1 and PR proteins, it is believed that SA is involved in downstream transcriptional expression of secretory pathway conferring vesicle transport mediated defenses against a broad spectrum of pathogens (Malamy et al., 1990; Yalpani et al., 1991; Wang et al., 2005; Matsye et al. 2012; Pant et al., 2014; Sharma et al. 2016). CHE belongs to a transcription factor (TF) family that not only binds to the CCA1 promotor fragment as a repressor of CCA1, but also binds to the promoter of ICS1 as an activator, correlating with the increase in expression of ICS1 and SA levels

both locally and systemically during pathogen attack (Wildermuth et al., 2002; Strawn et al., 2007; Pruneda-Paz et al., 2009; Zheng et al., 2015).

To further characterize the role of CCA1 in defense against plant biotrophic root pathogens (e.g. *H. glycines*), the expression level of *Gm*-CCA1-1 in *Gm*-CCA1-1-OE and *Gm*-CCA1-1-RNAi plants with respective controls has revealed a significant change in its expression. The amplitude and average expression level of *Gm*-CCA1-1 has been reduced more in the infected plant than uninfected plant roots among the *Gm*-CCA1-1-OE lines. However, no significant change in amplitude and expression level has been observed among the *Gm*-CCA1-1-RNAi lines. Since TFs (e.g. CHE) that bind to the promoter of CCA1 results in the dampening of its expression level its binding also induces ICS1 and SA accumulation upon pathogen infection, CCA1 could be involved in localized or systemic immune responses with multiple TFs allowing plants to anticipate pathogen attack at specific time of the day (Zhang et al., 2013; Wang et al., 2015; Zheng et al., 2015).

The levels of mRNA of *Gm*-CCA1-1 in both *Gm*-CCA1-1-OE and *Gm*-CCA1-1-RNAi lines cycled in light-dark cycles, peak in the late day (Figure 2.7 and Figure 2.9). Notably, the amplitude and average expression level has been observed to be decreased in infected roots as compared to uninfected roots (Figure 2.8 and Figure 2.10). Our study reinforces results of a recent study on human tumor cells (Filipski et al., 2005). In that analysis, the amplitude and overall expression of human circadian genes are repressed in tumor cells (Filipski et al., 2005). Furthermore, it has been recently gaining a great deal of attention that fusion and accumulation of cells progressing towards tumor development, even cancer through genetic alterations and chromosomal instability among

various other factors in animal tissues, changes the expression amplitude of clock genes (Yokota, 2000; Lu & Kang, 2009; Seyfried & Huysentruyt, 2013; Bastida-Ruiz et al., 2016). While spanning great evolutionary distances (animals-plant divergence) and pathosystems (animal tumor vs. nematode-induced syncytium), such formation of the SCN-induced syncytial cell might relate to animal tumor cell formation through the basic and ubiquitous altered circadian rhythms. Recent studies have demonstrated circadian clock components being involved in PAMP-triggered defense responses as well as R-gene mediated immune responses against biotrophic pathogens (Wang et al., 2011; Zhang et al., 2013). Moreover, both pathogenic infection and treatment with flg22 that mimics PAMP, could induce defense responses in plants with altered circadian rhythm and shortened period of CCA1 expression (Zhang et al., 2013).

Our findings of lower amplitude and average expression level of *Gm*-CCA1-1 among infected than uninfected plant roots, but still higher than controls, clearly demonstrate that the expression of a clock component has been altered during the infection process of *H. glycines*. A disrupted circadian rhythm might be a significant consequence of infection as clock components take part in global transcript regulation including regulating defense genes as well. In order to correlate and identify cross talk between clock component and defense genes, plant-pathogen interaction under light/dark (LD) as well as constant light (LL) could be performed simultaneously to separate genes solely regulated by clock but not by light.

Clock components and defense connections are vast in living cells. An integrative study of biological, physiological, biochemical and molecular approaches are a must in order to understand plant-pathogen interaction and role of circadian in immunity. A few

studies have been done, but have been restricted to the model plant *A. thaliana*. Our study of clock genes in *G. max* in relation to *H. glycines* infection could help to determine and predict the nature of the cross talk occurring between the circadian clock and defense gene expression. However, a broad and detailed genome-wide analysis along with biological approaches coupled with biochemical study could be helpful to obtain meaningful information regarding vast circadian network. Even, mathematical modelling could be the key in unravelling the interconnected loops of circadian clock and its components and possible involvement in plant immune responses along with constitutive rhythm activities.

References

Alabadí, D., Oyama, T., Yanovsky, M. J., Harmon, F. G., Más, P., & Kay, S. A. (2001). Reciprocal Regulation Between TOC1 and LHY/CCA1 Within the Circadian Clock. *Science*, *293*(5531), 880 LP-883. Retrieved from http://science.sciencemag.org/content/293/5531/880.abstract

Bastida-Ruiz, D., Van Hoesen, K., & Cohen, M. (2016). The dark side of cell fusion. *International Journal of Molecular Sciences*, *17*(5). https://doi.org/10.3390/ijms17050638

Bell-Pedersen, D., Cassone, V. M., Earnest, D. J., Golden, S. S., Hardin, P. E., Thomas, T. L., & Zoran, M. J. (2005). Circadian rhythms from multiple oscillators: lessons from diverse organisms. *Nature Reviews Genetics*, *6*, 544. Retrieved from http://dx.doi.org/10.1038/nrg1633

Bhardwaj, V., Meier, S., Petersen, L. N., Ingle, R. A., & Roden, L. C. (2011). Defence responses of *Arabidopsis thaliana* to infection by *Pseudomonas syringae* are regulated by the circadian clock. *PLoS ONE*, *6*(10), 1–8. https://doi.org/10.1371/journal.pone.0026968

Brown, S. A. (2014). Circadian clock-mediated control of stem cell division and differentiation: beyond night and day. *Development*, *141*(16), 3105–3111. https://doi.org/10.1242/dev.104851

Bybd, D. W., Kirkpatrick, T., Barker, K. R., & Barker, K. R. (1983). An improved technique for clearing and staining plant tissues for detection of nematodes. *Journal of Nematology*, *15*(1), 142–143. Retrieved from http://www.ncbi.nlm.nih.gov/pubmed/19295781%5Cnhttp://www.pubmedcentral.nih.gov/articlerender.fcgi?artid=PMC2618249

Cao, H., Bowling, S. A., & Gordon, A. S. (1994). Characterization of an *Arabidopsis* Mutant That 1 s Nonresponsive to lnducers of Systemic Acquired Resistance. *The Plant Cell*, *6*(November), 1583–1592. https://doi.org/10.1105/tpc.6.11.1583

Chandra-Shekara, A. C., Gupte, M., Navarre, D., Raina, S., Raina, R., Klessig, D., & Kachroo, P. (2006). Light-dependent hypersensitive response and resistance signaling against Turnip Crinkle Virus in *Arabidopsis*. *Plant Journal*, *45*(3), 320–334. https://doi.org/10.1111/j.1365-313X.2005.02618.x

Colgrove, A. L., & Niblack, T. L. (2008). Correlation of Female Indices From Virulence Assays on Inbred Lines and Field Populations of *Heterodera glycines*. *Journal of Nematology*, *40*(1), 39–45. Retrieved from http://journals.fcla.edu/jon/article/view/67762%5Cnhttp://www.ncbi.nlm.nih.gov/pmc/articles/PMC2586527

Covington, M. F., Maloof, J. N., Straume, M., Kay, S. A., & Harmer, S. L. (2008). Global transcriptome analysis reveals circadian regulation of key pathways in plant growth and development. *Genome Biology*, *9*(8). https://doi.org/10.1186/gb-2008-9-8-r130

Dixon, L. E., Knox, K., Kozma-Bognar, L., Southern, M. M., Pokhilko, A., & Millar, A. J. (2011). Temporal repression of core circadian genes is mediated through EARLY FLOWERING 3 in Arabidopsis. *Current Biology*, *21*(2), 120–125. https://doi.org/10.1016/j.cub.2010.12.013

Dodd, A. N., Salathia, N., Hall, A., Kévei, E., Tóth, R., Nagy, F., … Webb, A. A. R. (2005). Plant Circadian Clocks Increase Photosynthesis, Growth, Survival, and Competitive Advantage. *Science*, *309*(5734), 630 LP-633. Retrieved from http://science.sciencemag.org/content/309/5734/630.abstract

Doyle, M. R., Davis, S. J., Bastow, R. M., McWatters, H. G., Kozma-Bognar, L., Nagy, F., … Amasino, R. M. (2002). The ELF4 gene controls circadian rhythms and flowering time in *Arabidopsis thaliana*. *Nature*, *419*(6902), 74–77. https://doi.org/10.1038/nature00955.1.

Dunlap, J. C. (1999). Molecular bases for circadian clocks. *Cell*, *96*(2), 271–290. https://doi.org/10.1016/S0092-8674(00)80566-8

Evrard, A., Ndatimana, T., & Eulgem, T. (2009). FORCA, a promoter element that responds to crosstalk between defense and light signaling. *BMC Plant Biology*, *9*, 1–13. https://doi.org/10.1186/1471-2229-9-2

Ferre, E., Harmer, S., Harmon, F., & Yanovsky, M. (2005). Overlapping and Distinct Roles of PRR7 and PRR9 in the *Arabidopsis* Circadian Clock. *Cutis*, *15*(1), 47–54. https://doi.org/10.1016/j

Filipski, E., Innominato, P. F., Wu, M. W., Li, X. M., Iacobelli, S., Xian, L. J., & Lévi, F. (2005). Effects of light and food schedules on liver and tumor molecular clocks in mice. *Journal of the National Cancer Institute*, *97*(7), 507–517. https://doi.org/10.1093/jnci/dji083

Fukushima, A., Kusano, M., Nakamichi, N., Kobayashi, M., Hayashi, N., Sakakibara, H., … Saito, K. (2009). Impact of clock-associated *Arabidopsis* pseudo-response regulators in metabolic coordination. *Proceedings of the National Academy of Sciences*, *106*(17), 7251 LP-7256. Retrieved from http://www.pnas.org/content/106/17/7251.abstract

Genoud, T., Buchala, A. J., Chua, N. H., & Métraux, J. P. (2002). Phytochrome signalling modulates the SA-perceptive pathway in *Arabidopsis*. *Plant Journal*, *31*(1), 87–95. https://doi.org/10.1046/j.1365-313X.2002.01338.x

Gibon, Y., Bläsing, O. E., Palacios-Rojas, N., Pankovic, D., Hendriks, J. H. M., Fisahn, J., … Stitt, M. (2004). Adjustment of diurnal starch turnover to short days: Depletion of sugar during the night leads to a temporary inhibition of carbohydrate utilization, accumulation of sugars and post-translational activation of ADP-glucose pyrophosphorylase in the followin. *Plant Journal*, *39*(6), 847–862. https://doi.org/10.1111/j.1365-313X.2004.02173.x

Golden, A. M., Epps, J. M., Riggs, R. D., Duclos, L. A., Fox, J. A., & Bernard, R. L. (1970). Terminology and identity of infraspecific forms of the soybean cyst nematode (*Heterodera glycines*). *Plant Disease Reporter*.

Golinowski, W., Sobczak, M., Kurek, W., & Grymaszewska, G. (1997). The Structure of Syncytia BT - Cellular and Molecular Aspects of Plant-Nematode Interactions. In C. Fenoll, F. M. W. Grundler, & S. A. Ohl (Eds.) (pp. 80–97). Dordrecht: Springer Netherlands. https://doi.org/10.1007/978-94-011-5596-0_7

Graf, A., Schlereth, A., Stitt, M., & Smith, A. M. (2010). Circadian control of carbohydrate availability for growth in Arabidopsis plants at night. *Proc Natl Acad Sci U S A*, *107*(20), 9458–9463. https://doi.org/10.1073/pnas.0914299107/-/DCSupplemental.www.pnas.org/cgi/doi/10.1073/pnas.0914299107

Green, R. M., Tingey, S., Wang, Z. ., & Tobin E.M. (2002). Circadian Rhythms Confer a Higher Level of Fitness to *Arabidopsis* Plants. *Plant Physiology*, *129*(2), 576–584. https://doi.org/10.1104/pp.004374

Griebel, T., & Zeier, J. (2008). Light Regulation and Daytime Dependency of Inducible Plant Defenses in Arabidopsis: Phytochrome Signaling Controls Systemic Acquired Resistance Rather Than Local Defense. *Plant Physiology*, *147*(2), 790–801. https://doi.org/10.1104/pp.108.119503

Harmer, S. L., Hogenesch, J. B., Straume, M., Chang, H.-S., Han, B., Zhu, T., … Kay, S. A. (2000). Orchestrated Transcription of Key Pathways in Arabidopsis by the Circadian Clock. *Science*, *290*(5499), 2110 LP-2113. Retrieved from http://science.sciencemag.org/content/290/5499/2110.abstract

Hazen, S. P., Naef, F., Quisel, T., Gendron, J. M., Chen, H., Ecker, J. R., … Kay, S. A. (2009). Exploring the transcriptional landscape of plant circadian rhythms using genome tiling arrays. *Genome Biology*, *10*(2). https://doi.org/10.1186/gb-2009-10-2-r17

Hazen, S. P., Schultz, T. F., Pruneda-Paz, J. L., Borevitz, J. O., Ecker, J. R., & Kay, S. A. (2005). LUX ARRHYTHMO encodes a Myb domain protein essential for circadian rhythms. *Proceedings of the National Academy of Sciences of the United States of America*, *102*(29), 10387–10392. https://doi.org/10.1073/pnas.0503029102

Helfer, A., Nusinow, D. A., Chow, B. Y., Gehrke, A. R., Bulyk, M. L., & Kay, S. A. (2011). LUX ARRHYTHMO encodes a nighttime repressor of circadian gene expression in the *Arabidopsis* core clock. *Current Biology*, *21*(2), 126–133. https://doi.org/10.1016/j.cub.2010.12.021

Huang, W., Pérez-García, P., Pokhilko, A., Millar, A. J., Antoshechkin, I., Riechmann, J. L., & Mas, P. (2012). Mapping the Core of the *Arabidopsis* Circadian Clock Defines the Network Structure of the Oscillator. *Science*, *336*(6077), 75 LP-79. Retrieved from http://science.sciencemag.org/content/336/6077/75.abstract

Humphry, M., Bednarek, P., Kemmerling, B., Koh, S., Stein, M., Gobel, U., … Panstruga, R. (2010). A regulon conserved in monocot and dicot plants defines a functional module in antifungal plant immunity. *Proceedings of the National Academy of Sciences*, *107*(50), 21896–21901. https://doi.org/10.1073/pnas.1003619107

Iwasaki, H., & Kondo, T. (2000). The current state and problems of circadian clock studies in cyanobacteria. *Plant and Cell Physiology*, *41*(9), 1013–1020. https://doi.org/10.1093/pcp/pcd024

Jenkins, W. R. (1964). A rapid centrifugal-flotation technique for separating nematodes from soil. *Plant Disease Reporter*, *48*(9), 692.

Johansson, O. N., Fantozzi, E., Fahlberg, P., Nilsson, A. K., Buhot, N., Tör, M., & Andersson, M. X. (2014). Role of the penetration-resistance genes PEN1, PEN2 and PEN3 in the hypersensitive response and race-specific resistance in *Arabidopsis thaliana*. *Plant Journal*, *79*(3), 466–476. https://doi.org/10.1111/tpj.12571

Jones, M. G. K. (1981). Host cell responses to endoparasitic nematode attack: structure and function of giant cells and syncytia*. *Annals of Applied Biology*, *97*(3), 353–372. https://doi.org/10.1111/j.1744-7348.1981.tb05122.x

Klink, V. P., Alkharouf, N., MacDonald, M., & Matthews, B. (2005). Laser Capture Microdissection (LCM) and expression analyses of *Glycine max* (soybean) syncytium containing root regions formed by the plant pathogen *Heterodera glycines* (soybean cyst nematode). *Plant Molecular Biology*, *59*(6), 965–979. https://doi.org/10.1007/s11103-005-2416-7

Klink, V. P., Kim, K. H., Martins, V., MacDonald, M. H., Beard, H. S., Alkharouf, N. W., … Matthews, B. F. (2009). A correlation between host-mediated expression of parasite genes as tandem inverted repeats and abrogation of development of female *Heterodera glycines* cyst formation during infection of *Glycine max*. *Planta*, *230*(1), 53–71. https://doi.org/10.1007/s00425-009-0926-2

Lai, A. G., Doherty, C. J., Mueller-Roeber, B., Kay, S. A., Schippers, J. H. M., & Dijkwel, P. P. (2012). CIRCADIAN CLOCK-ASSOCIATED 1 regulates ROS homeostasis and oxidative stress responses. *Proceedings of the National Academy of Sciences*, *109*(42), 17129–17134. https://doi.org/10.1073/pnas.1209148109

Legnaioli, T., Cuevas, J., & Mas, P. (2009). TOC1 functions as a molecular switch connecting the circadian clock with plant responses to drought. *EMBO Journal*, *28*(23), 3745–3757. https://doi.org/10.1038/emboj.2009.297

Livak, K. J., & Schmittgen, T. D. (2001). Analysis of Relative Gene Expression Data Using Real-Time Quantitative PCR and the 2−ΔΔCT Method. *Methods*, *25*(4), 402–408. https://doi.org/https://doi.org/10.1006/meth.2001.1262

Lu, X., & Kang, Y. (2009). Cell fusion as a hidden force in tumor progression. *Cancer Research*, *69*(22), 8536–8539. https://doi.org/10.1158/0008-5472.CAN-09-2159

Lu, Y., Gehan, J. P., & Sharkey, T. . (2005). Daylength and Circadian Effects on Starch Degradation and Maltose Metabolism. *Plant Physiology*, *138*(4), 2280–2291. https://doi.org/10.1104/pp.105.061903

Mahalingam, R., & Skorupska, H. T. (1996). Cytological expression of early response to infection by *Heterodera glycines* Ichinohe in resistant P1 437654 soybean. *Genome*, *39*, 986–998.

Malamy, J., Carr, J. P., Klessig, D. F., & Raskin, I. (1990). Salicylic Acid: A Likely Endogenous Signal in the Resistance Response of Tobacco to Viral Infection. *Science*, *250*(4983), 1002 LP-1004. Retrieved from http://science.sciencemag.org/content/250/4983/1002.abstract

Matsye, P. D., Lawrence, G. W., Youssef, R. M., Kim, K. H., Lawrence, K. S., Matthews, B. F., & Klink, V. P. (2012). The expression of a naturally occurring, truncated allele of an α-SNAP gene suppresses plant parasitic nematode infection. *Plant Molecular Biology*, *80*(2), 131–155. https://doi.org/10.1007/s11103-012-9932-z

Matthews, B. F., Beard, H., MacDonald, M. H., Kabir, S., Youssef, R. M., Hosseini, P., & Brewer, E. (2013). Engineered resistance and hypersusceptibility through functional metabolic studies of 100 genes in soybean to its major pathogen, the soybean cyst nematode. *Planta*, *237*(5), 1337–1357. https://doi.org/10.1007/s00425-013-1840-1

Matthews, B. F., Macdonald, M. H., Thai, V. K., & Tucker, M. L. (2003). Molecular Characterization of Arginine Kinases in the Soybean Cyst Nematode (*Heterodera glycines*). *Journal of Nematology*, *35*(3), 252–258.

McClung, C. R. (2001). Circadian rhythms in plants. *Annual Review of Plant Physiology and Plant Molecular Biology*, *52*(4), 139–162. https://doi.org/10.1105/tpc.106.040980

McNeece, B., Sharma, K., Lawrence, G. W., Lawrence, K. S., & Klink, V. P. (2019). The mitogen activated protein kinase (MAPK) gene family functions as a cohort during the Glycine max defense response to Heterodera glycines. *Plant Physiology and Biochemistry*, 1–19. https://doi.org/https://doi.org/10.1016/j.plaphy.2019.01.018

Mizoguchi, T., Wheatley, K., Hanzawa, Y., Wright, L., Mizoguchi, M., Song, H. R., … Coupland, G. (2002). LHY and CCA1 are partially redundant genes required to maintain circadian rhythms in *Arabidopsis*. *Developmental Cell*, *2*(5), 629–641. https://doi.org/10.1016/S1534-5807(02)00170-3

N. Seyfried, Thomas; C. Huysentruyt, L. (2013). On the Origin of Cancer Metastasis. *Critical Reviews in Oncology*, *18*(1–2), 43–73. https://doi.org/10.1021/nl061786n.Core-Shell

Pant, S. R., Matsye, P. D., McNeece, B. T., Sharma, K., Krishnavajhala, A., Lawrence, G. W., & Klink, V. P. (2014). Syntaxin 31 functions in *Glycine max* resistance to the plant parasitic nematode *Heterodera glycines*. *Plant Molecular Biology*, *85*(1–2), 107–121. https://doi.org/10.1007/s11103-014-0172-2

Pant, S. R., McNeece, B. T., Sharma, K., Niruala, P., Burson, H. E., Lawrence, G. W., & Klink, V. P. (2016). The heterologous expression of a *Glycine max* homolog of NONEXPRESSOR OF PR1 (NPR1) and α-hydroxynitrile glucosidase suppresses parasitism by the root pathogen *Meloidogyne incognita* in *Gossypium hirsutum*. *Journal of Plant Interactions*, *11*(1), 41–52. https://doi.org/10.1080/17429145.2016.1163423

Park, D. H., Somers, D. E., Kim, Y. S., Choy, Y. H., Lim, H. K., Soh, M. S., … Nam, H. G. (1999). Control of Circadian Rhythms and Photoperiodic Flowering by the *Arabidopsis* GIGANTEA Gene. *Science*, *285*(5433), 1579 LP-1582. Retrieved from http://science.sciencemag.org/content/285/5433/1579.abstract

Pruneda-Paz, J. ., Breton, G., Para, A., & Kay, S. A. (2009). A Functional Genomics Approach Reveals CHE as a Component of the *Arabidopsis* Circadian Clock, *583*(October), 1481–1486.

Rawat, R., Takahashi, N., Hsu, P. Y., Jones, M. A., Schwartz, J., Salemi, M. R., … Harmer, S. L. (2011). REVEILLE8 and PSEUDO-REPONSE REGULATOR5 form a negative feedback loop within the *Arabidopsis* circadian clock. *PLoS Genetics*, *7*(3). https://doi.org/10.1371/journal.pgen.1001350

Roden, L. C., & Ingle, R. A. (2009). Lights, Rhythms, Infection: The Role of Light and the Circadian Clock in Determining the Outcome of Plant-Pathogen Interactions. *The Plant Cell Online*, *21*(9), 2546–2552. https://doi.org/10.1105/tpc.109.069922

Roux, M., Schwessinger, B., Albrecht, C., Chinchilla, D., Jones, A., Holton, N., … Zipfel, C. (2011). The *Arabidopsis* Leucine-Rich Repeat Receptor–Like Kinases BAK1/SERK3 and BKK1/SERK4 Are Required for Innate Immunity to Hemibiotrophic and Biotrophic Pathogens. *The Plant Cell*, *23*(6), 2440–2455. https://doi.org/10.1105/tpc.111.084301

Ruts, T., Matsubara, S., Wiese-Klinkenberg, A., & Walter, A. (2012). Aberrant temporal growth pattern and morphology of root and shoot caused by a defective circadian clock in *Arabidopsis thaliana*. *Plant Journal*, *72*(1), 154–161. https://doi.org/10.1111/j.1365-313X.2012.05073.x

Sawa, M., & Kay, S. A. (2011). GIGANTEA directly activates Flowering Locus T in *Arabidopsis thaliana*. *Proceedings of the National Academy of Sciences of the United States of America*, *2011*(28), 11698–11703. https://doi.org/10.1073/pnas.1106771108/-/DCSupplemental.www.pnas.org/cgi/doi/10.1073/pnas.1106771108

Schmitt, D. P., & Shannon, G. (1992). Differentiating Soybean Responses to *Heterodera glycines* Races. *Crop Science*, *32*, 275–277. https://doi.org/10.2135/cropsci1992.0011183X003200010056x

Sharma, K., Pant, S. R., McNeece, B. T., Lawrence, G. W., & Klink, V. P. (2016). Co-regulation of the *Glycine max* soluble N-ethylmaleimide-sensitive fusion protein attachment protein receptor (SNARE)-containing regulon occurs during defense to a root pathogen. *Journal of Plant Interactions*, *11*(1), 74–93. https://doi.org/10.1080/17429145.2016.1195891

Sobczak, M., & Golinowski, W. (2011). Cyst Nematodes and Syncytia BT - Genomics and Molecular Genetics of Plant-Nematode Interactions. In J. Jones, G. Gheysen, & C. Fenoll (Eds.) (pp. 61–82). Dordrecht: Springer Netherlands. https://doi.org/10.1007/978-94-007-0434-3_4

Strawn, M. A., Marr, S. K., Inoue, K., Inada, N., Zubieta, C., & Wildermuth, M. C. (2007). Arabidopsis isochorismate synthase functional in pathogen-induced salicylate biosynthesis exhibits properties consistent with a role in diverse stress responses. *Journal of Biological Chemistry*, *282*(8), 5919–5933. https://doi.org/10.1074/jbc.M605193200

Suarez-Lopez, P., Wheatley, K., Robson, F., Onouchi, H., Valverde, F., & Coupland, G. (2001). *CONSTANS* mediates between the circadian clock and the control of flowering in arabidopsis. *Nature*, *410*(April), 1116–1120.

Van Der Biezen, E. A., Freddie, C. T., Kahn, K., Parker, J. E., & Jones, J. D. G. (2002). Arabidopsis RPP4 is a member of the RPP5 multigene family of TIR-NB-LRR genes and confers downy mildew resistance through multiple signalling components. *Plant Journal*, *29*(4), 439–451. https://doi.org/10.1046/j.0960-7412.2001.01229.x

Veronese, P., Nakagami, H., Bluhm, B., AbuQamar, S., & Chen X. (2006). The Membrane-Anchored BOTRYTIS-INDUCED KINASE1 Plays Distinct Roles in Arabidopsis Resistance to Necrotrophic and Biotrophic Pathogens. *The Plant Cell Online*, *18*(1), 257–273. https://doi.org/10.1105/tpc.105.035576

Wang, D., Weaver, N., Kesarwani, M., & Dong, X. (2005). Induction of Protein Secretory Pathway Is Required for Systemic Acquired Resistance. *Science*, *308*(5724), 1036–1040. https://doi.org/10.1126/science.1108791

Wang, W., Barnaby, J. Y., Tada, Y., Li, H., Tör, M., Caldelari, D., … Dong, X. (2011). Timing of plant immune responses by a central circadian regulator. *Nature*, *470*(7332), 110–115. https://doi.org/10.1038/nature09766

Wang, X., Gao, J., Zhu, Z., Dong, X., Wang, X., Ren, G., … Kuai, B. (2015). TCP transcription factors are critical for the coordinated regulation of ISOCHORISMATE SYNTHASE 1 expression in Arabidopsis thaliana. *Plant Journal*, *82*(1), 151–162. https://doi.org/10.1111/tpj.12803

Wang, Z. Y., & Tobin, E. M. (1998). Constitutive expression of the CIRCADIAN CLOCK ASSOCIATED 1 (CCA1) gene disrupts circadian rhythms and suppresses its own expression. *Cell*, *93*(7), 1207–1217. https://doi.org/10.1016/S0092-8674(00)81464-6

Wijnen, H., & Young, M. W. (2006). Interplay of Circadian Clocks and Metabolic Rhythms. *Annual Review of Genetics*, *40*(1), 409–448. https://doi.org/10.1146/annurev.genet.40.110405.090603

Wildermuth, M. C., Dewdney, J., Wu, G., & Ausubel, F. M. (2002). Isochorismate synthase is required to synthesize salicylic acid for plant defence (vol 414, pg 562, 2001). *Nature*, *414*(6888), 562–565.

Yalpani, N., Silverman, P., Wilson, M. A., Kleier, D. A., & Raskin, I. (1991). Salicylic Acid Is a Systemic Signal and an Inducer of Pathogenesis-Related Proteins in Virus-Infected Tobacco. *The Plant Cell*, *3*(8), 809–818. https://doi.org/10.1105/tpc.3.8.809

Yokota, J. (2000). Tumor progression and metastasis. *Carcinogenesis*, *21*(3), 497–503. https://doi.org/10.1093/carcin/21.3.497

Yoshida, T., Mogami, J., & Yamaguchi-Shinozaki, K. (2014). ABA-dependent and ABA-independent signaling in response to osmotic stress in plants. *Current Opinion in Plant Biology*, *21*, 133–139. https://doi.org/10.1016/j.pbi.2014.07.009

Young, M. W. (1998). The molecular control of circadian behavioral rhythms and their entrainment in Drosophila. *Annual Review of Biochemistry*, *67*, 135–152. https://doi.org/10.1146/annurev.biochem.67.1.135

Zeier, J., Pink, B., Mueller, M., & Berger, S. (2004). Light conditions influence specific defence responses in incompatible plant?pathogen interactions: uncoupling systemic resistance from salicylic acid and PR-1 accumulation. *Planta*, *219*(4), 673–683. https://doi.org/10.1007/s00425-004-1272-z

Zhang, C., Xie, Q., Anderson, R. G., Ng, G., Seitz, N. C., Peterson, T., … Lu, H. (2013). Crosstalk between the Circadian Clock and Innate Immunity in *Arabidopsis*. *PLoS Pathogens*, *9*(6). https://doi.org/10.1371/journal.ppat.1003370

Zheng, X., Zhou, M., Yoo, H., Pruneda-Paz, J. L., Spivey, N. W., Kay, S. A., & Dong, X. (2015). Spatial and temporal regulation of biosynthesis of the plant immune signal salicylic acid. *Proceedings of the National Academy of Sciences*, *112*(30), 9166–9173. https://doi.org/10.1073/pnas.1511182112

CHAPTER III

XYLOGLUCAN-REMODELING XYLOGLUCAN ENDO-TRANSGLYCOSYLASE/ HYDROLASE (XTH) ON *G. MAX* DURING DEFENSE AGAINST THE *H. GLYCINES*

Abstract

Based on prior experiments, the level of *Gm*-XTH43 transcripts are elevated significantly in the cells undergoing resistance to *H. glycines*. The role of *Gm*-XTH43 protein might be involved in re-arranging or re-modelling XyG in an effort to establish a defense process at an otherwise functional feeding site. A high amount of XyG in tightly bound sugar in positively regulated gene expression and low amount in negatively regulated gene expression would confirm that XTH is key component for maintaining XyG chain length and extensibility. Besides XyG amount variation, molecular weights (MWs) of XyG have varied in such a way that *Gm*-XTH43-OE have led to lower molecular mass XyG than control. In contrast, *Gm*-XTH43-RNAi have led to higher molecular mass XyG than control. Such observations indicate an XTH association with cell wall strengthening by XTH-mediated remodeling of the XyG chain in cell wall architecture. However, the weight average MW (WAMW) identified through the gel permeation chromatography (GPC) must be regarded with caution as it might occur that MW sugars are not all XyGs but also multiple polysaccharides organization in the cell wall.

Introduction

The Plant cell wall

The plant body consists of root and shoot systems. After germination from the seed, the first formed plant body is primary plant body. However, most gymnosperms and angiosperms show an increase in the thickness of its body by means of secondary growth that occurs from a lateral meristem called the vascular cambium that produces xylem and phloem among other cell types. Most of the produced living secondary xylem cells rapidly die through targeted programmed cell death that occurs as those same cells deposit secondary cell wall material. The combined processes lead to the production of lignified, woody tissue. At the cellular level, the secondary wall is deposited after primary wall while the cell is increasing in size (Somerville et al., 2004). The plant cell wall is a complex and dynamic frame being a mixture of cellulose, hemicelluloses, pectins, proteins and phenolic compounds. The dry mass of the cell wall is approximately 30% cellulose, 30% hemicellulose and 35% pectin and approximately 1-5% being some structural proteins. Polymers such as cellulose and hemicellulose mostly provide rigidity to the wall while pectin provides fluidity through the gelatinous polysaccharide matrix (Ochoa et al., 2012). Cellulose is the principal component of plant cell wall, while it is found less in secondary wall than primary wall, which mainly determines the wall architecture. Cellulose is a repeating monomer of glucose and polymers that are bundled into micro-fibrils. The cellulose framework of the wall is interlocked by a cross-linked matrix of non-cellulosic polysaccharide molecules, known as hemicelluloses (Somerville et al., 2004; Liu et al., 2007; Scheller & Ulvskov, 2010). Hemicelluloses are polysaccharides that have a (1→4)-linked mono-sugar backbone. Most hemicelluloses

include XyGs, xylans, mannans and glucomannans. XyG is the most principal hemicellulose, composing up to 25% of the cell wall. XyG is linked via hydrogen bonds to the surface of adjacent cellulose microfibrils, thereby, forming a network with cellulose. Such a configuration may limit the extensibility of the cell wall by tethering adjacent micro-fibrils as well as functions such as its significant role in regulating cell enlargement and acting as a load bearing structure (Scheller & Ulvskov, 2010).

XyG structure and occurrence (particularly in soybean)

XyG is a branched polysaccharide having complex structure, with backbone (β1-4)-linked D-glucan, which is the same as cellulose (Hayashi et al., 1994). In addition to glucan backbone, three out of four glucose residues are substituted with α-xylosyl residues attached to the 6-position of β-glucosyl residues, and terminal galactose is attached to the 2-position of xylosyl residues by β-linkage (Umemura & Yuguchi, 2009). In different plants, heterogeneity of XyG occurs from either differences in molecular mass or the distribution of additional branching of galactosyl residues of fucosyl residues (Hayashi, 1989; Vanzin et al., 2002; Hoffman et al., 2005).

According to (Hayashi et al. (1980), two kinds of XyGs (with molecular masses of 180 kDa and 60 kDa) have been obtained from suspension-cultured soybean cells. The methylation and fragmentation analysis with endoglucanases have determined that each XyG is constructed of two kinds of oligosaccharide repeating units, a heptasaccharide (glucose/xylose, 4:3) and nonsaccharide (glucose/xylose/galactose/fucose, 4:3:1;1). Fucosylated subunits are predominant in soybean root XyG which is characteristically similar to bulk of *A. thaliana* root XyG (Pena et al., 2012; Muszyński et al., 2015).

Biosynthesis of XyG

The synthesis of the glucan backbone of XyG is believed to involve cellulose synthase-like family genes (Pauly et al., 2013). Since, the exogenous XyG fails to complex with newly formed cellulose microfibrils in the protoplast wall, the macromolecular organization involves a secretion of polysaccharides on the plasma membrane (Hayashi et al., 1980; Dwivany et al., 2009). Golgi bodies are involved in the synthesis and secretion of non-cellulosic polysaccharides destined for incorporation into the cell wall (Davis et al., 2010). Golgi are known to contain xyloglucan 4-β-glucosyltransferase and 6-α-xylosyltransferase. These enzymes are involved in incorporation of UDP-glucose, UDP-xylose to the XyG chain by concurrent transfer of glucose and xylose during XyG synthesis (Scheible & Pauly, 2004; Sterling et al., 2006). A total synthesis of XyG occurs in Golgi stacks before transport to the cell wall by secretory vesicles (Hayashi, 1989).

According to Gidding et al. (1980), the Golgi apparatus functions not only in the synthesis and export of XyG but also is involved in export of multi-enzyme complexes involved in cellulose synthesis. Such enzymes or other glycoproteins destined for secretion are transferred to Golgi from the endoplasmic reticulum (ER), via transition vesicles (Handford et al., 2006; Zhao & Colley, 2008). The synthesis of the backbone of XyG is believed to occur in the cisternae of the Golgi, while further branching of galactosylation and fucosylation may occur in the medial- and trans- Golgi as XyG matures (Cocuron et al., 2007; Chevalier et al., 2010). Matrix polysaccharides synthesized in the Golgi are transported to plasma membrane and apoplast by the conventional pathway via secretory vesicle (Kim & Brandizzi, 2016). The secretory

vesicle clusters (SVCs) containing the secretory carrier membrane protein mediate polysaccharide secretion not only in exocytosis but also in endocytosis during cell plate formation (Toyooka et al., 2009; Toyooka & Matsuoka, 2009).

Function of XyG

XyG is an important component of primary cell wall. It functions by performing key roles in cell enlargement during growth and also XyG metabolism, including its biosynthesis, remodeling and organization (Jia et al., 2005; Hayashi & Kaida, 2011). Consequently, XyG has a high impact on growth regulation and stress response to biotic/abiotic stresses (Jia et al., 2005; Hayashi & Kaida, 2011). A glucan backbone serves as a tether between cellulose microfibrils, contributing to the load bearing capacity of the cell wall (Takeda et al., 2002). A single XyG chain can adhere to multiple microfibrils via hydrogen bonds along its length, locally penetrating them and fastening the end of the tethers, that property greatly contributes to the cell architecture (Alonso-Simón et al., 2010). The cross-linking by XyG between perpendicular microfibrils (cellulose) may function as bracket linking between the parallel fibrils as beam (Mellerowicz et al., 2008). Therefore, during cell enlargement and during growth, the extension of the cell wall may be due to auxin-induced endo-1,4-β-glucanases functioning to hydrolyze the cross-linked XyG and resulting in the loosening of each cellulose micro-fibrils (Hayashi, 1989). The interaction between XyG and cellulose microfibril shows a greater binding capacity and is dependent on the surface area of the microfibrils. In addition, XyG probably not only binds to the surface of micro-fibrils but is also woven into the amorphous part (Hayashi et al., 1994). That property could be the reason that highly concentrated (24% KOH) is required for the extraction of XyG

(Hayashi & Kaida, 2011). XyG plays both structural and signaling roles and modify polysaccharides or oligosaccharide physical characteristics through their incorporation. A partial hydrolysis of XyG yields apoplastic XyG-derived oligosaccharides (XGOs) involved in modulating plant growth, morphogenesis and signal transduction (Fry, 2010).

XyG re-modeling XTHs [Xyloglucan endo-transglycosylase/hydrolase]

The xyloglucan endo-transglycosylase/hydrolases (XET/XTHs [XTH]) are a family of enzymes that specifically use XyG as a substrate and catalyze XET and/or XTH activities (Cosgrove, 2005). Since, the major structural components of plant cell walls are polysaccharide networks composed of pectins, hemicelluloses and celluloses, XTHs are important for precise arrangement and composition of these components for cell wall formation during growth, development and defense response (Rose et al.,2002; Matsui et al., 2005; Miedes et al., 2011). XTHs which can cut and rejoin XyG chains are considered a key agent regulating cell wall expansion and are also believed to be the enzyme responsible for the incorporation of newly synthesized XyG into the cell wall matrix (Fry et al., 1992; Liu et al., 2007; Genovesi et al., 2008). The role of XTHs has also been implicated in the cell wall degradation necessary for fruit ripening, abscission, cell wall strengthening that takes place during thigmomorphogenesis (Nishitani, 1998).

XTHs may also be involved in reversibly or irreversibly loosening of existing cell wall materials, especially the XyG chain (Thompson & Fry, 2001). In support of this hypothesis, XET activity is often related with growth. Moreover, XyG turnover is associated with rapid cell expansion such that XTH gene expression becomes highly induced in rapidly elongating tissues (Cho et al., 2006; Sasidharan & Pierik, 2010). XTHs can rearrange existing cell wall materials, in which pair of XyG molecules are catalyzed

for transglycosylation, both of partners having been previously hydrogen bonded to cellular microfibrils. Such reversible transglycosylation is a significant mechanism for wall loosening or strengthening during incremental wall expansion and certainly restores original wall strength (Fry, 1989; Fry et al., 1992; Nishitani, 1998). In addition, XTHs may also catalyze the integration of newly synthesized XyG into the cell wall through XET activity. In the meristem, the integration of XyG into the cell wall accompanies a process called vacuolation in which cell expansion is accompanied by maintenance of the thickness of the cell wall. The incoming XyG molecules (secreted via vesicle transport machinery) is grafted to an existing wall bound XyG integrating into the wall architecture (Shedletzky et al., 1990; Thompson et al., 1997; Thompson & Fry, 2001).

The plant cell wall, as an anatomical defense against biotic stresses

The plant cell wall acts as a mechanical barrier and also participates in signal transduction that allows plant to respond to changes in outer/or surface environment (Hématy et al., 2009; Sorensen et al., 2010). The complexity of cell wall polysaccharides and the formation of network determines the strength, flexibility and functionality during different stress responses (Gall et al., 2015; Tenhaken, 2015; Coolen et al., 2016).

Lignin, an aromatic polymer that is mainly deposited in secondary thickened cell wall, acts as physical barrier against initial pathogen colonization as well as preventing the spread of toxins or enzymes produced by the pathogens into host while also preventing the transfer of water/nutrients from the host cell to pathogens (Smith et al., 2007). Suberin, a lipophilic macro-molecule creates a barrier layer that prohibits the progression of pathogens. Soluble compounds associated with suberin polymers, such as phenolics or wax components may themselves acts as anti-pathogenic barriers (Lulai &

Corsini, 1998; Enstone et al., 2002; Huitema et al., 2004). Experiments have shown that the anatomical distribution of soybean root suberin acts in the structural resistance it has to *Phytophthora sojae* as a physiochemical barrier (Thomas et al., 2007). Another common plant response to pathogen attack, especially fungi, is the deposition of callose. Higher callose accumulation contributes to resistance against necrotrophic pathogens (Ellinger et al., 2013). It has been found in transgenic *A. thaliana* plants that expressing genes of stress-induced callose synthase exhibited early callose deposition at the sites of pathogen penetration (Naumann et al., 2013; Pogorelko et al., 2013; Voigt, 2014).

As an anatomical response against stresses, XyG which remains bound to cellulose micro-fibrils coating and cross-linking, results in an extensive XyG-cellulose network (Fry, 2010). XTHs proteins are responsible for cleavage and/or re-arrangement of the XyG backbone (Cosgrove, 2005; Park & Cosgrove, 2015). Recent studies have highlighted the defense role of XTH protein, found to have increased expression of XTHs in sites infected with pathogens (Albert et al., 2004; Pant et al., 2014).

G. max defense against *H. glycines*

A permanent feeding site is established when a *H. glycines* invades a *G. max* root and represses or controls the defense response and is then able to parasitize a pericycle or neighboring cell (Ithal et al., 2007; Putoff et al., 2007; Klink et al., 2010; Kandoth et al., 2011; Ibrahim et al., 2011). Altered gene expression occurs in the soybean root and syncytial cells for susceptible and resistant reactions in soybean roots infected by *H. glycines* occur (Klink et al., 2005, 2007b, 2009, 2010a, b; 2011 Matsye et al., 2011). If the plant is not resistant to the nematode, *H. glycines* establishes a feeding site. In contrast, if the soybean plant shows resistance to the parasite, the nematode will fail to

establish or will develop very slowly and/or die (Klink et al., 2005, 2007b, 2009, 2010a, b; 2011 Matsye et al., 2011). In *G. max*$_{[Peking/PI\ 548402]}$, a resistant cultivar, the collapse of syncytia is observed as early as 48 hour post infection (hpi), whereas the onset of the resistance response is much slower in *G. max*$_{[PI\ 209332],}$ in which syncytial degeneration occur within 8 to 10 days of post infection (Mahalingam & Skorupska, 1996).

The resistance process occurring in *G. max* against the *H. glycines* is quantitative, controlled by multiple loci (Abdelmajid et al., 2014; Jiao et al., 2015). However, the resistant locus *rhg1*, on its own, has shown to provide some resistance against nematodes of all *H. glycines* races (Kim et al., 2010). During resistance, the plant defense process demonstrates a more dynamic coexistence of gene expression that can interfere with deployment and engagement of the parasites by transducing signals as effective defense responses (Klink et al., 2007; Matsye et al., 2011). Among the very highly expressed genes present in syncytia undergoing defense, a soybean XTH homolog (*Gm*-XTH43) related to *A. thaliana* XTH (*At*-XTH) is one of them (Matsye et al., 2011; Pant et al., 2014; Klink et al., 2017). XTH is an enzyme responsible for XyG metabolism in the primary and secondary cell wall, enhancing the nurse cell development and may have central role in resistance to *H. glycines* infection (Matsye et al., 2011; Pant et al., 2014; Klink et al., 2017).

Study objectives

XTHs function as remodeling agents of XyG as well as promoting the integration of newly synthesized and secreted XyG into the cell wall as cell wall appositions (CWAs). CWAs are structures initiated during early infection, resulting in the development of a physical/chemical barrier to prevent cell penetration (Hardham et al.,

2008). CWA production involves the vesicular transport machinery processing the cargo through the Golgi apparatus. In one study, Albert et al. (2004) has found an increased expression of XTH in tomato occurring by the infection by the plant parasite *Cuscuta reflexa*, demonstrating the importance of XTH in the defense reaction. Nishikubo et al. (2011) has demonstrated that overexpression of some XTHs result in an initial shortening of the XyG chain length, maintaining well defined boundary. Similarly, in recent studies, Matsye et al. (2011) and Pant et al. (2014) have highlighted the defense role of *Gm*-XTH, a secretory protein, functioning in the resistance process occurring against the *H. glycines*.

Prior studies have identified a pool of 1,787 genes expressed specifically in the cells undergoing the resistant reaction (Klink et al., 2010; Matsye et al., 2011), further analyses have narrowed those genes down to approximately100 that are expressed to a higher absolute level in cells undergoing a defense response. That pool of genes has been examined in functional tests as candidate genes. Among them, *Gm*-XTH43 has been found to be expressed in high levels in nurse cells undergoing a defense response (Matsye et al. 2011). While a defense role of *Gm*-XTH43 has been demonstrated, determination of whether it performs a defense function and analysis of whether it has a role in inducing chemical changes of XyG in root remain unknown.

In the study presented here, the role of *Gm*-XTH43 in *G. max* on *H. glycines* parasitism is functionally assayed. As described in the previous chapter, the examination involves the molecular cloning of *Gm*-XTH43, in which the candidate gene is either overexpressed in a susceptible cultivar while in contrast, its expression is impaired by RNAi in a resistant genotype. The effect these transgenic lines have on *H. glycines*

parasitism are done as described in the previous chapter. For the determination of its possible role in XyG modification in cell wall restructuring, a cell wall polysaccharide analysis has been performed by polysaccharide fractionation proceeding with XyG assay and high-performance liquid chromatography (HPLC) of both genetically engineered and control soybean root samples. The results that are presented here provide insight into how plants express defense genes and regulate defense gene products, including a known secreted protein like XTH that is transported to the site of infection by the vesicle transport machinery. The results presented here provide insight into the mechanism that could limit cellular expansion or strengthen wall through xyloglucan remodeling or/and integration (of newly synthesized and secreted XyG), preventing access to *H. glycines* and *H. glycines* synthesized cell wall degrading enzymes. In turn XTH could prevent cellular expansion and syncytium development, perhaps, allowing an opportunity for other defense processes to overwhelm the *H. glycines*.

Materials and Methods

Material preparation

The transformed roots of *G. max* with *Gm*-XTH43 overexpressed in *G. max*$_{[\text{Williams 82/PI 518671}]}$ and *Gm*-XTH43 RNAi in *G. max*$_{[\text{Peking/PI 548402}]}$ along with pRAP15-OE-control and pRAP17-RNAi-control plants have been made as described previously. These transgenic roots then have been analyzed for chemical differences. Roots have been crushed in liquid nitrogen in an autoclaved and cooled mortar and pestle. After crushing, the samples have been kept at -80° C and freeze-dried (Labconco, Freezone® 4.5 Plus) until constant weight had been obtained. The samples weights have been recorded and then the samples kept at 4° C.

Removal of extractives

A procedure according to NREL/TP-510-42619 standard has been followed to remove extractives from the root samples (Sluiter et al., 2012). The samples have been wrapped in Kim-wipes and stapled into small packets. The samples have been first Soxhlet extracted in water for 15 hours and air-dried overnight. Air-dried samples have been returned into Soxhlet and extracted in 95% ethanol of 24 hours. Samples have been kept at room temperature for two days to allow evaporation of ethanol. The samples have been additionally dried in an oven at 50° C to constant mass (Heratherm ™ OMS60, Thermo Fisher Scientific ™). Again, the dry mass of the samples has been recorded before further processing.

Removal of starch, protein, and pectin

A gram of dry tissue of soybean roots contains 2.5 mg of proteins and 25 mg of starch (Finn & Brun, 1982; Rodrigues et al., 2012). Based on the literature, to remove starch, weighed root samples have been treated with porcine pancreas α-amylase (Sigma-Aldrich®). Then, 25 units of amylase (capable of releasing 25mg of starch) have been added per 1 gram of sample. Amylase has been diluted in sufficient volume of 100 mM Tris-HCL buffer (pH 7.0) to cover the sample. The de-starching reaction has been performed at 37° C for 3 hours. The solution has been centrifuged at 10,000 rpm for 5 minutes and the supernatant subsequently discarded.

To each gram of de-starched roots samples, 0.025 mg of Pierce™ Protease (Thermo Fisher Scientific ™), capable of removing 2.5 mg of protein, along with sufficient amount of 50 mM acetic acid (pH 8.0) to cover the sample material and the reaction has been carried out at 37° C for 4 hours. The solution has been centrifuged at

4,000 rpm for 8 minutes and the pellet washed with deionized water (10 ml). Upon removal of the supernatant, the pellet has been de-pectinated by boiling at 100° C in 50 mM EDTA (pH 6.8) for 15 minutes three times. The extracted pectin has been removed by centrifugation and de-pectinated samples have been further subjected to fractionation in 4% and 24% KOH solutions for extraction of loosely bound and tightly bound polysaccharides, respectively.

Polysaccharide fractionation

A procedure described by Nishikubo et al. (2011) has been followed to perform polysaccharide fractionation. Loosely bound hemicelluloses have been obtained by extracting the polysaccharides with three portions of 4% (w/v) KOH at room temperature on a rocker platform (first for 2 hours, then overnight, and finally for 2 minutes). The supernatants or extracts (loosely bound polysaccharides) of each step have been combined and labeled as 4% KOH extracts. The remaining root tissues have been extracted in three portions of a solution containing 24% (w/v) KOH and 0.02% (w/v) sodium borohydride ($NaBH_4$) in a similar manner (first for 2 hours, then overnight, and finally for 2 minutes). Three of these supernatant extracts (tightly bound polysaccharides) have been combined and labeled as 24% KOH extracts.

All KOH extractives have been neutralized with concentrated acetic acid on ice and dialyzed in a dialysis tubing (Spectra/Pro6® 1000 MWCO; Spectrum®) against water until the conductivity became lower than 1 mS. The dialyzed materials have been subjected to freeze-drying until constant weight was obtained.

XyG quantification

Freeze dried samples of 4% and 24% KOH-extracted polysaccharides have been diluted in water (app. 8 µg/µl) and heated at 80° C for 10 minutes. Lugol's solution (Fisher Scientific™) has been diluted 10 times to obtain approximately 20 mM I2 and 60 mM KI solution. Then, 30 µl of each sample have been mixed with 15.1 µl of diluted Lugol's solution and 151 µl of sodium sulfate solution (1.4 M), as per Kooiman (1957). Upon incubation for an hour at room temperature, the absorbance has been measured at 660 nm (Epoch ™, Biotek®). XyG contents of the samples have been calculated and expressed in mg/g freeze-dried tissue according to the standard curve of tamarind (*Tamarindus indica*) XyG (Megazyme™). XyG standards have been prepared at concentrations of 1,500, 1,000, 500, 250, 150 and 62.5 ppm. The difference in XyG quantities of 4% and 24% KOH extracts occurring between transgenic and control samples have been assessed by analysis of variance (ANOVA) Turkey test using SAS (SAS® Institute) software.

Molecular weight analysis by gel permeation chromatography (GPC)

The samples diluted to approximately 8 µg/µl extracted polysaccharides in distilled water have been analyzed for molecular weight. Six dextran GPC analytical standards (Sigma-Aldrich®) in range of 25 kDa to 1,400 kDa have been used for molecular weight calibration. The samples and the standards have been filtered through 0.2 µm filters and then analyzed by GPC using Refrectomax 520 RI (Thermo Fisher Scientific ™) detector and HPLC Finnigan Surveyor System (Thermo Fisher Scientific ™) controlled by Chromeleon ™ v.7 software (Thermo Scientific ™). The separation of MWs has been performed by Superose ™ 6 10/300 column (GE Healthcare ™), using

water mobile phase at the flow rate of 0.2 ml/min (back pressures 277 psi) over a period of 120 minutes. Each GPC spectra have been analyzed by Principal Component Analysis (PCA) in order to observe the difference in dimension of spectral data among genetically modified and control root samples and WAMWs have been determined for each spectrum using The Origin 2018 software (version 95E).

Results

Transgenic plant root identification

The *Gm*-XTH43 gene has been genetically transformed for overexpression into *G. max*$_{[\text{Williams 82/PI 518671}]}$ as described earlier. Likewise, the *Gm*-XTH43-RNAi construct has been transformed to *G. max*$_{[\text{Peking/PI 548402}]}$ as described earlier. The appropriate controls have also been made. Transformed roots exhibit eGFP expression (Figure 3.1) (Klink et al., 2009c; Matsye et al., 2012; Pant et al., 2014). The transgenic roots show similar root growth and maturity.

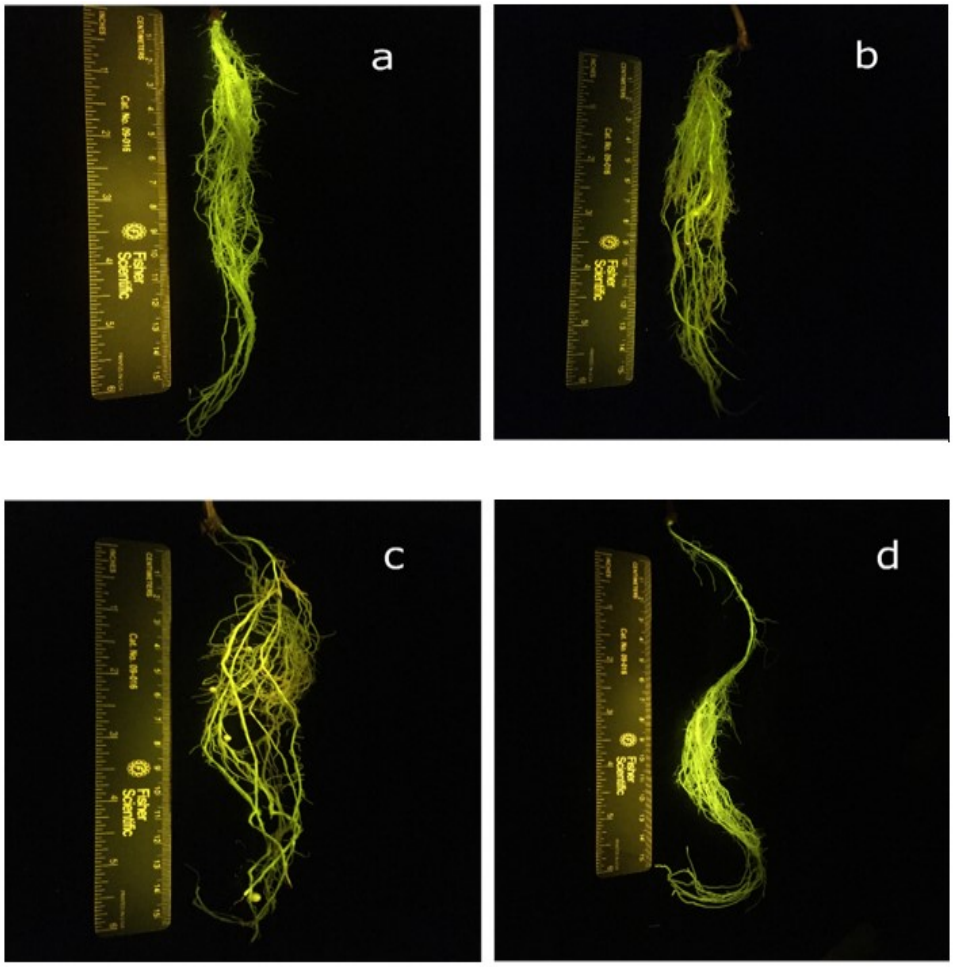

Figure 3.01 Genetically engineered roots of *G. max*. a. *Gm*-XTH-43-OE; b. Control (pRAP15 vector); c. *Gm*-XTH43-RNAi; d. Control (pRAP17 vector).

Total sugars in overexpressed/control plants

Among *Gm*-XTH43-OE and the pRAP15-control soybean root samples, although higher amounts of total sugars have accounted for the pRAP15-control plants (9.40 ±0.64%) than *Gm*-XTH43-OE plants (7.30 ±1.18%) of dry Soxhlet-extracted root material, as shown in Figure 3.2, the difference did not differ in a statistically significant manner. In case of both the pRAP15-control and *Gm*-XTH43-OE plants, tightly bound sugars (24% KOH extractions) have contributed to higher amounts of the dry Soxhlet-

extracted materials with 6.57 ±0.63% of the pRAP15-control, and 4.63 ±0.85% of *Gm*-XTH43-OE plants. The percentage of loosely bound sugars (4% KOH extractions) in general has contributed less to total sugars. In case of the pRAP15-control plants, loosely bound sugars have accounted for 2.83 ±0.34% of dry Soxhlet-extracted material. Likewise, in *Gm*-XTH43-OE plant, it has accounted for 2.66 ±0.63% of dry material from Soxhlet-extraction.

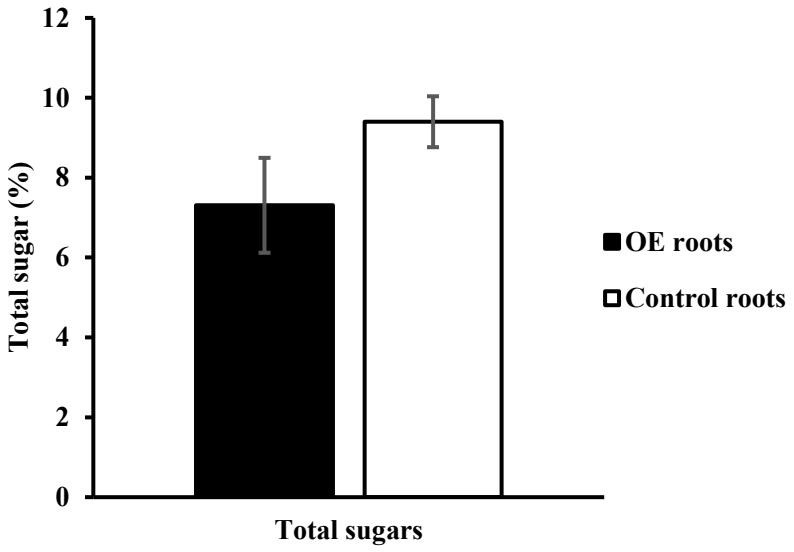

Figure 3.02 Total sugar percent of Soxhlet-extracted *Gm*-XTH43-OE and the pRAP15-control soybean root samples.

Note: (*) represents statistically significant difference $p < 0.05$ calculated by t-test using R-programming (Welch Two Sample t-test). Error bars represent standard error.

Amounts of XyG in overexpressed and control plants

Amounts of XyG has been tested in loosely bound, tightly bound, and total sugars. All the results are interpreted at 5% significance level. A significance difference ($p < 0.05$) of amounts (%) XyG in total sugars has been observed between the pRAP15-control and *Gm*-XTH43-OE plants, with average values of 7.26 ±0.25% and 13.21

±1.24%, respectively (Figure 3.3). Among tightly bound extraction (24% KOH extractions), the amount of XyG has shown a significance difference ($p < 0.05$) of amounts (%) as 5.36 ±0.07% detected in the pRAP15-control plants samples whereas, 11.21 ±1.28% has been detected in *Gm*-XTH43-OE soybean plants samples (Figure 3.4, A). However, the amount of XyG of loosely bound sugars did not differ significantly between *Gm*-XTH43-OE and the pRAP15-control sample types (Figure 3.4, B).

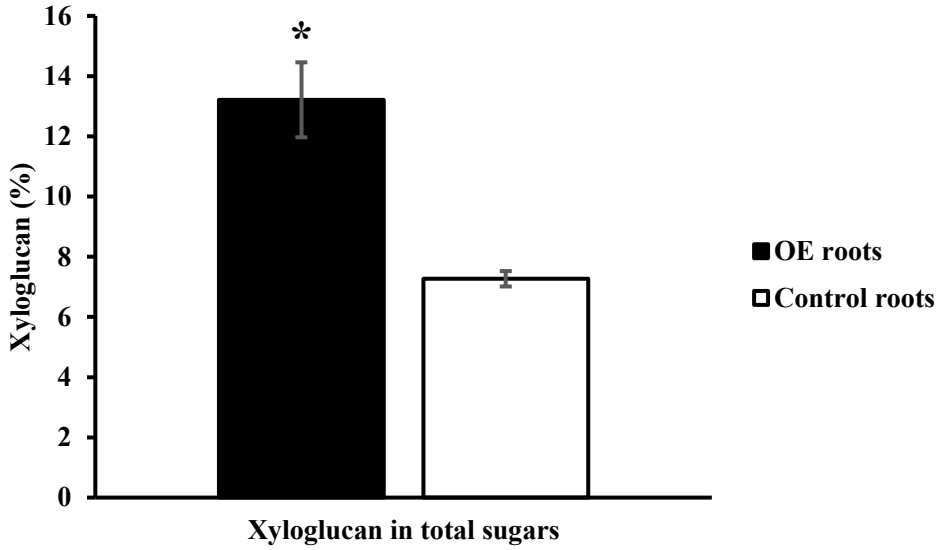

Figure 3.03 XyG percent amounts in total sugars of *Gm*-XTH43-OE and the pRAP15-control root samples of soybean plants.

Note: (*) represents statistically significant difference $p < 0.05$ calculated by t-test using R-programming (Welch Two Sample t-test). Error bars represent standard error.

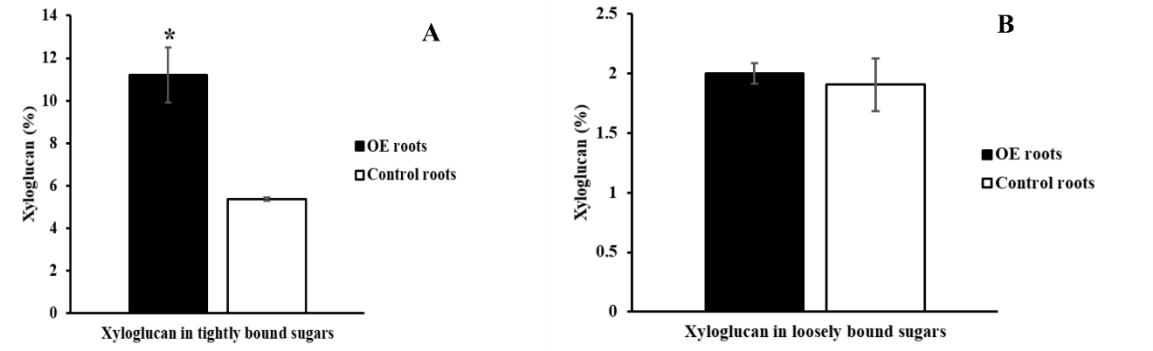

Figure 3.04 XyG percent amounts. A. XyG percent amounts of tightly bound sugars of *Gm*-XTH43-OE and the pRAP15-control root samples; B. XyG percent amounts of loosely bound sugars of overexpressed and the pRAP15-control root samples.

Note: (*) represents statistically significant difference $p < 0.05$ calculated by t-test using R-programming (Welch Two Sample t-test). Error bars represent standard error.

A total amount (%) of XyG detected has been calculated in total dry mass of soybean root tissue. In total, a significant difference ($p < 0.05$) has been observed in between the pRAP15-control and *Gm*-XTH43-OE plant samples, with an average amount of 0.23 ±0.005% and 0.47 ±0.05%, respectively (Figure 3.5).

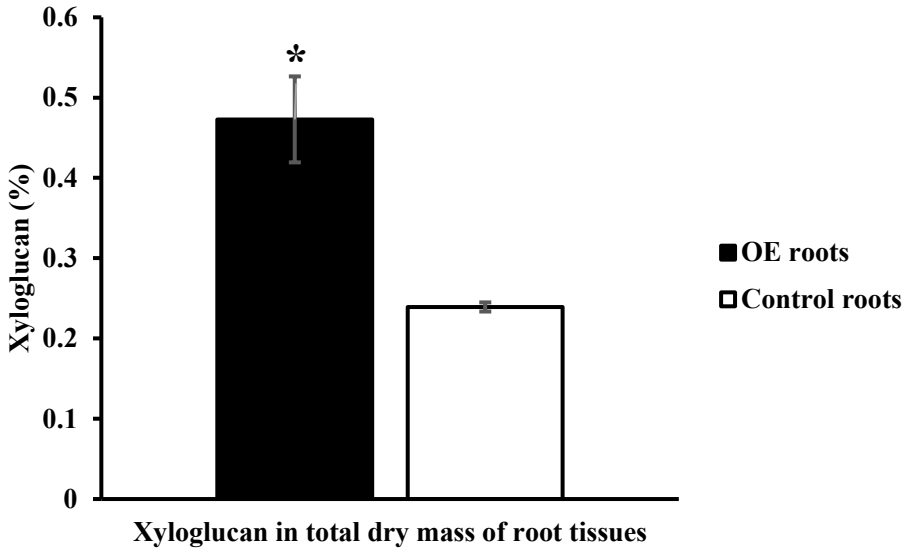

Figure 3.05 Total XyG percent amounts in total dry mass of the tissue of *Gm*-XTH43-OE and the pRAP15-control root samples of soybean plants.

Note: (*) represents statistically significant difference $p < 0.05$ calculated by t-test using R-programming (Welch Two Sample t-test). Error bars represent standard error.

Total sugars in RNA-interference/control plants

The total sugar amount between *Gm*-XTH43-RNAi and the pRAP17-control samples did not differ significantly, as shown in Figure 3.6. An amount of total sugars of 7.70 ±0.51% accounted for the pRAP17-control root samples and 6.89 ±0.65% for *Gm*-XTH43-RNAi of soybean root samples. Among tightly bound (24% KOH extracts) and loosely bound (4% KOH extracts) sugars, in general, has contributed in higher amounts to the dry Soxhlet-extracted root material with 3.98 ±0.71% of the pRAP17-control, and 4.35 ±0.39% of *Gm*-XTH43-RNAi plants. Similar results have been observed in loosely bound sugar as well, in which the pRAP17-control and *Gm*-XTH43-RNAi samples did not differ significantly, with average values of 3.72 ±0.20% in the pRAP17-control samples, whereas, 2.53 ±0.26% in *Gm*-XTH43-RNAi root sample of soybean roots.

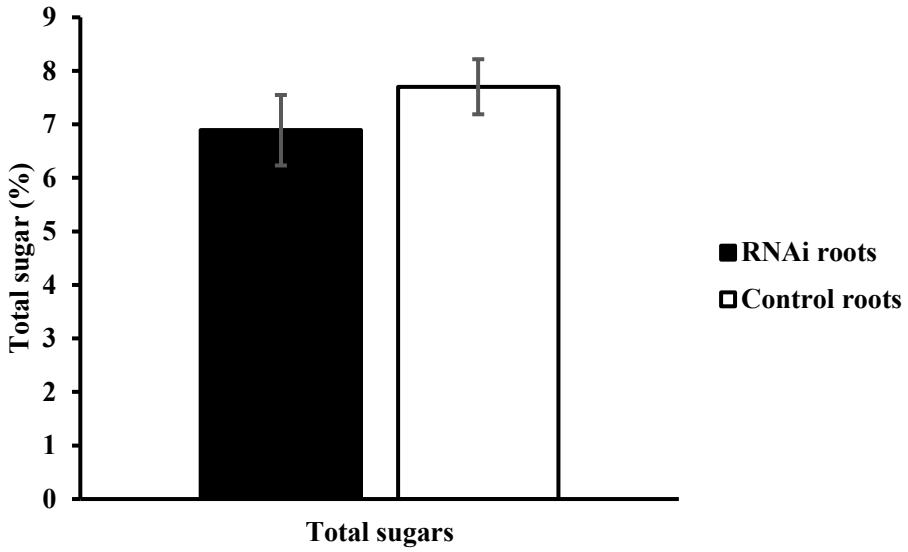

Figure 3.06 Total sugar percent of Soxhlet-extracted *Gm*-XTH43-RNAi and the pRAP17-control soybean root samples.

Note: (*) represents statistically significant difference $p < 0.05$ calculated by t-test using R-programming (Welch Two Sample t-test). Error bars represent standard error.

Amounts of XyG in RNA-interference/control plants

The amount of XyG present between the pRAP17-control and *Gm*-XTH43-RNAi root samples has been tested in loosely bound, tightly bound and total sugars. All results have been interpreted at 5% level of significance. The amount of XyG has been shown to be significantly different in total contents, with average values of 8.95 ±0.97% and 6.43 ±0.33% among the pRAP17-control and *Gm*-XTH43-RNAi plant samples, respectively, as shown in Figure 3.7. A significant difference has also been observed in XyG content in tightly bound sugars (24% KOH extracts), in which, 7.10 ±1.15% has been accounted for in the pRAP17-control and 4.70 ±0.18% has been accounted for *Gm*-XTH43-RNAi root samples (Figure 3.8, A). However, the amount of XyG did not differ significantly in between loosely bound sugar and control. An amount of 1.49 ±0.32% and 1.73 ±0.23%

has been accounted for in the pRAP17-control and *Gm*-XTH43-RNAi root samples respectively, as shown in Figure 3.8, B.

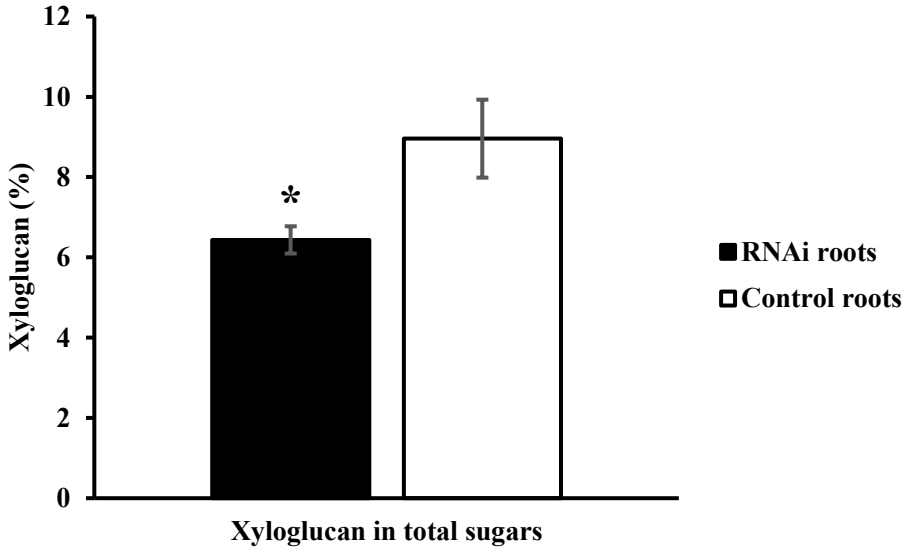

Figure 3.07 XyG percent amounts in total sugars of *Gm*-XTH43-RNAi and pRAP17-control root samples of soybean plants.

Note: (*) represents statistically significant difference $p < 0.05$ calculated by t-test using R-programming (Welch Two Sample t-test). Error bars represent standard error.

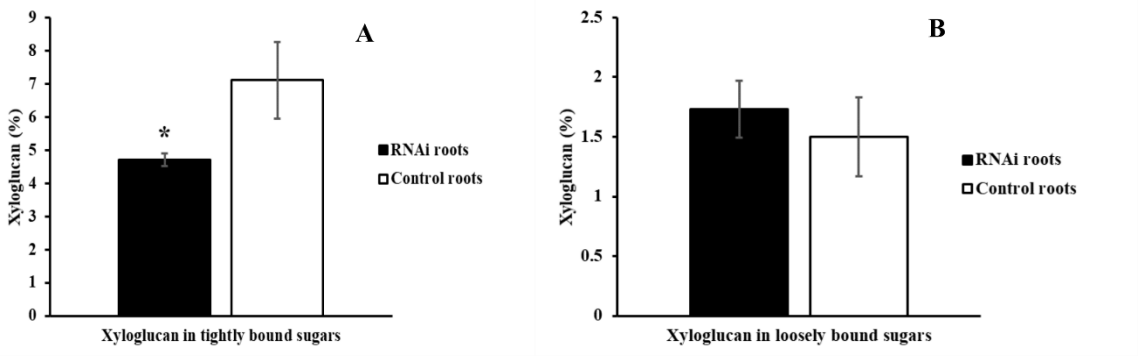

Figure 3.08 XyG percent amounts. A. XyG percent amounts of tightly bound sugars of *Gm*-XTH43-RNAi and pRAP17-control root samples; B. XyG percent amounts of loosely bound sugars of *Gm*-XTH43-RNAi and pRAP17-control root samples.

Note: (*) represents statistically significant difference $p < 0.05$ calculated by t-test using R-programming (Welch Two Sample t-test). Error bars represent standard error.

An amount of XyG in total dry weight of tissue has been calculated for control and *Gm*-XTH43-RNAi root samples. The amount of XyG has been observed to be higher in the pRAP17-control, accounting for 0.25 ±0.05% more than in RNAi, which has accounted for 0.16 ±0.03% of total dry weight of root tissue samples of soybean plants, as shown in Figure 3.9. However, the difference is not statistically significant.

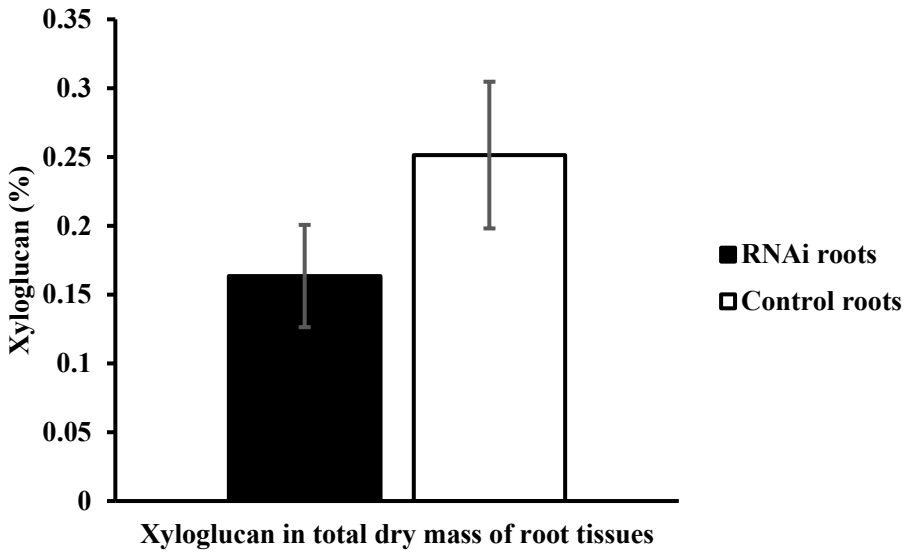

Figure 3.09 Total XyG percent amounts in total dry mass of the tissue of *Gm*-XTH43-RNAi and control root samples of soybean plants.

Note: (*) represents statistically significant difference $p < 0.05$ calculated by t-test using R-programming (Welch Two Sample t-test). Error bars represent standard error.

Gel permeation chromatography (GPC) analysis

The GPC analysis began by analyzing dextran standard controls. The GPC chromatograms of dextran standards ranging from 25 kDa to 1,400 kDa are shown in Figure 3.10. A consistent and clear peak of separation of the standards has been observed, demonstrating that the instrument performed consistent and stable throughout the sample analysis procedure.

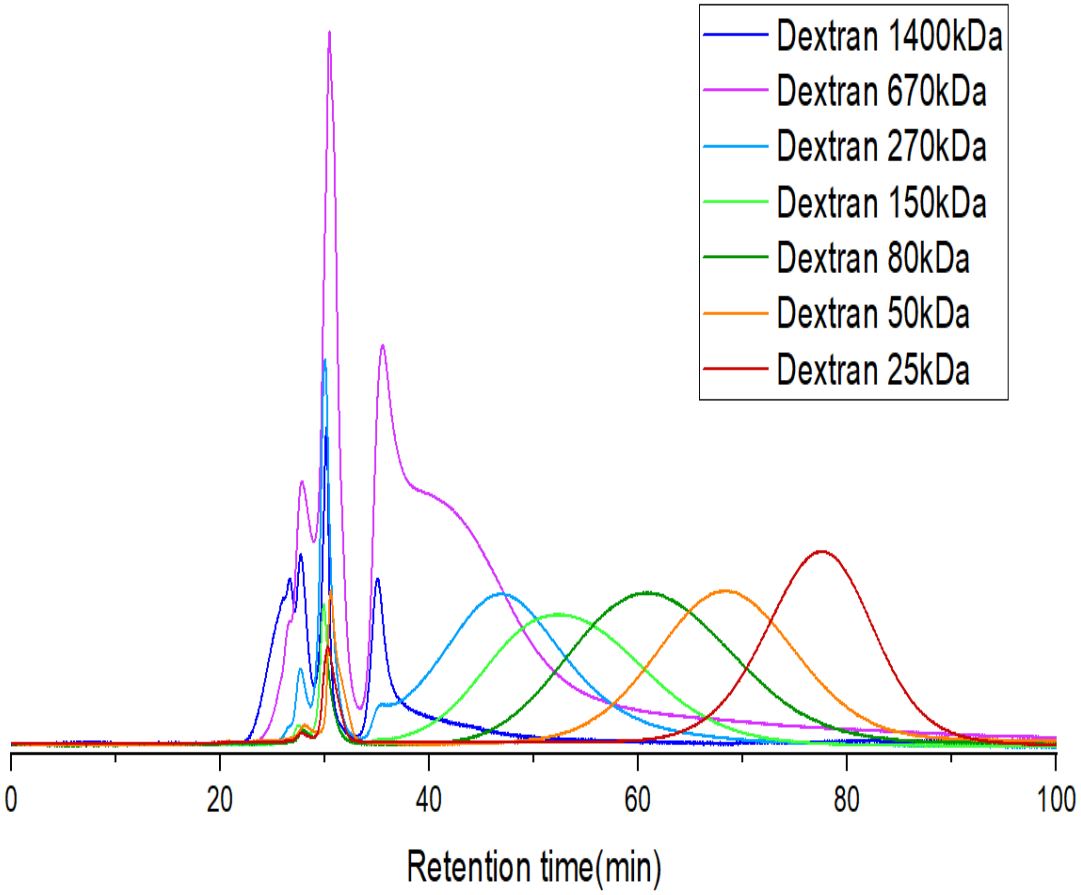

Figure 3.10 Area normalized GPC chromatograms of dextran standards (25-1,400 kDa).

Tightly bound sugars in *Gm*-XTH43-OE and control samples

A GPC analysis of tightly bound sugars (24% KOH extracts) of *Gm*-XTH43-OE and pRAP15-control root samples have shown a stable run with a constant baseline and MeOH peak (internal standard) remaining at constant elution time. Although, some differences have been seen between the replicate runs, overall, consistent chromatograms have been observed as shown in Figure 3.11. In general, as visible from Figure 3.11 and

Figure 3.12, and confirmed by PCA analysis (Appendix B, Figure B.1), the difference between the pRAP15-control (red chromatograms) and *Gm*-XTH43-OE roots (blue chromatograms) signifies the alteration in cell wall structural architecture due to *Gm*-XTH43 overexpression. The difference lies mainly in the section of the peaks eluted after 35 minutes, i.e. in sugars with size comparable to dextran standards with MW <270 kDa.

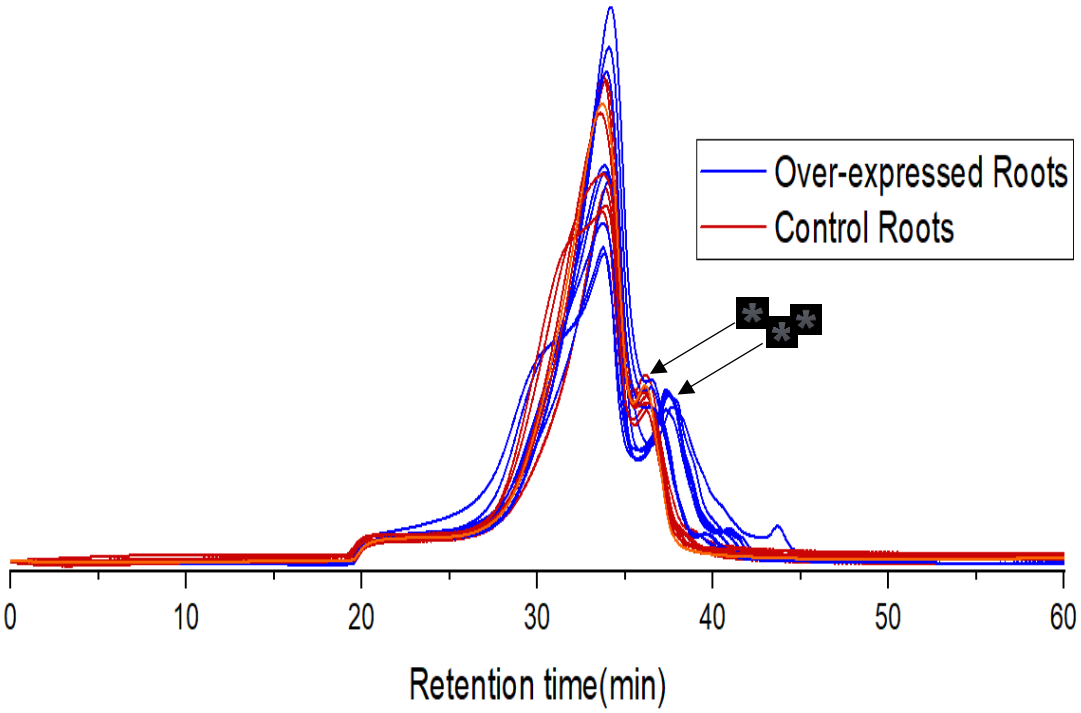

Figure 3.11 Area normalized chromatogram of tightly bound sugars in *Gm*-XTH43-OE (blue) and pRAP15-control (red) roots.

Note: The regions pointed by arrow head represents section of elution peaks where mainly the difference observed (*, control roots peak; **, Overexpressed roots peak)

For each chromatogram, the WAMW has been calculated (Appendix B, Table B.3). Overall, the pRAP15-control sample appears to have sugars with a higher MW, with an average value of 931.34 ±15.22 as compared to the *Gm*-XTH43-OE root samples which accounted for an average value of 860.94 ±10.57. The observed overall lower MW polysaccharides in the cell wall of the *Gm*-XTH43-OE soybean root samples suggests that the genetically modified plants would have shorter xyloglucan chains, and therefore smaller chains for nematode or related enzymatic access to those chains.

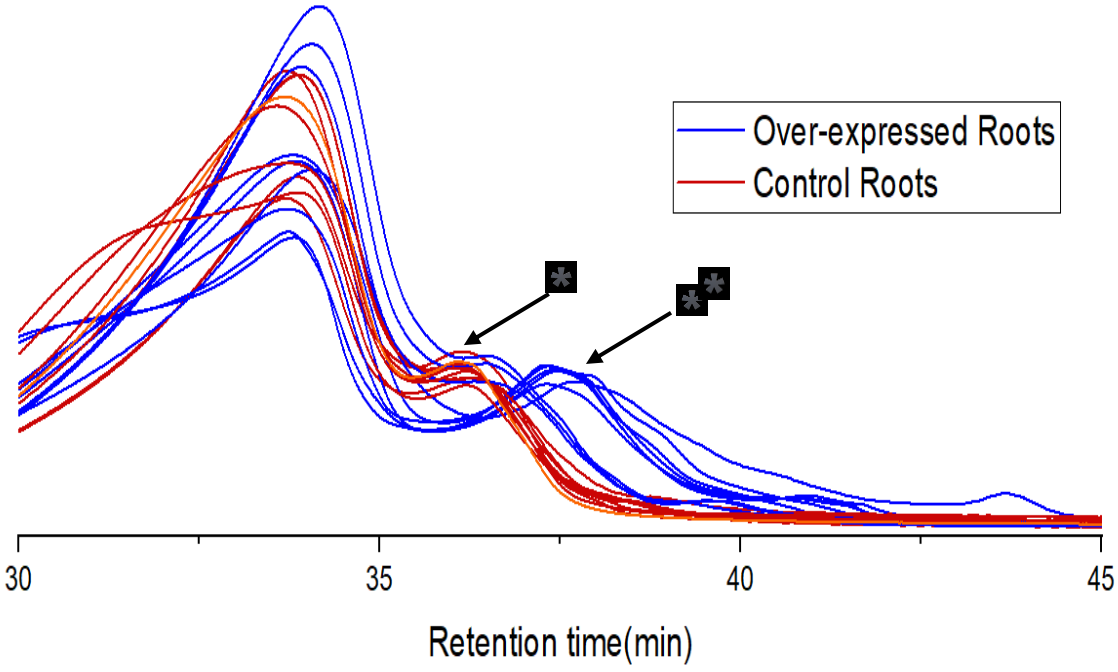

Figure 3.12 Magnified Higher and lower MW spectral region of area-normalized chromatograms (from Figure 3.11) of tightly bound sugars in *Gm*-XTH43-OE (blue) and pRAP15-control (red) roots.

Note: The regions pointed by arrow head represents section of elution peaks where mainly the difference observed (*, control roots peak; **, Overexpressed roots peak)

Loosely bound sugars in *Gm*-XTH43-OE and control samples

As visible from Figure 3.13 and Figure 3.14, loosely bound sugars (4% KOH extracts) have shown similar spectral differences occurring between pRAP15-control and *Gm*-XTH43-OE root samples to the differences between the tightly bound sugars. The major difference has also been observed in the region of dextran MW <270 kDa, with pRAP15-control samples (red chromatograms) showing higher MW peaks than *Gm*-XTH43-OE (blue chromatograms) in this region. The dimensional difference of spectra of pRAP15-control and *Gm*-XTH43-OE gene-modified root samples have also been differentiated through PCA, as shown in Appendix B (Figure B.3).

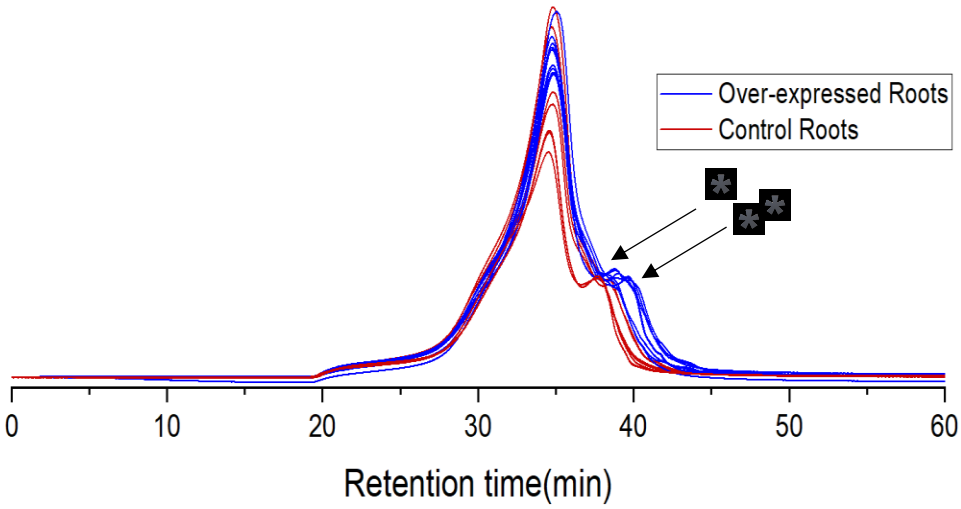

Figure 3.13 Area normalized chromatogram of loosely bound sugars in *Gm*-XTH43-OE (blue) and pRAP15-control (red) roots.

Note: The regions pointed by arrow head represents section of elution peaks where mainly the difference observed (*, control roots peak; **, Overexpressed roots peak)

When analyzing the spectral data to calculate the WAMW, a higher MW with average value of 813.86 ±5.17 has been accounted for in the pRAP15-control than the comparatively lower value of 741.69 ±9.10 that has been accounted for in the *Gm*-XTH43-OE root samples (Appendix B, Table B.5). In general, loosely bound sugars are expected to have a lower MW than tightly bound sugars. The similar pattern in loosely bound sugars to tightly bound sugars suggests that the genetically modified root of soybean plant, caused by *Gm*-XTH43 overexpression has altered the cell wall architecture, especially XyG, conferring shorter chain length which could confine the cellular environment required for parasitism.

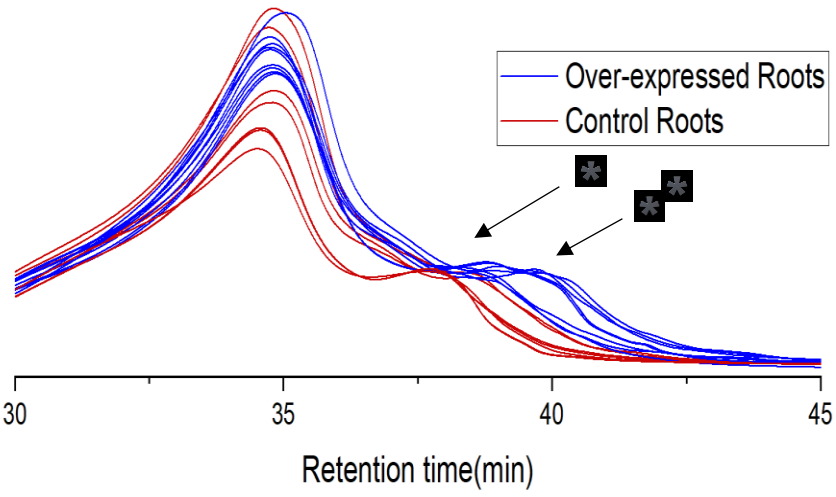

Figure 3.14 Magnified Higher and lower-MW spectral region of area-normalized chromatograms (from Figure 3.13) of loosely bound sugars in *Gm*-XTH43-OE (blue) and pRAP15-control (red) roots.

Note: The regions pointed by arrow head represents section of elution peaks where mainly the difference observed (*, control roots peak; **, Overexpressed roots peak)

Tightly bound sugars in *Gm*-XTH43-RNAi and control samples

GPC analysis of root samples isolated from roots genetically modified to express *Gm*-XTH43-RNAi have been compared to the appropriate pRAP17-control in tightly bound sugars showed difference between them as shown in Figure 3.15 and Figure 3.16. The difference in dimension of spectra revealed by PCA analysis of each chromatograms have been grouped into control and *Gm*-XTH43-RNAi as shown in Appendix B (Figure B.2). In contrast to the result in tightly bound sugars in *Gm*-XTH43-OE, the RNAi pRAP17-control samples appear to have sugars with lower MW in comparison to the *Gm*-XTH43-RNAi root samples, with average value of 846.80 ±5.90 in pRAP17-control samples as compared to the average value of 916.75 ±8.13 in *Gm*-XTH43-RNAi plant samples (Appendix B, Table B.4).

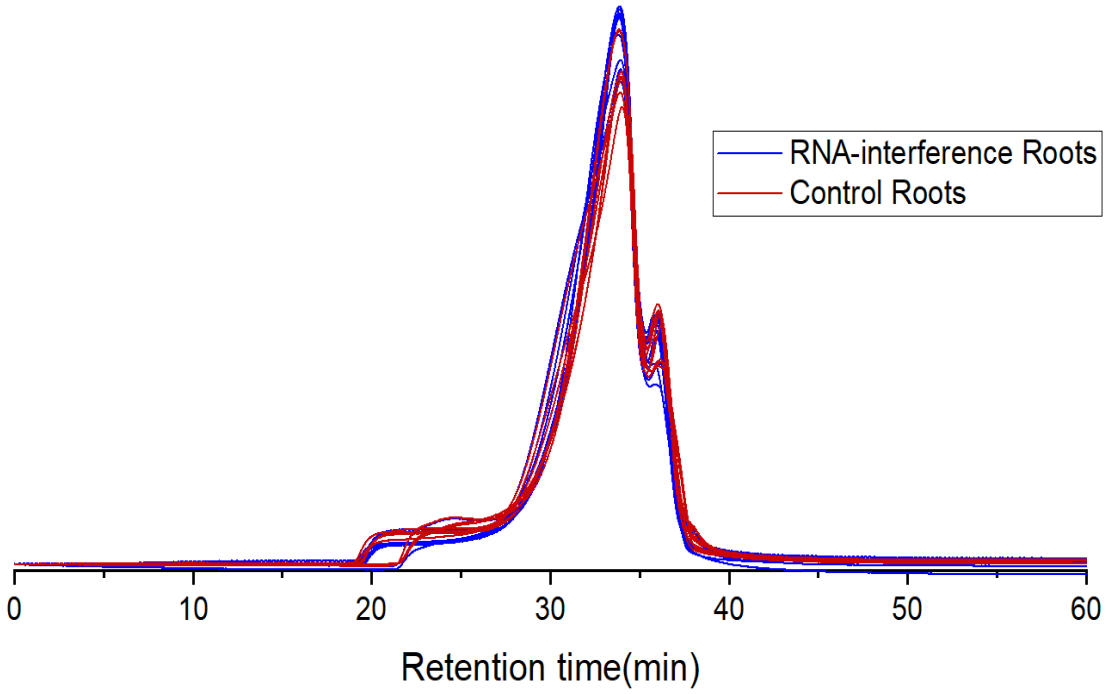

Figure 3.15 Area-normalized chromatograms of tightly bound sugars in *Gm*-XTH43-RNAi (blue) and pRAP17-control (red) roots.

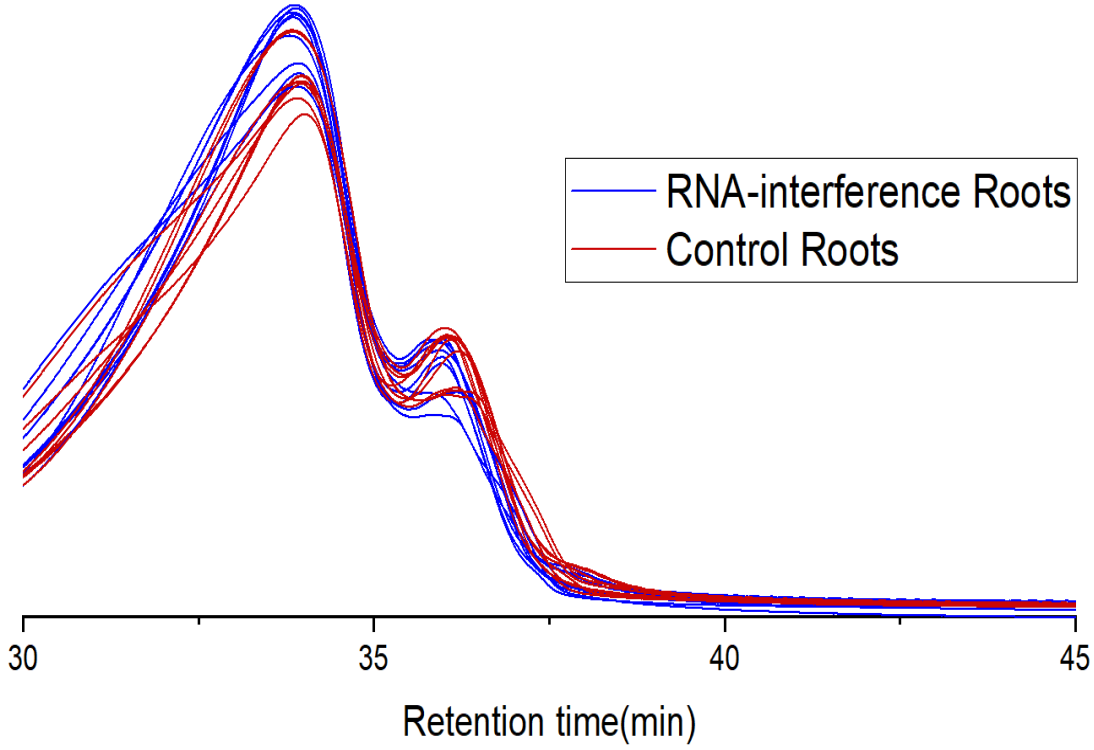

Figure 3.16 Magnified higher and lower-MW spectral region of area-normalized chromatograms (from Figure 3.15) of tightly bound sugars in *Gm*-XTH43-RNAi (blue) and pRAP17-control (red) roots.

Loosely bound sugars in *Gm*-XTH43-RNAi and control samples

Loosely bound sugars (4% KOH extracts) of *Gm*-XTH43-RNAi and pRAP17-control samples show similar spectral differences occurring between control and *Gm*-XTH43-RNAi plants, with a calculated average MW of 760.63 ±6.05 of pRAP17-control root samples and average MW of 775.35 ±4.64 of *Gm*-XTH43-RNAi soybean root samples (Appendix B, Table B.6). The observation that pRAP17-control samples have a lower MW than *Gm*-XTH43-RNAi samples suggests that the genetically modified plants would have longer xyloglucan chains as compared to *Gm*-XTH43-RNAi modified cell

wall architecture. This observation is the opposite of what was observed in the *Gm*-XTH43-OE experiment. The difference between the pRAP17-control (red chromatograms) and modified plants (blue chromatograms) lies mainly in the sections of the peaks that elute after 35 minutes (i.e. in sugars whose size is comparable to dextran standard below 270 kDa). Although the difference between the pRAP17-control and modified spectral profiles are minimal in appearance in chromatograms, the results confirm the lower MW that is accounted for in pRAP17-control samples as compared to the *Gm*-XTH43-RNAi-modified, signifying the role of *Gm*-XTH-43 in altering cell wall architecture.

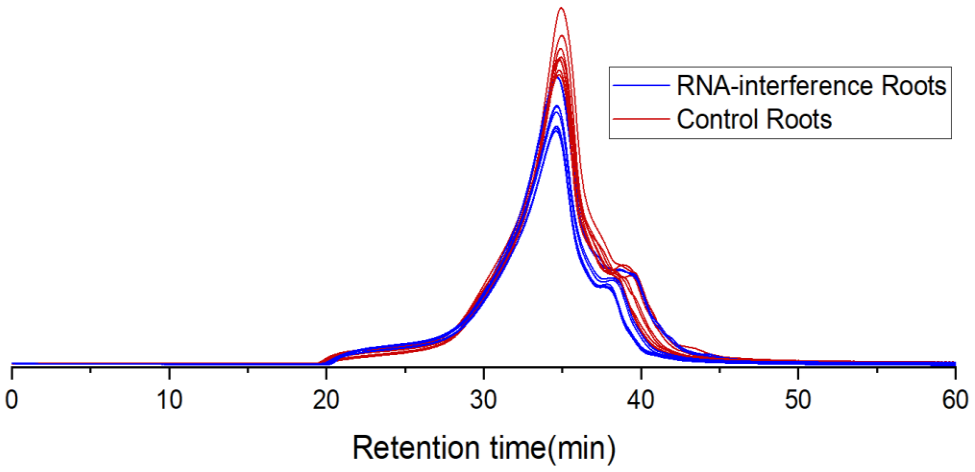

Figure 3.17 Area-normalized chromatograms of loosely bound sugars in *Gm*-XTH43-RNAi (blue) and pRAP17-control (red) roots.

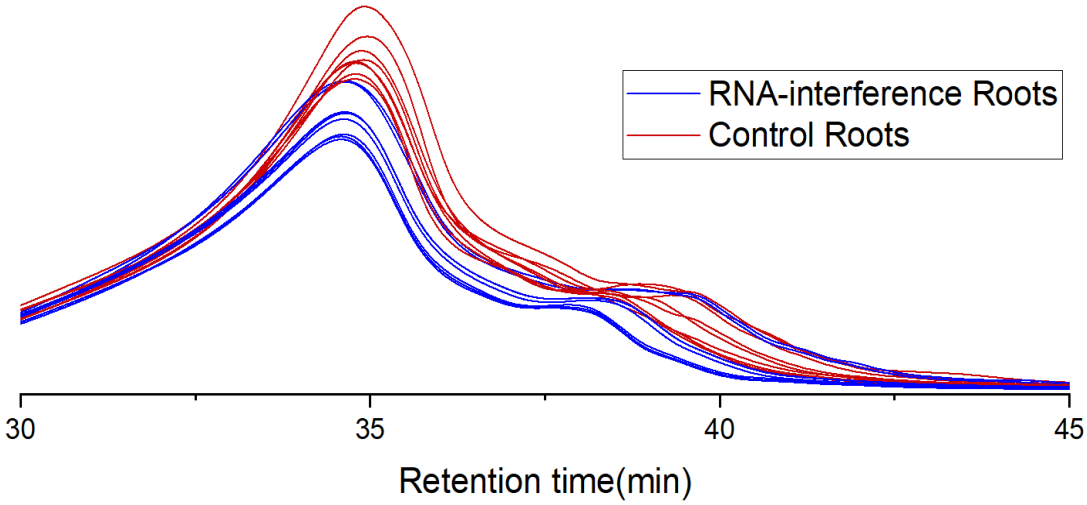

Figure 3.18 Magnified higher and lower-MW spectral region of area-normalized chromatograms (from Figure 3.17) of loosely bound sugars in *Gm*-XTH43-RNAi (blue) and pRAP17-control (red) roots.

Discussion

The role of *Gm*-XTH43 during the defense response that soybean has toward *H. glycines* has been confirmed in previous studies (Pant et al., 2014). Pant et al. (2014) has shown the suppression of *H. glycines* parasitism in soybean plants through *Gm*-XTH43 OE and RNAi approaches. Previous, experiments performed by Klink et al. (2010) have determined the extent to which *Gm*-XTH43 is expressed during the defense reaction of *G. max* against *H. glycines*. The high levels of *Gm*-XTH43 transcripts present in the cells undergoing resistance to *H. glycines* has revealed the role of XTH proteins could have in the defense process against pathogenic invasion (Klink et al., 2010; Matsye et al., 2011; Pant et al., 2014). The work presented here, in conjunction with the results of those of Pant et al. (2014), point towards the functional effect of *Gm*-XTH43 protein appears to

have in re-arranging or re-modelling of XyG to combat *H. glycines* as it attempts to establish a functional feeding site.

In this study, total XyG amounts have been shown to be higher in the root samples of *Gm*-XTH43-OE plants as compared to pRAP15-control plants. The results are in agreement with the findings of Nishikubo et al. (2011) that have reported an increase in overall XyG content in *Populus* sp. tissues that are overexpressing XTH. Nishikubo et al. (2011) has reported an increase in tightly bound XyG in the XTH-OE lines as compared to the wild type by approximately 20%, while decreasing the loosely bound fraction. The present study also has shown a significant difference in the XyG amounts of tightly bound sugars between XTH-OE and pRAP15-control plants, while loosely bound sugars with only a fraction of the difference between XTH-OE and pRAP15-control plants.

In order to better understand the role of XTH gene, an RNAi approach has then been used to obtain transformed roots as described by Klink et al. (2009). A lower amount of XyG has been obtained in *Gm*-XTH43-RNAi tissue as compared to pRAP17-control plants, in which, there was a significantly lower amount of XyG of tightly bound sugars in between *Gm*-XTH43-RNAi and pRAP17-control plants and fraction of the difference among *Gm*-XTH43-RNAi and pRAP17-control plants of loosely bound sugars. In a similar type of study that has been approached through the isolation of an XTH mutant in *A. thaliana*, Zhu et al. (2012) reported significantly reduced hemicellulose and total XyG content in the root sample of XTH-mutant plants.

The observation of a higher amount of XyG in tightly bound sugars than loosely bound sugars suggests that XyG is modified after deposition in the cell wall. XyG is

reported to change soon after deposition including increase in size, depolymerization and increment in amount during expansion (Talbott & Ray, 1992; Thompson et al., 1997; Tokumoto et al., 2002; Kerr & Fry, 2003; Popper & Fry, 2005). Several rearrangements do occur during transition stages of the cell wall and a transition of loosely bound sugars to tightly bound to cellulose microfibrils into tightly bound network have been observed to happen along with these transitions (Bourquin, 2002; Nishikubo et al., 2011). Although in previous studies it has been found that modified XTH activity has a mixed effect on XyG, a definitive role of XTH has been revealed by Nishikubo et al. (2011) in which XTH activity has been reported to promote XyG incorporation into the cell wall of tightly bound fraction (Herbers et al., 2001; Liu et al., 2007; Genovesi et al., 2008; Miedes et al., 2011; Zhu et al., 2012). Moreover, changes in mono-sugar composition of hemicellulose fractions have been reported. The results demonstrate higher XyG amounts to be positively expressed and lower to be negatively regulated by the XTH gene. These observations indicate the key role of XTH in developmental XyG rearrangement that the metabolic processes of genes involve in the generation of XyG in the plant cell. These observations support, experimentally, the hypothesis that XTH activity incorporates newly synthesized XyG to xyloglucan network through transglycosylation, increasing the net amount of XyG content of the wall. Consequently, in cells that do not synthesize XyG, XTH may act only in their rearrangement.

XTH is considered a key component for maintaining the chain length and extensibility of cellulose- XyG network (Jan et al., 2004; Shin et al., 2006). The function of XTH appears to be more complex than a simple role in cell expansion catalyzed through depolymerization of XyG as reported, but also inhibiting root and root hair

elongation along with the broadening of root and root hairs indicating enhanced radial expansion (Hayashi, 1989; Talbott & Ray, 1992; Jan et al., 2004; Liu et al., 2007; Liu et al., 2007; Cavalier et al., 2008; Maris et al., 2009).

In the present study, WAMW of genetically modified and control root samples have been determined taking dextrans ranging from 25 kDa to 1,400 kDa as standards. The MWs have varied in such a way that *Gm*-XTH43-OE leads to a lower molecular mass than the pRAP15-control samples while *Gm*-XTH43-RNAi leads to a higher molecular mass than pRAP17-control samples. These results indicate that shortening of the XyG chain length in *Gm*-XTH43-OE and increasing chain length in *Gm*-XTH43-RNAi roots occurs as compared to their respective control roots. In a similar study, Nishikubo et al. (2011) also reported the shift toward lower molecular mass XyG within the main peak and higher content of low molecular mass XyG from the samples of XTH-OE lines in *Populus* species. Similarly, Herbers et al. (2001) noted an increase in XyG size by 20% when XTH expression is suppressed. Although, there have been dubious explanations of the role of XTH in cell wall morphogenesis in many plant species, a high expression level of the XTH gene in the region of active wall formation indicates role in wall deposition and wall remodeling even after enlargement has ceased (Fry et al., 1992; Antosiewicz et al., 1997; Vissenberg et al., 2001; Takeda et al., 2002; Hyodo et al., 2003; Yokoyama et al., 2004). The observed evidence argues for *Gm*-XTH43 being involved in the incorporation of XyG molecules into the cell wall through transglycosylation. The observation of lower MW XyG in *Gm*-XTH43-OE transgenic lines and higher MW XyG in *Gm*-XTH43-RNAi transgenic lines than their respective control plants might be

associated with cell wall strengthening by XTH-mediated remodeling of XyG chain in cell wall architecture.

The XyG chain length estimation, based on WAMW obtained through GPC, must be regarded with caution as they are sensitive to conformation (Park & Cosgrove, 2015). It is plausible that the observation of MW sugars is not all XyG, but also the result of multiple polysaccharide reorganization in cell wall. GPC columns are generally calibrated with dextran backbone [α-1,6-D-glucan with 5% α-(1,3)-glucose substitution] and is generally insensitive to xyloglucans <10-20 kDa (Hayashi, 1989; Talbott & Ray, 1992; Gaborieau & Castignolles, 2011; Köhnke et al., 2011). Thus, the MW data must be best interpreted as relative rather than absolute size. Also, the conformation of XyG may vary on the degree of substitution of side chain residues, acetylation pattern and undoubtedly, different biological sources and stages of same material that could attribute to the observed differences.

For the future, it is recommended for mono-sugar analysis obtained through HPLC to be performed according to Sluiter et al. (2012). In those procedures, the composition of the extracted polysaccharide gives extensive data regarding actual cell wall modification by compositional changes in the polysaccharide microfibril. The XyG backbone attributes a relatively rigid conformation whose flexibility is mainly dependent on side the chain and their interaction to other components of cell wall (Gidley et al., 1991; Muller et al., 2011). Also recommended would be a different approach of estimating chain length by use of microdissection and use of electron microscopy (EM). Although these methods do not reveal the chemical components, a broad perspective of

cell wall extensibility could reveal the functionality of XTH gene in cell wall architecture especially XyG remodeling.

Furthermore, understanding the complex organization of wall, characterizing the cellular, structural and chemical composition could be useful for the basis of biofuel and bioproduct manufacturing. Although the focus of this study has been to understand the role of XTH genes up against nematode resistance in soybean, it is possible that XTH mediated XyG modification can be used for prevention of biological, chemical and/or mechanical damage. Consequently, in turn, would be useful for overall improvement of the properties of bioproducts/biofuels.

References

Abdelmajid, K. M., Ramos, L., Hyten, D., Bond, J., Bendahmane, A., Arelli, P. R., … Ave, B. (2014). Quantitative Trait Loci (QTL) that Underlie SCN Resistance in Soybean [*Glycine max* (L .) Merr .] PI438489B by " Hamilton " Re- combinant Inbred Line (RIL) Population, *1*(3), 29–38. https://doi.org/10.5147/ajpb.2014.0140

Albert, M., Werner, M., Proksch, P., Fry, S. C., & Kaldenhoff, R. (2004). The cell wall-modifying xyloglucan endotransglycosylase/hydrolase LeKTH1 is expressed during the defence reaction of tomato against the plant parasite Cuscuta reflexa. *Plant Biology*, *6*(4), 402–407. https://doi.org/10.1055/s-2004-817959

Alonso-Simón, A., Neumetzler, L., García-Angulo, P., Encina, A. E., Acebes, J. L., Álvarez, J. M., & Hayashi, T. (2010). Plasticity of xyloglucan composition in bean (*Phaseolus vulgaris*)-cultured cells during habituation and dehabituation to lethal concentrations of dichlobenil. *Molecular Plant*, *3*(3), 603–609. https://doi.org/10.1093/mp/ssq011

Antosiewicz, D. M., Purugganan, M. M., Polisensky, D. H., & Braam, J. (1997). Cellular localization of *Arabidopsis* xyloglucan endotransglycosylase-related proteins during development and after wind stimulation. *Plant Physiology*, *115*(4), 1319–1328. https://doi.org/115/4/1319 [pii]

Bourquin, V. (2002). Xyloglucan Endotransglycosylases Have a Function during the Formation of Secondary Cell Walls of Vascular Tissues. *The Plant Cell Online*, *14*(12), 3073–3088. https://doi.org/10.1105/tpc.007773

Cavalier, D. M., Lerouxel, O., Neumetzler, L., Yamauchi, K., Reinecke, A., Freshour, G., … Keegstra, K. (2008). Disrupting Two *Arabidopsis thaliana* Xylosyltransferase Genes Results in Plants Deficient in Xyloglucan, a Major Primary Cell Wall Component. *The Plant Cell Online*, *20*(6), 1519–1537. https://doi.org/10.1105/tpc.108.059873

Chevalier, L., Bernard, S., Ramdani, Y., Lamour, R., Bardor, M., Lerouge, P., … Driouich, A. (2010). Subcompartment localization of the side chain xyloglucan-synthesizing enzymes within Golgi stacks of tobacco suspension-cultured cells. *Plant Journal*, *64*(6), 977–989. https://doi.org/10.1111/j.1365-313X.2010.04388.x

Cho, S. K., Kim, J. E., Park, J. A., Eom, T. J., & Kim, W. T. (2006). Constitutive expression of abiotic stress-inducible hot pepper CaXTH3, which encodes a xyloglucan endotransglucosylase/hydrolase homolog, improves drought and salt tolerance in transgenic Arabidopsis plants. *FEBS Letters*, *580*(13), 3136–3144. https://doi.org/10.1016/j.febslet.2006.04.062

Cocuron, J.-C., Lerouxel, O., Drakakaki, G., Alonso, A. P., Liepman, A. H., Keegstra, K., … Wilkerson, C. G. (2007). A gene from the cellulose synthase-like C family encodes a beta-1,4 glucan synthase. *Proceedings of the National Academy of Sciences of the United States of America*, *104*(20), 8550–8555. https://doi.org/10.1073/pnas.0703133104

Coolen, S., Proietti, S., Hickman, R., Davila Olivas, N. H., Huang, P. P., Van Verk, M. C., … Van Wees, S. C. M. (2016). Transcriptome dynamics of *Arabidopsis* during sequential biotic and abiotic stresses. *The Plant Journal : For Cell and Molecular Biology*, *86*(3), 249–267. https://doi.org/10.1111/tpj.13167

Cosgrove, D. J. (2005). Growth of the plant cell wall. *Nature Reviews Molecular Cell Biology*, *6*(11), 850–861. https://doi.org/10.1038/nrm1746

Davis, J., Brandizzi, F., Liepman, A. H., & Keegstra, K. (2010). Arabidopsis mannan synthase CSLA9 and glucan synthase CSLC4 have opposite orientations in the Golgi membrane. *Plant Journal*, *64*(6), 1028–1037. https://doi.org/10.1111/j.1365-313X.2010.04392.x

Dwivany, F. M., Yulia, D., Burton, R. A., Shirley, N. J., Wilson, S. M., Fincher, G. B., … Doblin, M. S. (2009). The CELLULOSE-SYNTHASE LIKE C (CSLC) family of barley includes members that are integral membrane proteins targeted to the plasma membrane. *Molecular Plant*, *2*(5), 1025–1039. https://doi.org/10.1093/mp/ssp064

Ellinger, D., Naumann, M., Falter, C., Zwikowics, C., Jamrow, T., Manisseri, C., … Voigt, C. A. (2013). Elevated Early Callose Deposition Results in Complete Penetration Resistance to Powdery Mildew in *Arabidopsis*. *Plant Physiology*, *161*(3), 1433–1444. https://doi.org/10.1104/pp.112.211011

Enstone, D. E., Peterson, C. A., & Ma, F. (2002). Root endodermis and exodermis: Structure, function, and responses to the environment. *Journal of Plant Growth Regulation*, *21*(4), 335–351. https://doi.org/10.1007/s00344-003-0002-2

Finn, G. A., & Brun, W. A. (1982). Effect of Atmospheric CO_2 Enrichment on Growth , Nonstructural Carbohydrate Content , and Root Nodule Activity in Soybean Published by : American Society of Plant Biologists (ASPB) Stable URL : http://www.jstor.org/stable/4267201 Linked references are a, *69*(2), 327–331.

Fry, S. C. (1989). The structure and functions of xyloglucan. *Journal of Experimental Botany*, *40*(1), 1–11. https://doi.org/10.1093/jxb/40.1.1

Fry, S. C. (2010). *Cell Wall Polysaccharide Composition and Covalent Crosslinking*. *Annual Plant Reviews* (Vol. 41). https://doi.org/10.1002/9781444391015.ch1

Fry, S. C., Smith, R. C., Renwick, K. F., Martin, D. J., Hodge, S. K., & Matthews, K. J. (1992). Xyloglucan endotransglycosylase, a new wall-loosening enzyme activity from plants. *Biochemical Journal*, *282*(3), 821–828. https://doi.org/10.1042/bj2820821

Gaborieau, M., & Castignolles, P. (2011). Size-exclusion chromatography (SEC) of branched polymers and polysaccharides. *Analytical and Bioanalytical Chemistry*, *399*(4), 1413–1423. https://doi.org/10.1007/s00216-010-4221-7

Gall, H., Philippe, F., Domon, J.-M., Gillet, F., Pelloux, J., & Rayon, C. (2015). Cell Wall Metabolism in Response to Abiotic Stress. *Plants*, *4*(1), 112–166. https://doi.org/10.3390/plants4010112

Genovesi, V., Fornalé, S., Fry, S. C., Ruel, K., Ferrer, P., Encina, A., … Caparrós-Ruiz, D. (2008). ZmXTH1, a new xyloglucan endotransglucosylase/hydrolase in maize, affects cell wall structure and composition in *Arabidopsis thaliana*. *Journal of Experimental Botany*, *59*(4), 875–889. https://doi.org/10.1093/jxb/ern013

Giddings, T. H., Brower, D. L., & Andrew Staehelin, L. (1980). Visualization of particle complexes in the plasma membrane of *Micrasterias denticulata* associated with the formation of cellulose fibrils in primary and secondary cell walls. *Journal of Cell Biology*, *84*(2), 327–339. https://doi.org/10.1083/jcb.84.2.327

Gidley, M. J., Lillford, P. J., Rowlands, D. W., Lang, P., Dentini, M., Crescenzi, V., … Reid, J. S. G. (1991). Structure and solution properties of tamarind-seed charide, *214*, 299–314.

Handford, M., Rodriguez-Furlán, C., & Orellana, A. (2006). Nucleotide-sugar transporters: Structure, function and roles in vivo. *Brazilian Journal of Medical and Biological Research*, *39*(9), 1149–1158. https://doi.org/10.1590/S0100-879X2006000900002

Hardham, A. R., Takemoto, D., & White, R. G. (2008). Rapid and dynamic subcellular reorganization following mechanical stimulation of *Arabidopsis* epidermal cells mimics responses to fungal and oomycete attack. *BMC Plant Biology*, *8*, 1–15. https://doi.org/10.1186/1471-2229-8-63

Hayashi, T. (1989). Xyloglucans in the primary cell wall. *Annu. Rev. Plant Physiol. Mol. Biol.*, *40*, 139–168.

Hayashi, T., & Kaida, R. (2011). Functions of xyloglucan in plant cells. *Molecular Plant*, *4*(1), 17–24. https://doi.org/10.1093/mp/ssq063

Hayashi, T., Kato, Y., & Mastuda, K. (1980). xylogluacn from suspension cultured soybean cells.pdf. *Plant and Cell Physiology*, 1405–1418.

Hayashi, T., Takeda, T., Ogawa, K., & Mitsuishi, Y. (1994). Effects of the degree of polymerization on the binding of xyloglucans to cellulose. *Plant & Cell Physiology*, *35*(6), 893–899. Retrieved from http://www.ncbi.nlm.nih.gov/pubmed/7981962

Hématy, K., Cherk, C., & Somerville, S. (2009). Host-pathogen warfare at the plant cell wall. *Current Opinion in Plant Biology*, *12*(4), 406–413. https://doi.org/10.1016/j.pbi.2009.06.007

Herbers, K., Lorences, E. P., Barrachina, C., & Sonnewald, U. (2001). Functional characterisation of _*Nicotiana tabacum*_ xyloglucan endotransglycosylase (NtXET-1): generation of transgenic tobacco plants and changes in cell wall xyloglucan. *Planta*, *212*(2), 279–287. https://doi.org/10.1007/s004250000393

Hoffman, M., Jia, Z., Peña, M. J., Cash, M., Harper, A., Blackburn, A. R., … York, W. S. (2005). Structural analysis of xyloglucans in the primary cell walls of plants in the subclass Asteridae. *Carbohydrate Research*, *340*(11), 1826–1840. https://doi.org/10.1016/j.carres.2005.04.016

Huitema, E., Bos, J. I. B., Tian, M., Win, J., Waugh, M. E., & Kamoun, S. (2004). Linking sequence to phenotype in Phytophthora-plant interactions. *Trends in Microbiology*, *12*(4), 193–200. https://doi.org/10.1016/j.tim.2004.02.008

Hyodo, H., Yamakawa, S., Takeda, Y., Tsuduki, M., Yokota, A., Nishitani, K., & Kohchi, T. (2003). Active gene expression of a xyloglucan endotransglucosylase/hydrolase gene, XTH9, in inflorescence apices is related to cell elongation in *Arabidopsis thaliana*. *Plant Molecular Biology*, *52*(2), 473–482. https://doi.org/10.1023/A:1023904217641

Ibrahim, H. M. M., Hosseini, P., Alkharouf, N. W., Hussein, E. H. A., Gamal El-Din, A. E. K. Y., Aly, M. A. M., & Matthews, B. F. (2011). Analysis of Gene expression in soybean (*Glycine max*) roots in response to the root knot nematode *Meloidogyne incognita* using microarrays and KEGG pathways. *BMC Genomics*, *12*(1), 220. https://doi.org/10.1186/1471-2164-12-220

Ithal, N., Recknor, J., Nettleton, D., Hearne, L., Maier, T., Baum, T. J., & Mitchum, M. G. (2007). Parallel Genome-Wide Expression Profiling of Host and Pathogen During Soybean Cyst Nematode Infection of Soybean. *Molecular Plant-Microbe Interactions*, *20*(3), 293–305. https://doi.org/10.1094/MPMI-20-3-0293

Jan, A., Yang, G., Nakamura, H., Ichikawa, H., Kitano, H., Matsuoka, M., … Komatsu, S. (2004). Characterization of a xyloglucan endotransglucosylase gene that is up-regulated by gibberellin in rice. *Plant Physiology*, *136*(3), 3670–3681. https://doi.org/10.1104/pp.104.052274

Jia, Z., Cash, M., Darvill, A. G., & York, W. S. (2005). NMR characterization of endogenously O-acetylated oligosaccharides isolated from tomato (*Lycopersicon esculentum*) xyloglucan. *Carbohydrate Research*, *340*(11), 1818–1825. https://doi.org/10.1016/j.carres.2005.04.015

Jiao, Y., Vuong, T. D., Liu, Y., Meinhardt, C., Liu, Y., Joshi, T., … Nguyen, H. T. (2015). Identification and evaluation of quantitative trait loci underlying resistance to multiple HG types of soybean cyst nematode in soybean PI 437655. *Theoretical and Applied Genetics*, *128*(1), 15–23. https://doi.org/10.1007/s00122-014-2409-5

Kandoth, P. K., Ithal, N., Recknor, J., Maier, T., Nettleton, D., Baum, T. J., & Mitchum, M. G. (2011). The Soybean Rhg1 Locus for Resistance to the Soybean Cyst Nematode *Heterodera glycines* Regulates the Expression of a Large Number of Stress- and Defense-Related Genes in Degenerating Feeding Cells. *Plant Physiology*, *155*(4), 1960–1975. https://doi.org/10.1104/pp.110.167536

Kerr, E. M., & Fry, S. C. (2003). Pre-formed xyloglucans and xylans increase in molecular weight in three distinct compartments of a maize cell-suspension culture. *Planta*, *217*(2), 327–339. https://doi.org/10.1007/s00425-003-1027-2

Kim, M., Hyten, D. L., Bent, A. F., & Diers, B. W. (2010). Fine Mapping of the SCN Resistance Locus rhg1-b from PI 88788. *The Plant Genome Journal*, *3*(2), 81. https://doi.org/10.3835/plantgenome2010.02.0001

Kim, S. J., & Brandizzi, F. (2016). The plant secretory pathway for the trafficking of cell wall polysaccharides and glycoproteins. *Glycobiology*, *26*(9), 940–949. https://doi.org/10.1093/glycob/cww044

Klink, V. P., Hosseini, P., Matsye, P., Alkharouf, N. W., & Matthews, B. F. (2009). A gene expression analysis of syncytia laser microdissected from the roots of the *Glycine max* (soybean) genotype PI 548402 (Peking) undergoing a resistant reaction after infection by *Heterodera glycines* (soybean cyst nematode). *Plant Molecular Biology* (Vol. 71). https://doi.org/10.1007/s11103-009-9539-1

Klink, V. P., Hosseini, P., Matsye, P. D., Alkharouf, N. W., & Matthews, B. F. (2010). Syncytium gene expression in *Glycine max*[PI 88788]roots undergoing a resistant reaction to the parasitic nematode *Heterodera glycines*. *Plant Physiology and Biochemistry*, *48*(2–3), 176–193. https://doi.org/10.1016/j.plaphy.2009.12.003

Klink, V. P., Kim, K. H., Martins, V., MacDonald, M. H., Beard, H. S., Alkharouf, N. W., … Matthews, B. F. (2009). A correlation between host-mediated expression of parasite genes as tandem inverted repeats and abrogation of development of female *Heterodera glycines* cyst formation during infection of Glycine max. *Planta*, *230*(1), 53–71. https://doi.org/10.1007/s00425-009-0926-2

Klink, V. P., Overall, C. C., Alkharouf, N. W., MacDonald, M. H., & Matthews, B. F. (2007). Laser capture microdissection (LCM) and comparative microarray expression analysis of syncytial cells isolated from incompatible and compatible soybean (*Glycine max*) roots infected by the soybean cyst nematode (*Heterodera glycines*). *Planta*, *226*(6), 1389–1409. https://doi.org/10.1007/s00425-007-0578-z

Klink, V. P., Sharma, K., Pant, S. R., McNeece, B., Niraula, P., & Lawrence, G. W. (2017). Components of the SNARE-containing regulon are co-regulated in root cells undergoing defense. *Plant Signaling and Behavior*, *12*(2), 1–19. https://doi.org/10.1080/15592324.2016.1274481

Köhnke, T., Östlund, Å., & Brelid, H. (2011). Adsorption of arabinoxylan on cellulosic surfaces: Influence of degree of substitution and substitution pattern on adsorption characteristics. *Biomacromolecules*, *12*(7), 2633–2641. https://doi.org/10.1021/bm200437m

Kooiman, P. (1957). Amyloids of seed plants. *Nature*, *179*, 107–109.

Liu, Y. B., Lu, S. M., Zhang, J. F., Liu, S., & Lu, Y. T. (2007). A xyloglucan endotransglucosylase/hydrolase involves in growth of primary root and alters the deposition of cellulose in *Arabidopsis*. *Planta*, *226*(6), 1547–1560. https://doi.org/10.1007/s00425-007-0591-2

Lulai, E. C., & Corsini, D. L. (1998). Differential deposition of suberin phenolic and aliphatic domains and their roles in resistance to infection during potato tuber (*Solanum tuberosum* L.) wound-healing. *Physiological and Molecular Plant Pathology*, *53*(4), 209–222. https://doi.org/10.1006/pmpp.1998.0179

Mahalingam, R., & Skorupska, H. T. (1996). Cytological expression of early response to infection by *Heterodera glycines* Ichinohe in resistant P1 437654 soybean. *Genome*, *39*, 986–998.

Maris, A., Suslov, D., Fry, S. C., Verbelen, J. P., & Vissenberg, K. (2009). Enzymic characterization of two recombinant xyloglucan endotransglucosylase/hydrolase (XTH) proteins of *Arabidopsis* and their effect on root growth and cell wall extension. *Journal of Experimental Botany*, *60*(13), 3959–3972. https://doi.org/10.1093/jxb/erp229

Matsui, A., Yokoyama, R., Seki, M., Ito, T., Shinozaki, K., Takahashi, T., … Nishitani, K. (2005). AtXTH27 plays an essential role in cell wall modification during the development of tracheary elements. *Plant Journal*, *42*(4), 525–534. https://doi.org/10.1111/j.1365-313X.2005.02395.x

Matsye, P. D., Kumar, R., Hosseini, P., Jones, C. M., Tremblay, A., Alkharouf, N. W., … Klink, V. P. (2011). Mapping cell fate decisions that occur during soybean defense responses. *Plant Molecular Biology*, *77*(4–5), 513–528. https://doi.org/10.1007/s11103-011-9828-3

Matsye, P. D., Lawrence, G. W., Youssef, R. M., Kim, K. H., Lawrence, K. S., Matthews, B. F., & Klink, V. P. (2012). The expression of a naturally occurring, truncated allele of an α-SNAP gene suppresses plant parasitic nematode infection. *Plant Molecular Biology*, *80*(2), 131–155. https://doi.org/10.1007/s11103-012-9932-z

Mellerowicz, E. J., Immerzeel, P., & Hayashi, T. (2008). Xyloglucan: The molecular muscle of trees. *Annals of Botany*, *102*(5), 659–665. https://doi.org/10.1093/aob/mcn170

Miedes, E., Zarra, I., Hoson, T., Herbers, K., Sonnewald, U., & Lorences, E. P. (2011). Xyloglucan endotransglucosylase and cell wall extensibility. *Journal of Plant Physiology*, *168*(3), 196–203. https://doi.org/10.1016/j.jplph.2010.06.029

Muller, F., Manet, S., Jean, B., Chambat, G., Boué, F., Heux, L., & Cousin, F. (2011). SANS measurements of semiflexible xyloglucan polysaccharide chains in water reveal their self-avoiding statistics. *Biomacromolecules*, *12*(9), 3330–3336. https://doi.org/10.1021/bm200881x

Muszyński, A., O'Neill, M. A., Ramasamy, E., Pattathil, S., Avci, U., Peña, M. J., … Carlson, R. W. (2015). Xyloglucan, galactomannan, glucuronoxylan, and rhamnogalacturonan I do not have identical structures in soybean root and root hair cell walls. *Planta*, *242*(5), 1123–1138. https://doi.org/10.1007/s00425-015-2344-y

Naumann, M., Somerville, S. C., & Voigt, C. A. (2013). Differences in early callose deposition during adapted and non-adapted powdery mildew infection of resistant *Arabidopsis* lines. *Plant Signaling and Behavior*, *8*(6), 10–13. https://doi.org/10.4161/psb.24408

Nishikubo, N., Takahashi, J., Roos, A. A., Derba-Maceluch, M., Piens, K., Brumer, H., … Mellerowicz, E. J. (2011). Xyloglucan endo-Transglycosylase-Mediated Xyloglucan Rearrangements in Developing Wood of Hybrid Aspen. *Plant Physiology*, *155*(1), 399–413. https://doi.org/10.1104/pp.110.166934

Nishitani, K. (1998). Construction and restructuring of the cellulose-xyloglucan framework in the apoplast as mediated by the xyloglucan related protein family - A hypothetical scheme. *Journal of Plant Research*, *111*(1101), 159–166. https://doi.org/10.1007/BF02507162

Ochoa-Villarreal, M., Aispuro-Hernndez, E., Vargas-Arispuro, I., & ngel, M. (2012). Plant Cell Wall Polymers: Function, Structure and Biological Activity of Their Derivatives. *Polymerization*, (May 2014). https://doi.org/10.5772/46094

Pant, S. R., Matsye, P. D., McNeece, B. T., Sharma, K., Krishnavajhala, A., Lawrence, G. W., & Klink, V. P. (2014). Syntaxin 31 functions in *Glycine max* resistance to the plant parasitic nematode *Heterodera glycines*. *Plant Molecular Biology*, *85*(1–2), 107–121. https://doi.org/10.1007/s11103-014-0172-2

Park, Y. B., & Cosgrove, D. J. (2015). Xyloglucan and its interactions with other components of the growing cell wall. *Plant and Cell Physiology*, *56*(2), 180–194. https://doi.org/10.1093/pcp/pcu204

Pauly, M., Gille, S., Liu, L., Mansoori, N., de Souza, A., Schultink, A., & Xiong, G. (2013). Hemicellulose biosynthesis. *Planta*, *238*(4), 627–642. https://doi.org/10.1007/s00425-013-1921-1

Pena, M. J., Kong, Y., York, W. S., & O'Neill, M. A. (2012). A Galacturonic Acid-Containing Xyloglucan Is Involved in Arabidopsis Root Hair Tip Growth. *The Plant Cell*, *24*(11), 4511–4524. https://doi.org/10.1105/tpc.112.103390

Pogorelko, G., Lionetti, V., Fursova, O., Sundaram, R. M., Qi, M., Whitham, S. A., … Zabotina, O. A. (2013). *Arabidopsis* and *Brachypodium distachyon* Transgenic Plants Expressing *Aspergillus nidulans* Acetylesterases Have Decreased Degree of Polysaccharide Acetylation and Increased Resistance to Pathogens. *Plant Physiology*, *162*(1), 9–23. https://doi.org/10.1104/pp.113.214460

Popper, Z. A., & Fry, S. C. (2005). Widespread occurrence of a covalent linkage between xyloglucan and acidic polysaccharides in suspension-cultured angiosperm cells. *Annals of Botany*, *96*(1), 91–99. https://doi.org/10.1093/aob/mci153

Puthoff, D. P., Ehrenfried, M. L., Vinyard, B. T., & Tucker, M. L. (2007). GeneChip profiling of transcriptional responses to soybean cyst nematode, *Heterodera glycines*, colonization of soybean roots. *Journal of Experimental Botany*, *58*(12), 3407–3418. https://doi.org/10.1093/jxb/erm211

Rodrigues, E. P., Torres, A. R., da Silva Batista, J. S., Huergo, L., & Hungria, M. (2012). A simple, economical and reproducible protein extraction protocol for proteomics studies of soybean roots. *Genetics and Molecular Biology*, *35*(SUPPL.1), 348–352. https://doi.org/10.1590/S1415-47572012000200016

Rose, J. K. C., Braam, J., Fry, S. C., & Nishitani, K. (2002). The XTH family of enzymes involved in xyloglucan endotransglycosylation and endohyrdolosis: Current perspectives and a new unifying nomenclature. *Plant Cell Physiol.*, *43*(12), 1421–1435. https://doi.org/10.1093/pcp/pcf171

Sasidharan, R., & Pierik, R. (2010). Cell wall modification involving XTHs controls phytochrome-mediated petiole elongation in *Arabidopsis thaliana*. *Plant Signaling & Behavior*, *5*(11), 1491–1492. https://doi.org/10.4161/psb.5.11.13643

Scheible, W. R., & Pauly, M. (2004). Glycosyltransferases and cell wall biosynthesis: Novel players and insights. *Current Opinion in Plant Biology*, *7*(3), 285–295. https://doi.org/10.1016/j.pbi.2004.03.006

Scheller, H. V., & Ulvskov, P. (2010). Hemicelluloses. *Annual Review of Plant Biology*, *61*(1), 263–289. https://doi.org/10.1146/annurev-arplant-042809-112315

Shedletzky, E., Shmuel, M., Delmer, D. P., & Lamport, D. T. A. (1990). Adaptation and Growth of Tomato Cells on the Herbicide 2,6-Dichlorobenzonitrile Leads to Production of Unique Cell Walls Virtually Lacking a Cellulose-Xyloglucan Network. *Plant Physiol*, *94*, 980–987. https://doi.org/10.1104/pp.94.3.980

Shin, Y. K., Yum, H., Kim, E. S., Cho, H., Gothandam, K. M., Hyun, J., & Chung, Y. Y. (2006). BcXTH1, a Brassica campestris homologue of Arabidopsis XTH9, is associated with cell expansion. *Planta*, *224*(1), 32–41. https://doi.org/10.1007/s00425-005-0189-5

Sluiter, a., Hames, B., Ruiz, R., Scarlata, C., Sluiter, J., Templeton, D., & Crocker, D. (2012). NREL/TP-510-42618 analytical procedure - Determination of structural carbohydrates and lignin in Biomass. *Laboratory Analytical Procedure (LAP)*, (April 2008), 17. https://doi.org/NREL/TP-510-42618

Smith, A. H., Gill, W. M., Pinkard, E. A., & Mohammed, C. L. (2007). Anatomical and histochemical defence responses induced in juvenile leaves of Eucalyptus globulus and Eucalyptus nitens by Mycosphaerella infection. *Forest Pathology*, *37*(6), 361–373. https://doi.org/10.1111/j.1439-0329.2007.00502.x

Somerville, C., Bauer, S., Brininstool, G., Facette, M., Hamann, T., Milne, J., … Youngs, H. (2004). Toward a systems approach to understanding plant cell walls. *Science*, *306*(5705), 2206–2211. https://doi.org/10.1126/science.1102765

Sorensen, I., Domozych, D., & Willats, W. G. T. (2010). How Have Plant Cell Walls Evolved? *Plant Physiology*, *153*(2), 366–372. https://doi.org/10.1104/pp.110.154427

Sterling, J. D., Atmodjo, M. A., Inwood, S. E., Kumar Kolli, V. S., Quigley, H. F., Hahn, M. G., & Mohnen, D. (2006). Functional identification of an *Arabidopsis* pectin biosynthetic homogalacturonan galacturonosyltransferase. *Proceedings of the National Academy of Sciences*, *103*(13), 5236–5241. https://doi.org/10.1073/pnas.0600120103

Takeda, T., Furuta, Y., Awano, T., Mizuno, K., Mitsuishi, Y., & Hayashi, T. (2002). Suppression and acceleration of cell elongation by integration of xyloglucans in pea stem segments. *Proceedings of the National Academy of Sciences*, *99*(13), 9055–9060. https://doi.org/10.1073/pnas.132080299

Talbott, L. D., & Ray, P. M. (1992). Changes in molecular size of previously deposited and newly synthesized pea cell wall matrix polysaccharides : effects of auxin and turgor. *Plant Physiology*, *98*(1), 369–379. https://doi.org/10.1104/pp.98.1.369

Tenhaken, R. (2015). Cell wall remodeling under abiotic stress. *Frontiers in Plant Science*, *5*(January), 1–9. https://doi.org/10.3389/fpls.2014.00771

Thomas, R., Fang, X., Ranathunge, K., Anderson, T. R., Peterson, C. A., & Bernards, M. A. (2007). Soybean Root Suberin: Anatomical Distribution, Chemical Composition, and Relationship to Partial Resistance to *Phytophthora sojae*. *Plant Physiology*, *144*(1), 299–311. https://doi.org/10.1104/pp.106.091090

Thompson, J. E., & Fry, S. C. (2001). Restructuring of wall-bound xyloglucan by transglycosylation in living plant cells. *Plant Journal*, *26*(1), 23–34. https://doi.org/10.1046/j.1365-313X.2001.01005.x

Thompson, J. E., Smith, R. C., & Fry, S. C. (1997). Isopycnic Centrifugation in Caesium Trifluoroacetate. *Pharmacia*, *708*, 699–708.

Tokumoto, H. (2002). Changes in the Sugar Composition and Molecular Mass Distribution of Matrix Polysaccharides during Cotton Fiber Development. *Plant and Cell Physiology*, *43*(4), 411–418. https://doi.org/10.1093/pcp/pcf048

Toyooka, K., Goto, Y., Asatsuma, S., Koizumi, M., Mitsui, T., & Matsuoka, K. (2009). A Mobile Secretory Vesicle Cluster Involved in Mass Transport from the Golgi to the Plant Cell Exterior. *The Plant Cell Online*, *21*(4), 1212–1229. https://doi.org/10.1105/tpc.108.058933

Toyooka, K., & Matsuoka, K. (2009). Exo- and endocytotic trafficking of SCAMP2. *Plant Signaling & Behavior*, *4*(12), 1196–1198. https://doi.org/10.4161/psb.4.12.10075

Umemura, M., & Yuguchi, Y. (2009). Solvation of xyloglucan in water/alcohol systems by molecular dynamics simulation. *Cellulose*, *16*(3), 361–371. https://doi.org/10.1007/s10570-009-9278-0

Vanzin, G. F., Madson, M., Carpita, N. C., Raikhel, N. V, Keegstra, K., & Reiter, W.-D. (2002). The mur2 mutant of *Arabidopsis thaliana* lacks fucosylated xyloglucan because of a lesion in fucosyltransferase AtFUT1. *Proceedings of the National Academy of Sciences of the United States of America*, *99*(5), 3340–3345. https://doi.org/10.1073/pnas.052450699

Vissenberg, K., Fry, S. C., & Verbelen, J. P. (2001). Root hair initiation is coupled to a highly localized increase of xyloglucan endotransglycosylase action in *Arabidopsis* roots. *Plant Physiology*, *127*(3), 1125–1135. https://doi.org/10.1104/pp.010295

Voigt, C. A. (2014). Callose-mediated resistance to pathogenic intruders in plant defense-related papillae. *Frontiers in Plant Science*, *5*(April), 1–6. https://doi.org/10.3389/fpls.2014.00168

Yokoyama, R., Rose, J. K. C., & Nishitani, K. (2004). A Surprising Diversity and Abundance of Xyloglucan Endotransglucosylase / Hydrolases in Rice . Classification and Expression Analysis 1. *Society*, *134*(March), 1088–1099. https://doi.org/10.1104/pp.103.035261.sis

Zhao, W., & Colley, K. J. (2008). Nucleotide sugar transporters of the Golgi apparatus. *The Golgi Apparatus: State of the Art 110 Years after Camillo Golgi's Discovery*, 190–206. https://doi.org/10.1007/978-3-211-76310-0_13

Zhu, X. F., Shi, Y. Z., Lei, G. J., Fry, S. C., Zhang, B. C., Zhou, Y. H., … Zheng, S. J. (2012). XTH31, Encoding an in Vitro XEH/XET-Active Enzyme, Regulates Aluminum Sensitivity by Modulating in Vivo XET Action, Cell Wall Xyloglucan Content, and Aluminum Binding Capacity in *Arabidopsis*. *The Plant Cell*, *24*(11), 4731–4747. https://doi.org/10.1105/tpc.112.106039

CHAPTER IV

REGULATION OF OTHER DEFENSE GENES INVOLVED IN *G. MAX* UP AGAINST *H. GLYCINES* BY CIRCADIAN CLOCK ASSOCIATED 1-1 (CCA1-1)

Abstract

The circadian clock has been studied and its role as an endogenous regulator in developmental and physiological events have been well documented. In animals, an interaction between the immune system and circadian clock has been proven. Now, in recent studies, the clock-immune interaction is evident indicating circadian clock controlling plant innate immunity. In the analysis presented here, the gene expression of a panel of proven defense genes in *Gm*-CCA1-1-OE and *Gm*-CCA1-1-RNAi root samples have revealed a significant role of clock gene expression occurring in root cells undergoing defense to parasitism by *H. glycines*. In *G. max*, *Gm*-NDR1-1, usually associated with RPM1-INTERACTING PROTEIN 4 (*Gm*-RIN4-4), appears to function in defense by inducing the expression of *Gm*-CCA1-1. *Gm*-CCA1-1 is shown here to drive the expression of mitogen activating protein kinases (MAPKs) differently depending on either pathogen triggered immunity (PTI) or effector triggered immunity (ETI) branches of defense signaling. Besides interacting with defense genes, *Gm*-CCA1-1 induces the expression of *Gm*-XTH43. In a coordinated and rhythmic fashion, expression

controlled by clock genes responds to external stimuli and even may anticipate any changes in any particular event over the clock's 24 hour periodicity.

Introduction

The circadian clock intrinsically limits certain biochemical or physiological processes by effectively directing resources. It's role as an endogenous regulator in developmental and physiological events have been well documented in many organisms (Bell-Pedersen et al., 2005; Yakir et al., 2007). The plant circadian oscillator consists of an interlocking feedback loop. The main clock component, CCA1 is involved in activating *PRR* genes and repressing the expression of *TOC1*, *LUX*, *ELF3* and *ELF4* (Young, 1998; Park et al., 1999; Dunlap, 1999; Iwasaki & Kondo, 2000; Doyle et al., 2002; Mizoguchi et al., 2002; Hazen et al., 2005). *PRR* genes are involved in negative feedback inhibition of CCA1. Also, there is another feedback loop that occurs in the evening, Evening complex (EC), a trimeric protein assembly of LUX, ELF3 and ELF4 switches off the expression of *PRR*, resuming *CCA1* transcription (Ferre et al., 2005; Rawat et al., 2011). Another key transcription factor within the loop is TOC1, which in association with another component GI, induces *CCA1* expression (Dixon et al., 2011; Helfer et al., 2011; Huang et al., 2012).

Recent studies have indicated a possible interaction occurring between circadian clock genes and genes involved in defense signaling. This bidirectional regulation of the immune system in animals has been validated (Duhart et al., 2013; Scheiermann et al., 2013). Now, the clock-immune interaction is evident in plants indicating circadian clock in controlling plant innate immunity (Zhang et al., 2013). The circadian clock makes plants able to anticipate daily changes in abiotic and biotic factors, enhancing the immune

system (Lai et al., 2012; Yoshida et al., 2014). The clock components, when examined for their involvement in plant defense signaling towards possible pathogenic attack, proved to be true. The plant defense response, in an anticipation of likely pathogen attack, triggers both basal and R-gene mediated resistance and even cross-talk with other defense products (Wang et al., 2011; Zhang et al., 2013). These actions signify the importance of circadian rhythm and associated genes.

The defense genes involved in both R-gene specific programmed cell death (PCD) and general basal resistance is controlled positively and/or negatively by the main clock component CCA1 (Wang & Tobin, 1998; Harmer et al., 2000; Wang et al., 2011). There is a cross-talk between clock and defense activation of AtGRP7, which performs roles in floral transition, development and stress tolerance and plant defense. AtGRP7, as a slave constituent of oscillator, has been found to be affected in arrhythmic *CCA1* mutants (*cca1-1*) and *CCA1*-OE plants that shortens circadian period (Zhang et al., 2013). On the other hand, infection of both virulent and avirulent *P. syringae* strains shortens circadian period and similar feedback regulation recapitulates with flg22 treatment suggesting PTI induced by flg22 feedbacks to regulate clock activity (Bhardwaj et al., 2011; Zhang et al., 2013).

The circadian clock regulates the expression of members of the MAPK gene family, based on their particular function or network they are connected to different physiological and/or biochemical signal transduction processes. The clock regulates the expression of MAPK pathway by phosphorylation, thus activating signaling cascades further downstream (Bennett et al., 2013; Goldsmith & Bell-Pedersen, 2013; Jagodzik et al., 2018). These processes create rhythms in MAPK signal transduction along with

endogenous response pathway (Bennett et al., 2013; Goldsmith & Bell-Pedersen, 2013; Jagodzik et al., 2018). The MAPK cascade transduces input information in a discrete stepwise series of phosphorylation events from MAPKKKs (MEKKs), to MAPKKs (MEKs) to MAPKs (MPKs) (Ichimura et al., 2002; Jonak et al., 2002). However, in some of the instances or events, MAPKs function independently through autophosphorylation (Nagy et al., 2015). Expression of different suites of proven defense genes for PTI and ETI have been affected by MAPKs (McNeece et al., 2019). Thus, these observations demonstrate broad and possibly a coordinated influence on the outcome of pathogen infection in plants (Matsye et al., 2011, 2012; Pant et al., 2014; Sharma et al., 2016; McNeece et al., 2017; Klink et al., 2017).

NDR1, a plasma membrane (PM) protein, is activated during ETI (Mackey et al., 2002; Day et al., 2006). NDR1, in association with RIN4, activates ETI (Day et al., 2006). However, RIN4 can function independently of NDR1 performing negative regulation downstream in the absence of pathogen (Belkhadir et al., 2004). Another key protein found to be highly expressed in response to plant pathogen is XTH, a secretory protein, which is transported to site of infection through vesicle transport machinery through Golgi apparatus (Albert et al., 2004; Matsye et al., 2011; Pant et al., 2014; Sharma et al., 2016; McNeece et al., 2017). XTHs are responsible for either precise arrangement of XyG or incorporation of newly synthesized XyG into the cell wall matrix (Nishitani, 1998; Rose et al., 2002; Nishikubo et al., 2011;).

In the analysis presented here, the role of the main clock oscillator, CCA1, has been examined in *G. max* regarding its involvement in signal transduction, conferring both basal and R-gene mediated innate immunity to *H. glycines*. The aim here has been to

interconnect the circadian rhythm with early response kinases (MAPKs), NDR1, RIN4 and XTH proteins all already proven to be involved in defense against *H. glycines* (Matsye et al., 2012; Pant et al., 2014; Sharma et al., 2016; McNeece et al., 2017; McNeece et al., 2019). The present study examines the broad spectrum of expression of circadian clock and plant defense genes. The results show the relative expression and even cross talk occurring among them that could be interpreted and manipulated to identify novel ways of defense that have not been demonstrated before.

Materials and methods

Gene expression analyses

The transgenic plants have been made according to the procedures described earlier. The genes under transgenic analysis in this chapter are *G. max* homologs of GI-1, CCA1-1 (Chapter 2) and defense MAPKs (MAPK2, MAPK3-1, MAPK4-1, MAPK5-3, MAPK6-2, MAPK13-1, MAPK16-4 and MAPK20-2) and XTH43 (Pant et al., 2014; (McNeece et al., 2019). The qPCR analyses have been performed as drescibed previously using the $2^{-\Delta\Delta C}{}_{t}$ method that has been used to calculate the fold change in gene expression caused by genetic engineering event according to prior published methods (Livak & Schmittgen, 2001; Sharma et al., 2016; McNeece et al., 2017).

Results

Framework

The identification of *Gm*-NDR1-1 as a resistance gene, as well as the demonstration that its overexpression induces *Gm*-CCA1-1 expression (Figure 4.1), elucidates the regulatory role of *Gm*-CCA1-1 in defense (McNeece et al., 2017). The role

of NDR1 in defense extends beyond the activation of ETI to cellular and physiological response signal including activation of MAPKs (Century et al., 1995; Knepper et al., 2011). R-protein mediated signaling occurring during the pathogenic attack involves RIN4 interacting with NDR1 (Day et al., 2006), however, RIN4 can negatively regulate disease resistance downstream, independently of NDR1 in the absence of pathogen (Belkhadir et al., 2004). The circadian regulation of expression of MAPK pathway by phosphorylation occurs, thus activating further cascades downstream and explaining how the circadian clock generates rhythms in MAPK signal transduction along with stress response pathways endogenously (Bennett et al., 2013; Goldsmith & Bell-Pedersen, 2013; Jagodzik et al., 2018). In defense against plant pathogen, the cytoplasmic receptor FLAGELLIN-LIKE SIGNALING 2 (FLS2) recognizes invaders mediated by flg22 detection (Zipfel et al., 2004). In response by host plant, triggers early responses such as activation of MAPK cascades, accumulation of reactive oxygen species (ROS), production of nitric oxide (NO), as well as induces R-gene mediated response associated with SA-induced or mediated pathway that involves pathogenesis-related proteins (Delaney et al., 1994; Low & Merida, 1996; Glazebrook, 2005; Garcia-brugger et al., 2006; Ku et al., 2006). Other processes include vesicle transport machinery proteins such as syntaxin and VAMPs through Golgi apparatus leading to extensive hypersensitive reaction (HR) and SAR (Veronese et al., 2006; Matsye et al., 2012; Pant et al., 2014; Sharma et al., 2016). There is cross talk occurring between circadian clock and defense signaling by flg22, serving as an input signal to regulate clock activity (Wang et al., 2011; Zhang et al., 2013). Furthermore, XTH, an enzyme responsible for remodeling of

XyG in the cell wall, is expressed highly in response to plant pathogens (Albert et al., 2004; Pant et al., 2014).

Co-regulation of *Gm*-CCA1-1 occurs with *Gm*-NDR1-1 and *Gm*-RIN4-4

The OE and RNAi of *Gm*-CCA1-1 has been shown to confer resistance against *H. glycines* as demonstrated by a FI analysis (CHAPTER II). The qPCR analysis of *Gm*-CCA1-1 expression level in *Gm*-NDR1-1-OE and *Gm*-NDR1-1-RNAi samples (Figure 4.1) demonstrates that *Gm*-NDR1-1-OE induces the transcription of *Gm*-CCA1-1 while *Gm*-NDR1-1-RNAi reduces *Gm*-CCA1-1, respectively.

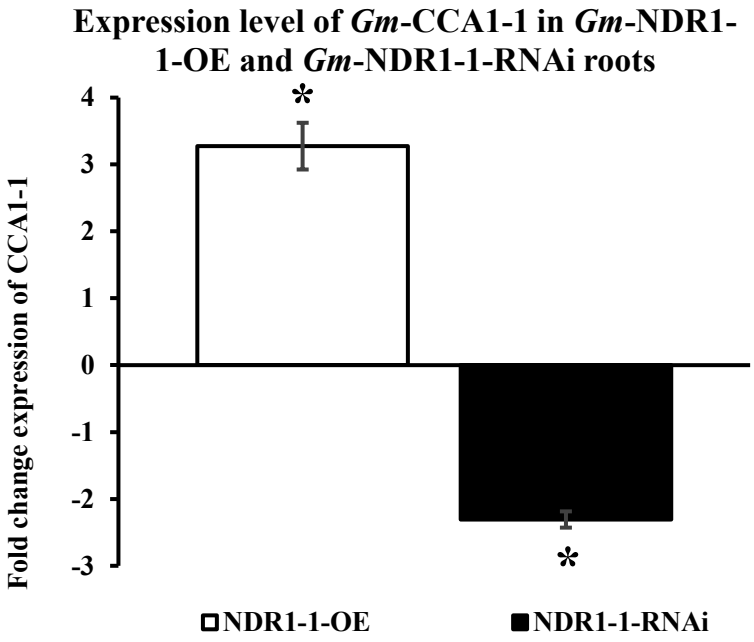

Figure 4.01 Induced expression of *Gm*-CCA1-1 in *Gm*-NDR1-1-OE and reduced expression in *Gm*-NDR1-1 RNAi.

Note: Three biological independent replicates were considered and run in triplicate. Error bars are standard error. * Statistically significant $p < 0.05$, determined using Mann-Whitney-Wilcoxon Rank Sum Test.

Furthermore, *Gm*-RIN4-4-OE roots have elevated levels of *Gm*-CCA1-1 while *Gm*-RIN4-4-RNAi has reduced the expression level of *Gm*-CCA1-1 (Figure 4.2)

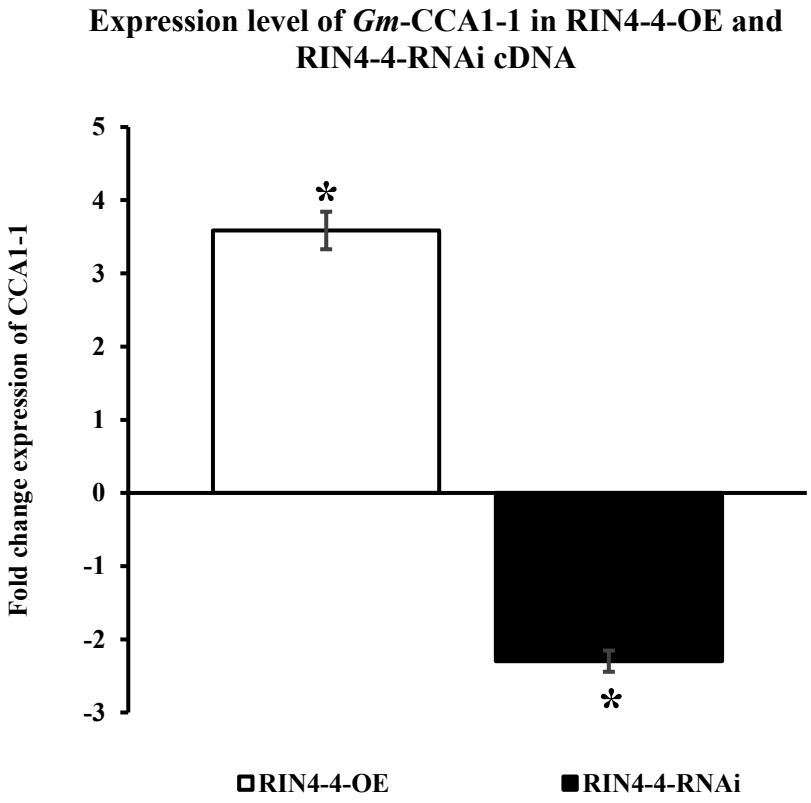

Figure 4.02 Induced expression of *Gm*-CCA1-1 in *Gm*-RIN4-4-OE and reduced expression in *Gm*-RIN4-4-RNAi.

Note: Three biological independent replicates were considered and run in triplicate. Error bars are standard error. * Statistically significant $p < 0.05$, determined using Mann-Whitney-Wilcoxon Rank Sum Test.

Our data clearly indicate that the *Gm*-CCA1-1 and *Gm*-NDR1-1 are co-regulated with defense activation feeding back to alter clock activity. The expression of *Gm*-NDR1-1 has been found to be induced in *Gm*-CCA1-1-OE and reduced in expression in *Gm*-CCA1-1-RNAi roots as shown in Figure 4.3.

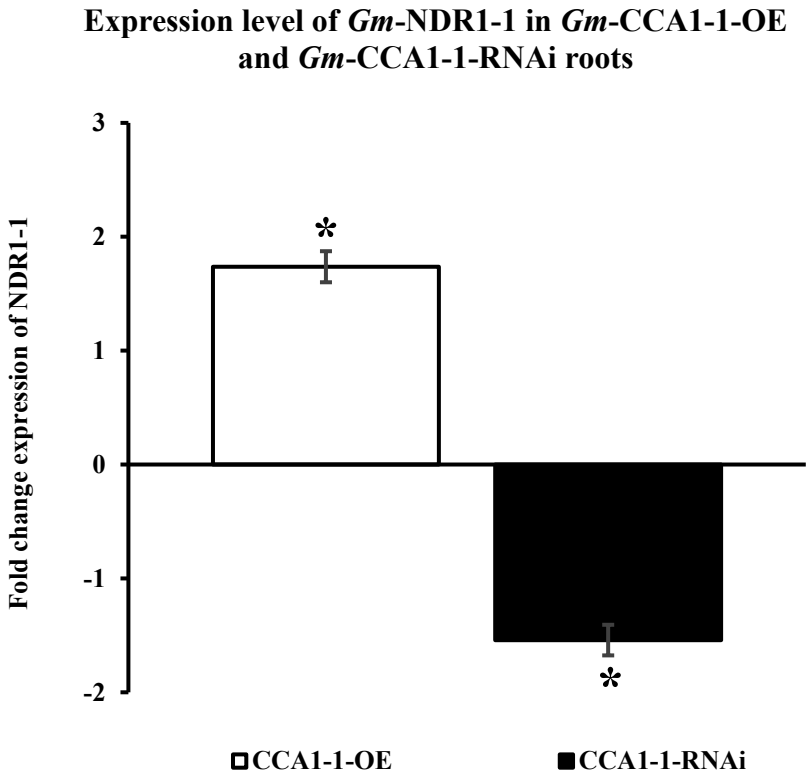

Figure 4.03 Induced expression of *Gm*-NDR1-1 in *Gm*-CCA1-1-OE and reduced expression in *Gm*-CCA1-1-RNAi.

Note: Three biological independent replicates were considered and run in triplicate. Error bars are standard error. * Statistically significant $p < 0.05$, determined using Mann-Whitney-Wilcoxon Rank Sum Test.

G. max MAPKs are regulated by the circadian main oscillator _Gm_-CCA1-1 as a part of signaling cascade

Gene expression of 9 different defense MAPKs have been analyzed in both *Gm*-CCA1-1-OE samples as well as *Gm*-CCA1-1 RNAi samples. mRNA has been isolated from these transgenic roots at different time points of a day (Samples have been taken in four hour intervals upto 24 hours starting from 4:00 AM). *Gm*-CCA1-1 has shown a pattern of expression when overexpressed or undergoing RNAi, peaking late in the day,

at about 8 PM (16 hours from the beginning of the experiment) in a 24-hour day-night condition (CHAPTER II).

Relative mRNA fold change expression of 9 *Gm*-MAPKs have been checked in *Gm*-CCA1-1-OE root samples at 7 different time points of a day. An arbitrary cutoff of ± 1.5 fold, $p < 0.05$ is considered differential expression (Pant et al., 2014). Overexpression of *Gm*-CCA1-1 in *G. max* has shown increased as well as decreased relative transcript levels of MAPKs at different time points. The most increased relative transcript level has been found for *Gm*-MAPK4-1 at the 16 hour time point (8:00 PM). Similarly, the most reduced level of expression has been observed for *Gm*-MAPK13-1 that has also occurred at the16 hour time point (8:00 PM) (Figure 4.4 and Appendix C).

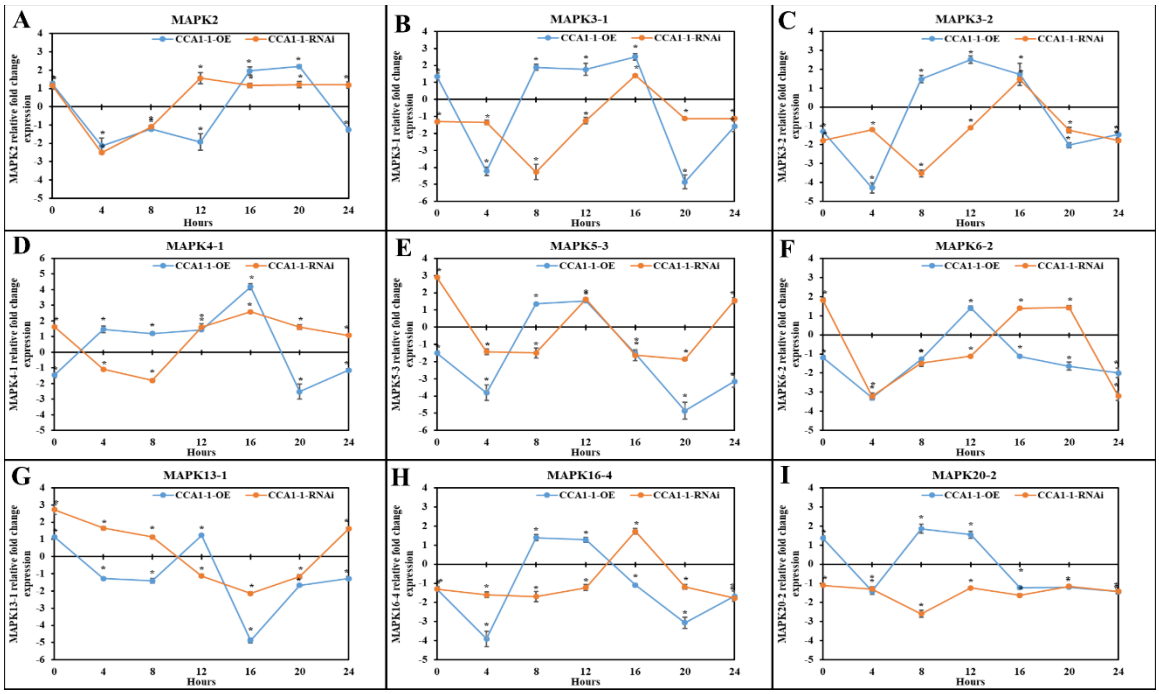

Figure 4.04 Expression pattern of *Gm*-MAPKs in *Gm*-CCA1-1-OE and RNAi lines in 24 hours. Nine different defense MAPKs have been used to examine their relative expression [A=MAPK2; B=MAPK3-1; C=MAPK3-2; D=MAPK4-1; E=MAPK5-3; F=MAPK6-2; G=MAPK13-1; H=MAPK16-4; I=MAPK20-2].

Note: Relative increase or decrease of transcript is considered as a fold change ±1.5, respectively. (*) represents ($p < 0.05$) statistically significant calculated for replicated qPCR analyses through t-test (Yuan et al., 2006). Values for standard error are indicated by bar

Relative fold abundance among the *Gm*-MAPKs in *Gm*-CCA1-1-RNAi samples has shown that the most expressed is *Gm*-MAPK5-3 at the zero hour time point (4:00 AM). In contrast, while the *Gm*-CCA1-1-RNAi has reduced the expression of most of MAPKs, the most reduced expression has been observed for *Gm*-MAPK3-1 at the 8 hour time point (12:00 PM) (Figure 4.4 and Appendix C).

As depicted from Figure 4.4 and Appendix C, the general pattern of expression observed to be higher during a day time (12:00PM to 8:00PM) for MAPK3-1, MAPK3-2

and MAPK4-1 in *Gm*-CCA1-1-OE. In contrast, *Gm*-CCA1-RNAi lines has reduced the expression of the same subsets of MAPKs (MAPK3-1, MAPK3-2, MAPK4-1) during early day time period (8:00AM to 12:00PM). Among 9 defense MAPKs, the expression of MAPK20-2, MAPK16-4, MAPK6-2, has been observed to be reduced in both *Gm*-CCA1-1-OE and *Gm*-CCA1-1-RNAi lines during most of the time points for 24 hours (Figure 4.4).

Gm*-CCA1-1 can influence the expression of target proteins relating to vesicle transport in *G. max* defense against *H. glycines

Gene expression experiments that are presented here have shown *Gm*-XTH43, a secretory protein transported into the site of pathogenic attack, to be induced in *Gm*-CCA1-1-OE lines (Figure 4.5) (Pant et al., 2014; Sharma et al., 2016). In contrast, *Gm*-XTH43 expression is suppressed in *Gm*-CCA1-1-RNAi lines (Figure 4.5) (Pant et al., 2014; Sharma et al., 2016). Furthermore, the *Gm*-NDR1-1 associated protein *Gm*-RIN4-4 has also been shown as an inducer of *Gm*-XTH43 as qPCR studies show *Gm*-XTH43 is increased in each of the *Gm*-RIN4-4-OE line while being decreased in *Gm*-RIN4-4-RNAi lines (Figure 4.6).

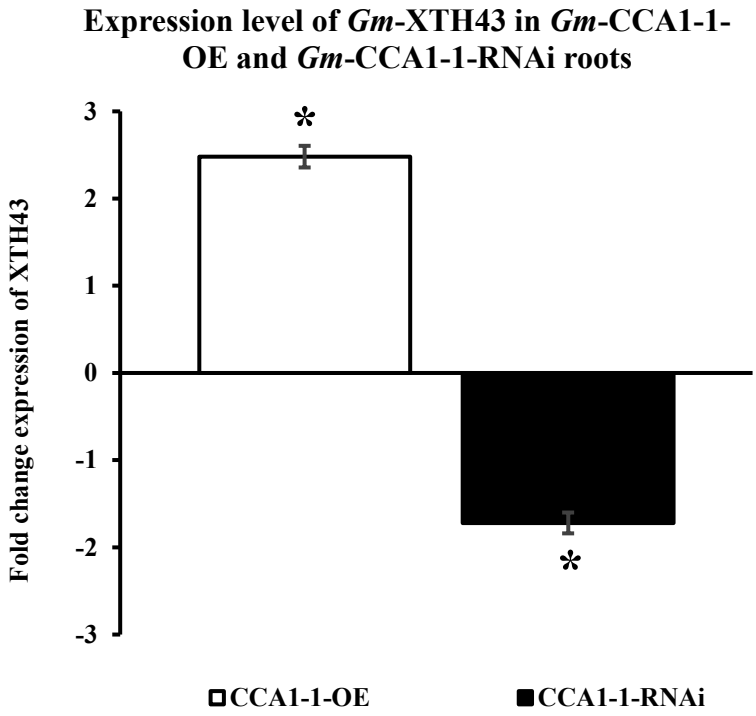

Figure 4.05 Induced expression of *Gm*-XTH43 in *Gm*-CCA1-1-OE and reduced expression in *Gm*-CCA1-1-RNAi lines.

Note: Three biological independent replicates have been considered and run in triplicate. Error bars are standard error. * Statistically significant $p < 0.05$, determined using Mann-Whitney-Wilcoxon Rank Sum Test.

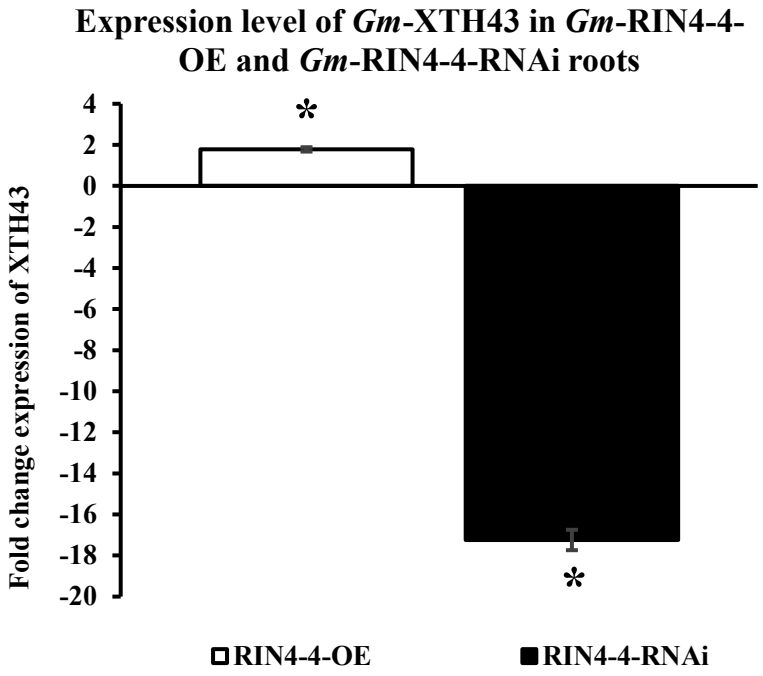

Figure 4.06 Induced expression of *Gm*-XTH43 in *Gm*-RIN4-4-OE and reduced expression in *Gm*-RIN4-4-RNAi.

Note: Three biological independent replicates have been considered and run in triplicate. Error bars are standard error. * Statistically significant $p < 0.05$, determined using Mann-Whitney-Wilcoxon Rank Sum Test.

Discussion

While the role of NDR1, along with another associated protein RIN4 has been identified as functioning in defense activation following perception of the pathogen, the intrinsic role of these proteins anticipating the possible pathogen attack has been addressed by the present study in *G. max* (Day et al., 2006; McNeece et al., 2017). NDR1, a PM localized protein, has an NDR1-RIN4 interaction on the N-terminal portion of NDR1 which is required for activation of ETI (Mackey et al., 2002; Day et al., 2006).

The role of *Gm*-NDR1-1 as a plant nematode defense protein has already been demonstrated, first identified to be highly expressed in syncytia formed at the feeding site of *H. glycines* undergoing the process of resistance (Klink et al., 2007, 2010, 2017; Matsye et al., 2012; Pant et al., 2014; Sharma et al., 2016; McNeece et al., 2017). The defense role of *Gm*-NDR1-1 is further corroborated with an association with *Gm*-RIN4-4 protein which is also expressed during the defense response in the syncytium (McNeece et al., 2017).

In *G. max*, *Gm*-NDR1-1 induces *Gm*-CCA1-1 expression which is the internal immune modulator. In *A. thaliana*, the role of CCA1 has been shown to mediate both basal and R-gene mediated PTI and ETI in plant defense against biotrophic plant pathogens (Wang et al., 2011; Zhang et al., 2013). The results presented here indicate that there is even cross talk between the circadian clock and defense signaling as *Gm*-NDR1-1 is observed to be induced in *Gm*-CCA1-1-OE plants and suppressed in *Gm*-CCA1-1-RNAi plants. These results are consistent with the defense signaling by pathogen-responsive genes in *A. thaliana* coding for AtGRP7 and FLS2 which are circadian regulated (Heintzen et al., 1997; Molina et al., 1997; Zhang et al., 2013).

In this study, a direct transcriptional control of defense *Gm*-MAPKs identified in an earlier analysis by the circadian clock has been discovered (McNeece et al., 2019). Although *Gm*-CCA1-1 could be affecting post-transcriptional signaling after pathogen recognition via receptors and phosphorylation cascades, only the expression of MAPKs has been elucidated here. The clock control of MAPK gene regulation would be expected as both are considered evolutionarily conserved and, thus, have had long time frames to establish cross-talk. Consistent with this idea, several higher eukaryotic model systems

have showed rhythms in phosphorylated forms of MAPKs (Williams et al., 2001; Hayashi et al., 2001, 2003; Coogan & Piggins, 2003; Hasegawa & Cahill, 2004; Vitalini et al., 2007).

We have demonstrated that the *Gm*-CCA1-1 regulates transcript levels differently among MAPKs, most of them peaking in their expression in the subjective evening/night while few are peaking in the subjective morning/day. The most abundant MAPK in transcript level has been observed for *Gm*-MAPK4-1, which has been shown to function as a defense gene family in different plant pathosystems (Qiu et al., 2008; Andreasson & Ellis, 2010; Zhou et al., 2014; Zhang et al., 2016; McNeece et al., 2019). Experiments that have been presented here show that overexpressing *Gm*-CCA1-1 results in the induction of subset of *Gm*-MAPKs, including MAPK2, MAPK3-1, MAPK3-2, MAPK4-1, MAPK5-3 and MAPK20-2, occurring at least at one time point. However, the expression of The *Gm*-MAPKs, including MAPK6-2, MAPK13-1 and MAPK16-4 remain unchanged. The result from *Gm*-CCA1-1-RNAi experiments show suppressed expression of all the defense MAPKs occurring at least at one time point of a day. Some of the MAPKs, including MAPK2, MAPK4-1, MAPK5-3, MAPK6-2 MAPK13-1, MAPK16-4, happen to be induced even in *Gm*-CCA1-1 RNAi samples. Complex forms of gene expression relating to *Gm*-MAPK-OE and *Gm*-MAPK-RNAi have been observed to be occurring within this gene family (McNeece et al., 2019). However, in some of these cases, the *Gm*-CCA1-1-RNAi lines appear to have altered the timing of MAPK expression (Figure 4.4).

The clock components affect defense MAPK gene expression in different ways. Some MAPKs are constitutively active, driving an intrinsic defense response (Genot et

al., 2017). Other MAPKs activate other defense genes, resulting in both PTI and ETI branches of defense signaling that reflect their biological function (Xiong & Yang, 2003; Ren et al., 2006; Wang et al., 2016). Such observations reflect the fact that circadian clock functions in cooperative manner with existing MAPK signaling pathway kinases. In one way, clock components induce a subset of MAPKs that are involved in defense responses by activating a signaling cascade which ultimately increases the expression of a number of defense genes. Other possibilities include the coordinately controlled kinase pathways occurring in rhythmic fashion in a way that would respond to external stimuli allowing an organism to anticipate any change in a particular event within the 24 hour periodicity.

Our experimental approach used to analyze the expression of *Gm*-XTH43 in *Gm*-CCA1-1-OE and *Gm*-CCA1-1-RNAi roots demonstrate their interconnection. *Gm*-CCA1-1 induces expression of *Gm*-XTH43 when overexpressed and suppressed in the RNAi lines. These results corroborate the defense role of circadian rhythm-mediated physiological processes in the plant, particularly enhancing the defense process involving *Gm*-XTH43 which is transported by vesicle machinery through Golgi apparatus (Albert et al., 2004; Matsye et al., 2011; Pant et al., 2014; Sharma et al., 2016; McNeece et al., 2017). In this study, the level of *Gm*-XTH43 has been shown to be expressed in *Gm*-RIN4-4-OE lines and highly suppressed in *Gm*-RIN4-4-RNAi lines, respectively. These results indicate that *Gm*-RIN4-4 functions independently or functions in association with the *Gm*-NDR1-1 signal, involved in protein cargo machinery in order to transport secretory protein to the site of infection including *Gm*-XTH43 protein. XTH has been shown to function by remodeling existing XyG chains or integrating newly synthesized

XyG, resulting in physical/chemical barrier (Hardham et al., 2008; Nishikubo et al., 2011). These observations provide insight into how circadian components regulates defense gene and defense gene products like *Gm*-XTH43, which are transported to site of infection by vesicle transport. Such a mechanism is supposed to limit cellular expansion or strengthen wall through XyG remodeling or/and integration, preventing access to plant pathogens and/or cell wall degrading enzymes secreted by the pathogens.

References

Albert, M., Werner, M., Proksch, P., Fry, S. C., & Kaldenhoff, R. (2004). The cell wall-modifying xyloglucan endotransglycosylase/hydrolase LeKTH1 is expressed during the defence reaction of tomato against the plant parasite *Cuscuta reflexa*. *Plant Biology*, *6*(4), 402–407. https://doi.org/10.1055/s-2004-817959

Andreasson, E., & Ellis, B. (2010). Convergence and specificity in the *Arabidopsis* MAPK nexus. *Trends in Plant Science*, *15*(2), 106–113. https://doi.org/10.1016/j.tplants.2009.12.001

Belkhadir, Y., Nimchuk, Z., Hubert, D. A., Mackey, D., & Dangl, J. L. (2004). *Arabidopsis* RIN4 Negatively Regulates Disease Resistance Mediated by RPS2 and RPM1 Downstream or Independent of the NDR1 Signal Modulator and Is Not Required for the Virulence Functions of Bacterial Type III Effectors, *16*(October), 2822–2835. https://doi.org/10.1105/tpc.104.024117.mammalian

Bell-Pedersen, D., Cassone, V. M., Earnest, D. J., Golden, S. S., Hardin, P. E., Thomas, T. L., & Zoran, M. J. (2005). Circadian rhythms from multiple oscillators: lessons from diverse organisms. *Nature Reviews Genetics*, *6*, 544. Retrieved from http://dx.doi.org/10.1038/nrg1633

Bennett, L. D., Beremand, P., Thomas, T. L., & Bell-pedersen, D. (2013). Circadian Activation of the Mitogen-Activated Protein Kinase MAK-1 Facilitates Rhythms in Clock-Controlled Genes in *Neurospora crassa*, *12*(1), 59–69. https://doi.org/10.1128/EC.00207-12

Bhardwaj, V., Meier, S., Petersen, L. N., Ingle, R. A., & Roden, L. C. (2011). Defence responses of arabidopsis thaliana to infection by pseudomonas syringae are regulated by the circadian clock. *PLoS ONE*, *6*(10), 1–8. https://doi.org/10.1371/journal.pone.0026968

Century, K. S., Holubt, E. B., & Staskawiczt, B. J. (1995). NDRJ , a locus of Arabidopsis thaliana that is required for disease resistance to both a bacterial and a fungal pathogen, *92*(July), 6597–6601.

Coogan, A. N., & Piggins, H. D. (2003). Circadian and Photic Regulation of Phosphorylation of ERK1/2 and Elk-1 in the Suprachiasmatic Nuclei of the Syrian Hamster. *The Journal of Neuroscience*, *23*(7), 3085–3093. https://doi.org/10.1523/JNEUROSCI.23-07-03085.2003

Day, B., Dahlbeck, D., & Staskawicz, B. J. (2006). NDR1 Interaction with RIN4 Mediates the Differential Activation of Multiple Disease Resistance Pathways in *Arabidopsis*, *18*(October), 2782–2791. https://doi.org/10.1105/tpc.106.044693

Delaney, T. P., Uknes, S., Vernooij, B., Friedrich, L., Weymann, K., Negrotto, D., … Ryals, J. (1994). A Central Role of Salicylic Acid in Plant Disease Resistance. *Science*, *266*(5188), 1247 LP-1250. https://doi.org/10.1126/science.266.5188.1247

Dixon, L. E., Knox, K., Kozma-Bognar, L., Southern, M. M., Pokhilko, A., & Millar, A. J. (2011). Temporal repression of core circadian genes is mediated through EARLY FLOWERING 3 in *Arabidopsis*. *Current Biology*, *21*(2), 120–125. https://doi.org/10.1016/j.cub.2010.12.013

Doyle, M. R., Davis, S. J., Bastow, R. M., McWatters, H. G., Kozma-Bognar, L., Nagy, F., … Amasino, R. M. (2002). The ELF4 gene controls circadian rhythms and flowering time in *Arabidopsis thaliana*. *Nature*, *419*(6902), 74–77. https://doi.org/10.1038/nature00955.1.

Duhart, J. M., Leone, M. J., Paladino, N., Evans, J. A., Castanon-cervantes, O., Alec, J., & Golombek, D. A. (2013). Suprachiasmatic Astrocytes Modulate the Circadian Clock in Response to TNF- α. https://doi.org/10.4049/jimmunol.1300450

Dunlap, J. C. (1999). Molecular bases for circadian clocks. *Cell*, *96*(2), 271–290. https://doi.org/10.1016/S0092-8674(00)80566-8

Ferre, E., Harmer, S., Harmon, F., & Yanovsky, M. (2005). Overlapping and Distinct Roles of PRR7 and PRR9 in the *Arabidopsis* Circadian Clock. *Cutis*, *15*(1), 47–54. https://doi.org/10.1016/j

Garcia-brugger, A., Lamotte, O., Vandelle, E., Bourque, S., Lecourieux, D., Poinssot, B., … Pugin, A. (2006). Early Signaling Events Induced by Elicitors of Plant Defenses, *19*(7), 711–724.

Genot, B., Lang, J., Berriri, S., Garmier, M., Gilard, F., & Pateyron, S. (2017). Constitutively Active *Arabidopsis* MAP Kinase 3 Triggers Defense Responses Involving Salicylic Acid and SUMM2, *174*(June), 1238–1249. https://doi.org/10.1104/pp.17.00378

Glazebrook, J. (2005). A GAINST B IOTROPHIC AND N ECROTROPHIC. https://doi.org/10.1146/annurev.phyto.43.040204.135923

Goldsmith, C. S., & Bell-pedersen, D. (2013). Diverse Roles for MAPK Signaling in Circadian Clocks, 1–35. https://doi.org/10.1016/B978-0-12-407703-4.00001-3.Diverse

Goldsmith, C. S., & Bell-Pedersen, D. (2013). Chapter One - Diverse Roles for MAPK Signaling in Circadian Clocks. In T. Friedmann, J. C. Dunlap, & S. F. B. T.-A. in G. Goodwin (Eds.) (Vol. 84, pp. 1–39). Academic Press. https://doi.org/https://doi.org/10.1016/B978-0-12-407703-4.00001-3

Hardham, A. R., Takemoto, D., & White, R. G. (2008). Rapid and dynamic subcellular reorganization following mechanical stimulation of *Arabidopsis* epidermal cells mimics responses to fungal and oomycete attack. *BMC Plant Biology*, *8*, 1–15. https://doi.org/10.1186/1471-2229-8-63

Harmer, S. L., Hogenesch, J. B., Straume, M., Chang, H.-S., Han, B., Zhu, T., … Kay, S. A. (2000). Orchestrated Transcription of Key Pathways in *Arabidopsis* by the Circadian Clock. *Science*, *290*(5499), 2110 LP-2113. Retrieved from http://science.sciencemag.org/content/290/5499/2110.abstract

Hasegawa, M., & Cahill, G. M. (2004). Regulation of the circadian oscillator in Xenopus retinal photoreceptors by protein kinases sensitive to the stress-activated protein kinase inhibitor, SB 203580. *Journal of Biological Chemistry*, *279*(21), 22738–22746. https://doi.org/10.1074/jbc.M401389200

Hayashi, Y., Sanada, K., & Fukada, Y. (2001). Circadian and photic regulation of MAP kinase by Ras- and protein phosphatase-dependent pathways in the chick pineal gland. *FEBS Letters*, *491*(1–2), 71–75. https://doi.org/10.1016/S0014-5793(01)02153-6

Hayashi, Y., Sanada, K., Hirota, T., Shimizu, F., & Fukada, Y. (2003). p38 Mitogen-activated Protein Kinase Regulates Oscillation of Chick Pineal Circadian Clock. *Journal of Biological Chemistry*, *278*(27), 25166–25171. https://doi.org/10.1074/jbc.M212726200

Hazen, S. P., Schultz, T. F., Pruneda-Paz, J. L., Borevitz, J. O., Ecker, J. R., & Kay, S. A. (2005). LUX ARRHYTHMO encodes a Myb domain protein essential for circadian rhythms. *Proceedings of the National Academy of Sciences of the United States of America*, *102*(29), 10387–10392. https://doi.org/10.1073/pnas.0503029102

Heintzen, C., Nater, M., Apel, K., & Staiger, D. (1997). At GRP7 , a nuclear RNA-binding protein as a component of a circadian-regulated negative feedback loop in *Arabidopsis thaliana*, *94*(August), 8515–8520.

Helfer, A., Nusinow, D. A., Chow, B. Y., Gehrke, A. R., Bulyk, M. L., & Kay, S. A. (2011). LUX ARRHYTHMO encodes a nighttime repressor of circadian gene expression in the *Arabidopsis* core clock. *Current Biology*, *21*(2), 126–133. https://doi.org/10.1016/j.cub.2010.12.021

Huang, W., Pérez-García, P., Pokhilko, A., Millar, A., Antoshechkin, I., Riechmann, L., & Mas, P. (2012). Mapping the Core of the *Arabidopsis* Circadian Clock Defines the Network Structure of the Oscillator. *Science*, *338*(November), 643–646.

Ichimura, K., Shinozaki, K., Tena, G., Sheen, J., Henry, Y., Champion, A., … Walker, J. C. (2002). Mitogen-activated protein kinase cascades in plants: a new nomenclature. *Trends in Plant Science*, *7*(7), 301–308. https://doi.org/https://doi.org/10.1016/S1360-1385(02)02302-6

Iwasaki, H., & Kondo, T. (2000). The current state and problems of circadian clock studies in cyanobacteria. *Plant and Cell Physiology*, *41*(9), 1013–1020. https://doi.org/10.1093/pcp/pcd024

Jagodzik, P., Tajdel-zielinska, M., & Ciesla, A. (2018). Mitogen-Activated Protein Kinase Cascades in Plant Hormone Signaling, *9*(October), 1–26. https://doi.org/10.3389/fpls.2018.01387

Jonak, C., Ökrész, L., Bögre, L., & Hirt, H. (2002). Complexity, Cross Talk and Integration of Plant MAP Kinase Signalling. *Current Opinion in Plant Biology*, *5*(5), 415–424. https://doi.org/https://doi.org/10.1016/S1369-5266(02)00285-6

Klink, V. P., Alkharouf, N., MacDonald, M., & Matthews, B. (2005). Laser Capture Microdissection (LCM) and expression analyses of *Glycine max* (soybean) syncytium containing root regions formed by the plant pathogen *Heterodera glycines* (soybean cyst nematode). *Plant Molecular Biology*, *59*(6), 965–979. https://doi.org/10.1007/s11103-005-2416-7

Klink, V. P., Hosseini, P., Matsye, P. D., Alkharouf, N. W., & Matthews, B. F. (2010). Syncytium gene expression in *Glycine max*[PI 88788]roots undergoing a resistant reaction to the parasitic nematode *Heterodera glycines*. *Plant Physiology and Biochemistry*, *48*(2–3), 176–193. https://doi.org/10.1016/j.plaphy.2009.12.003

Klink, V. P., Kim, K. H., Martins, V., MacDonald, M. H., Beard, H. S., Alkharouf, N. W., … Matthews, B. F. (2009). A correlation between host-mediated expression of parasite genes as tandem inverted repeats and abrogation of development of female *Heterodera glycines* cyst formation during infection of *Glycine max*. *Planta*, *230*(1), 53–71. https://doi.org/10.1007/s00425-009-0926-2

Klink, V. P., Overall, C. C., Alkharouf, N. W., MacDonald, M. H., & Matthews, B. F. (2007). Laser capture microdissection (LCM) and comparative microarray expression analysis of syncytial cells isolated from incompatible and compatible soybean (*Glycine max*) roots infected by the soybean cyst nematode (*Heterodera glycines*). *Planta*, *226*(6), 1389–1409. https://doi.org/10.1007/s00425-007-0578-z

Klink, V. P., Sharma, K., Pant, S. R., Mcneece, B., Lawrence, G. W., Klink, V. P., … Lawrence, W. (2017). Components of the SNARE-containing regulon are co-regulated in root cells undergoing defense. *Plant Signaling & Behavior*, *12*(2), 1–19. https://doi.org/10.1080/15592324.2016.1274481

Knepper, C., Savory, E. A., & Day, B. (2011). The role of NDR1 in pathogen perception and plant defense signaling, *6*(8), 1114–1116. https://doi.org/10.4161/psb.6.8.15843

Ku, I., Qutob, D., Kemmerling, B., Engelhardt, S., Gust, A. A., Luberacki, B., … Nu, T. (2006). Phytotoxicity and Innate Immune Responses Induced by Nep1-Like Proteins, *18*(December), 3721–3744. https://doi.org/10.1105/tpc.106.044180

Lai, A. G., Doherty, C. J., Mueller-Roeber, B., Kay, S. A., Schippers, J. H. M., & Dijkwel, P. P. (2012). CIRCADIAN CLOCK-ASSOCIATED 1 regulates ROS homeostasis and oxidative stress responses. *Proceedings of the National Academy of Sciences*, *109*(42), 17129–17134. https://doi.org/10.1073/pnas.1209148109

Livak, K. J., & Schmittgen, T. D. (2001). Analysis of Relative Gene Expression Data Using Real-Time Quantitative PCR and the 2−ΔΔCT Method. *Methods*, *25*(4), 402–408. https://doi.org/https://doi.org/10.1006/meth.2001.1262

Low, P. S., & Merida, J. R. (1996). The oxidative burst in plant defense: Function and signal transduction. *Physiologia Plantarum*, *96*(3), 533–542. https://doi.org/10.1111/j.1399-3054.1996.tb00469.x

Mackey, D., Iii, B. F. H., Wiig, A., Dangl, J. L., Hill, C., & Carolina, N. (2002). RIN4 Interacts with *Pseudomonas syringae* Type III Effector Molecules and Is Required for RPM1-Mediated Resistance in Arabidopsis, *108*, 743–754.

Matsye, P. D., Kumar, R., Hosseini, P., Jones, C. M., Tremblay, A., Alkharouf, N. W., … Klink, V. P. (2011). Mapping cell fate decisions that occur during soybean defense responses. *Plant Molecular Biology*, *77*(4–5), 513–528. https://doi.org/10.1007/s11103-011-9828-3

Matsye, P. D., Lawrence, G. W., Youssef, R. M., Kim, K. H., Lawrence, K. S., Matthews, B. F., & Klink, V. P. (2012). The expression of a naturally occurring, truncated allele of an α-SNAP gene suppresses plant parasitic nematode infection. *Plant Molecular Biology*, *80*(2), 131–155. https://doi.org/10.1007/s11103-012-9932-z

Matthews, B. F., Beard, H., MacDonald, M. H., Kabir, S., Youssef, R. M., Hosseini, P., & Brewer, E. (2013). Engineered resistance and hypersusceptibility through functional metabolic studies of 100 genes in soybean to its major pathogen, the soybean cyst nematode. *Planta*, *237*(5), 1337–1357. https://doi.org/10.1007/s00425-013-1840-1

McNeece, B., Sharma, K., Lawrence, G. W., Lawrence, K. S., & Klink, V. P. (2019). The mitogen activated protein kinase (MAPK) gene family functions as a cohort during the Glycine max defense response to Heterodera glycines. *Plant Physiology and Biochemistry*, 1–19. https://doi.org/https://doi.org/10.1016/j.plaphy.2019.01.018

McNeece, B. T., Pant, S. R., Sharma, K., Niruala, P., Lawrence, G. W., & Klink, V. P. (2017). A *Glycine max* homolog of NON-RACE SPECIFIC DISEASE RESISTANCE 1 (NDR1) alters defense gene expression while functioning during a resistance response to different root pathogens in different genetic backgrounds. *Plant Physiology and Biochemistry*, *114*, 60–71. https://doi.org/10.1016/j.plaphy.2017.02.022

McNeece, B. T., Sharma, K., Lawrence, G. W., Lawrence, K. S., & Klink, V. P. (2018). Mitogen activated protein kinases function as a cohort during a plant defense response. *BioRxiv*, 396192. https://doi.org/10.1101/396192

Mizoguchi, T., Wheatley, K., Hanzawa, Y., Wright, L., Mizoguchi, M., Song, H. R., … Coupland, G. (2002). LHY and CCA1 are partially redundant genes required to maintain circadian rhythms in Arabidopsis. *Developmental Cell*, *2*(5), 629–641. https://doi.org/10.1016/S1534-5807(02)00170-3

Molina, A., Mena, M., Carbonero, P., & Garcia-Olmedo, F. (1997). Differential expression of pathogen-responsive genes encoding two types of glycine-rich proteins in barley. *Plant Molecular Biology*, *33*(5), 803–810.

Nagy, S. K., Darula, Z., Kállai, B. M., Bögre, L., Bánhegyi, G., Medzihradszky, K. F., … Mészáros, T. (2015). Activation of AtMPK9 through autophosphorylation that makes it independent of the canonical MAPK cascades. *Biochemical Journal*, *467*(1), 167 LP-175. https://doi.org/10.1042/BJ20141176

Nishikubo, N., Takahashi, J., Roos, A. A., Derba-Maceluch, M., Piens, K., Brumer, H., … Mellerowicz, E. J. (2011). Xyloglucan endo-Transglycosylase-Mediated Xyloglucan Rearrangements in Developing Wood of Hybrid Aspen. *Plant Physiology*, *155*(1), 399–413. https://doi.org/10.1104/pp.110.166934

Nishitani, K. (1998). Construction and restructuring of the cellulose-xyloglucan framework in the apoplast as mediated by the xyloglucan related protein family - A hypothetical scheme. *Journal of Plant Research*, *111*(1101), 159–166. https://doi.org/10.1007/BF02507162

Pant, S. R., Matsye, P. D., McNeece, B. T., Sharma, K., Krishnavajhala, A., Lawrence, G. W., & Klink, V. P. (2014). Syntaxin 31 functions in *Glycine max* resistance to the plant parasitic nematode *Heterodera glycines*. *Plant Molecular Biology*, *85*(1–2), 107–121. https://doi.org/10.1007/s11103-014-0172-2

Park, D. H., Somers, D. E., Kim, Y. S., Choy, Y. H., Lim, H. K., Soh, M. S., … Nam, H. G. (1999). Control of Circadian Rhythms and Photoperiodic Flowering by the Arabidopsis GIGANTEA Gene. *Science*, *285*(5433), 1579 LP-1582. Retrieved from http://science.sciencemag.org/content/285/5433/1579.abstract

Qiu, J. L., Fiil, B. K., Petersen, K., Nielsen, H. B., Botanga, C. J., Thorgrimsen, S., … Petersen, M. (2008). Arabidopsis MAP kinase 4 regulates gene expression through transcription factor release in the nucleus. *EMBO Journal*, *27*(16), 2214–2221. https://doi.org/10.1038/emboj.2008.147

Rawat, R., Takahashi, N., Hsu, P. Y., Jones, M. A., Schwartz, J., Salemi, M. R., … Harmer, S. L. (2011). REVEILLE8 and PSEUDO-REPONSE REGULATOR5 form a negative feedback loop within the *Arabidopsis* circadian clock. *PLoS Genetics*, *7*(3). https://doi.org/10.1371/journal.pgen.1001350

Ren, D., Yang, K., Li, G., Liu, Y., Zhang, S., & Nonse-like. (2006). Activation of Ntf4 , a Tobacco Mitogen-Activated Protein Kinase , during Plant Defense Response and Its Involvement in Hypersensitive, *141*(August), 1482–1493. https://doi.org/10.1104/pp.106.080697.addition

Rose, J. K. C., Braam, J., Fry, S. C., & Nishitani, K. (2002). The XTH family of enzymes involved in xyloglucan endotransglycosylation and endohyrdolosis: Current perspectives and a new unifying nomenclature. *Plant Cell Physiol.*, *43*(12), 1421–1435. https://doi.org/10.1093/pcp/pcf171

Scheiermann, C., Kunisaki, Y., & Frenette, P. S. (2013). Circadian control of the immune system. *Nature Reviews Immunology*, *13*, 190. Retrieved from https://doi.org/10.1038/nri3386

Sharma, K., Pant, S. R., McNeece, B. T., Lawrence, G. W., & Klink, V. P. (2016). Co-regulation of the *Glycine max* soluble N-ethylmaleimide-sensitive fusion protein attachment protein receptor (SNARE)-containing regulon occurs during defense to a root pathogen. *Journal of Plant Interactions*, *11*(1), 74–93. https://doi.org/10.1080/17429145.2016.1195891

Veronese, P., Nakagami, H., Bluhm, B., AbuQamar, S., & Chen X. (2006). The Membrane-Anchored BOTRYTIS-INDUCED KINASE1 Plays Distinct Roles in *Arabidopsis* Resistance to Necrotrophic and Biotrophic Pathogens. *The Plant Cell Online*, *18*(1), 257–273. https://doi.org/10.1105/tpc.105.035576

Vitalini, M. W., de Paula, R. M., Goldsmith, C. S., Jones, C. A., Borkovich, K. A., & Bell-Pedersen, D. (2007). Circadian rhythmicity mediated by temporal regulation of the activity of p38 MAPK. *Proceedings of the National Academy of Sciences*, *104*(46), 18223–18228. https://doi.org/10.1073/pnas.0704900104

Wang, F., Wang, C., Yan, Y., Jia, H., & Guo, X. (2016). Overexpression of Cotton GhMPK11 Decreases Disease Resistance through the Gibberellin Signaling Pathway in Transgenic *Nicotiana benthamiana*, *7*(May), 1–16. https://doi.org/10.3389/fpls.2016.00689

Wang, W., Barnaby, J. Y., Tada, Y., Li, H., Tör, M., Caldelari, D., … Dong, X. (2011). Timing of plant immune responses by a central circadian regulator. *Nature*, *470*(7332), 110–115. https://doi.org/10.1038/nature09766

Wang, Z. Y., & Tobin, E. M. (1998). Constitutive expression of the CIRCADIAN CLOCK ASSOCIATED 1 (CCA1) gene disrupts circadian rhythms and suppresses its own expression. *Cell*, *93*(7), 1207–1217. https://doi.org/10.1016/S0092-8674(00)81464-6

Williams, J. A., Su, H. S., Bernards, A., Field, J., & Sehgal, A. (2001). A Circadian Output in Drosophila Mediated by Neurofibromatosis-1 and Ras/MAPK. *Science*, *293*(5538), 2251 LP-2256. https://doi.org/10.1126/science.1063097

Xiong, L., & Yang, Y. (2003). Disease Resistance and Abiotic Stress Tolerance in Rice Are Inversely Modulated by an Abscisic Acid – Inducible Mitogen-Activated Protein Kinase, *15*(March), 745–759. https://doi.org/10.1105/tpc.008714.ported

Yakir, E., Hilman, D., Harir, Y., & Green, R. M. (2007). Regulation of output from the plant circadian clock, *274*, 335–345. https://doi.org/10.1111/j.1742-4658.2006.05616.x

Yoshida, T., Mogami, J., & Yamaguchi-Shinozaki, K. (2014). ABA-dependent and ABA-independent signaling in response to osmotic stress in plants. *Current Opinion in Plant Biology*, *21*, 133–139. https://doi.org/10.1016/j.pbi.2014.07.009

Young, M. W. (1998). The molecular control of circadian behavioral rhythms and their entrainment in Drosophila. *Annual Review of Biochemistry*, *67*, 135–152. https://doi.org/10.1146/annurev.biochem.67.1.135

Yuan, J. S., Reed, A., Chen, F., & Jr, C. N. S. (2006). Statistical analysis of real-time PCR data, *12*, 1–12. https://doi.org/10.1186/1471-2105-7-85

Zhang, C., Xie, Q., Anderson, R. G., Ng, G., Seitz, N. C., Peterson, T., … Lu, H. (2013). Crosstalk between the Circadian Clock and Innate Immunity in *Arabidopsis*. *PLoS Pathogens*, *9*(6). https://doi.org/10.1371/journal.ppat.1003370

Zhang, X., Wang, G., Gao, J., Nie, M., Liu, W., & Xia, Q. (2016). Functional analysis of NtMPK2 uncovers its positive role in response to *Pseudomonas syringae* pv. tomato DC3000 in tobacco. *Plant Molecular Biology*, *90*(1–2), 19–31. https://doi.org/10.1007/s11103-015-0391-1

Zhou, J., Wu, S., Chen, X., Liu, C., Sheen, J., Shan, L., & He, P. (2014). The *Pseudomonas syringae* effector HopF2 suppresses Arabidopsis immunity by targeting BAK1. *Plant Journal*, *77*(2), 235–245. https://doi.org/10.1111/tpj.12381

Zipfel, C., Robatzek, S., Navarro, L., Oakeley, E. J., Jones, J. D. G., Felix, G., & Boller, T. (2004). Bacterial disease resistance in *Arabidopsis* through flagellin perception. *Nature*, *428*, 764. Retrieved from https://doi.org/10.1038/nature02485

CHAPTER V

CONCLUSION

The work presented here, along with determining the functional effect of clock oscillator genes against the plant root nematode *H. glycines*, demonstrates the expression pattern of clock component *Gm*-CCA1-1 in *G. max* roots in 24-hours day-night (LD) condition. The expression of circadian clock genes has been examined along with results of recent studies which have identified genes expressed to higher levels during the defense response in *G. max* against *H. glycines* parasitism (Klink et al., 2007; Klink et al., 2017; Matsye et al., 2011, 2012; Pant et al., 2014; Sharma et al., 2016; McNeece et al., 2017). The study presented here has demonstrated the involvement of circadian clock with other defense genes that could trigger PTI or ETI and there is even cross-talk occurring between clock components and defense genes. The observation of induced expression of *Gm*-XTH43, which is secretory protein transported by vesicle transport machinery, corroborates that the clock likely controls the systemic immune response in plant cell against biotrophic pathogens.

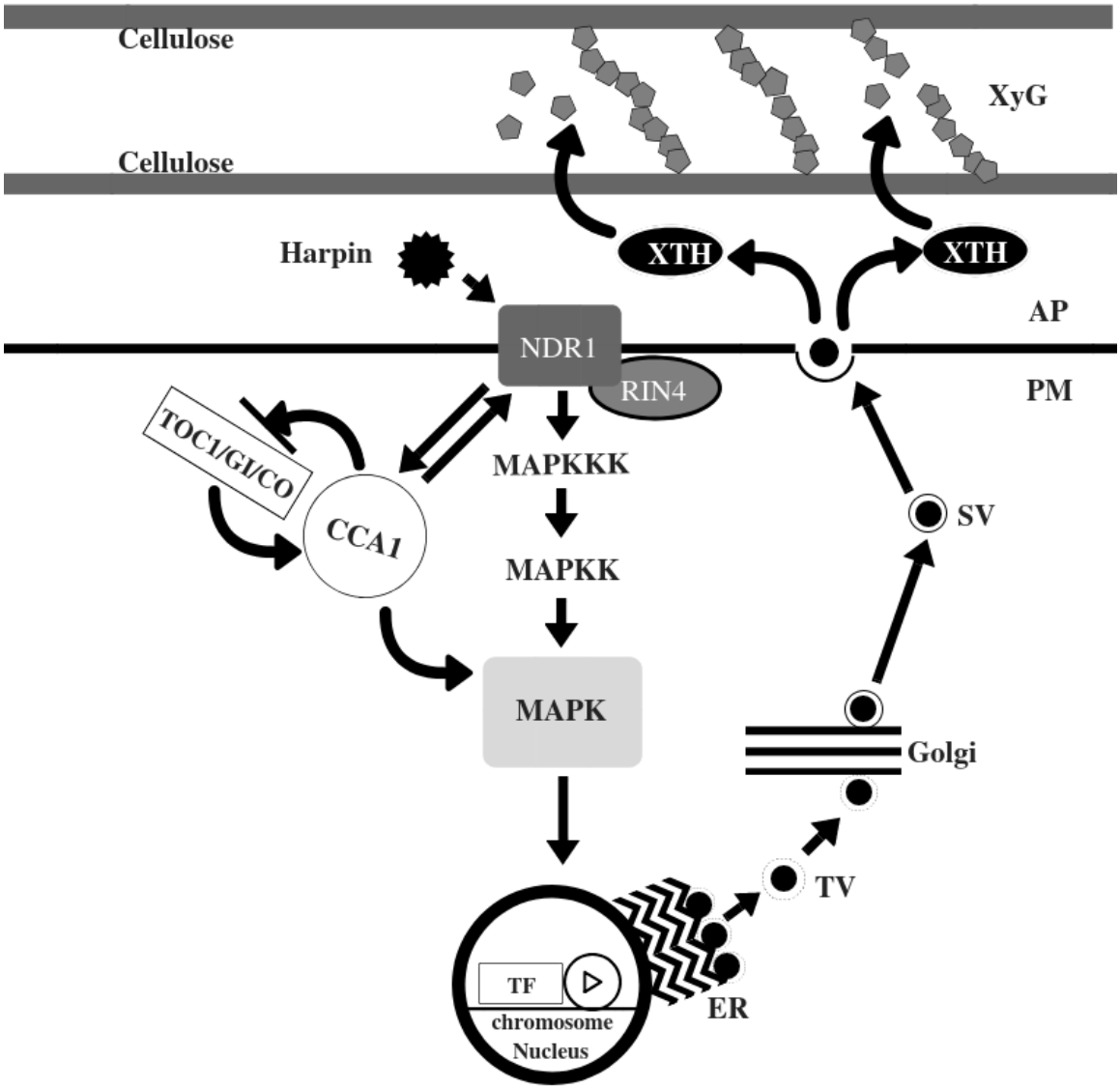

Figure 5.01 Defense model. *G. max* NDR1(*Gm*-DNR1-1) induced by effector (Harpin). NDR1 is associated with another transmembrane protein RIN4(*Gm*-RIN4-4). NDR1 is capable of inducing MAPKs cascade and CCA1 (*Gm*-CCA1-1) or even cross talking with each other. CCA1 is activated by TOC1/GI/CO (*Gm*-TOC1-1/*Gm*-GI-1/*Gm*-CO-4). MAPKs induces the transcription and translation of protein products like XTH (*Gm*-XTH43) that suppresses *H. glycines* parasitism in *G. max*.

Note: [TF, transcription factor; ER, endoplasmic reticulum; SV, secretory vesicle; TV, transition vesicle; PM, plasma membrane; AP, apoplast; XyG, xyloglucan]

***Gm*-CCA1-1 along with other clock component genes function during the defense process in the root**

The experiments presented here show that *Gm*-CCA1-1 functions in the resistance process that *G. max* has toward *H. glycines*. The results of a functional effect of other clock oscillators such as *Gm*-TOC1-1, *Gm*-GI-1, *Gm*-CO-4 genes against the root nematode suggests that collectively, the clock oscillator enhances resistance against biotrophic pathogen such as *H. glycines* in the root system. The functional experiment used to determine gene involvement in defense has characterized *Gm*-CCA1-1 as the most likely to confer resistance more than the other clock components. In the *Gm*-CCA1-1-OE lines, a statistically significantly lower amount of *H. glycines* parasitism has been identified in the wr (FI=34.9, SD=3.8) and pg (FI=29.9, SD=3.7) analyses. Similarly, in the *Gm*-CCA1-1-RNAi lines also a statistically significant increase in parasitism has been observed in both wr (FI=408.7, SD=10.06) and pg (FI=445.7, SD=38.2). The functional effect of other clock oscillator *Gm*-TOC1-1, *Gm*-GI-1, *Gm*-CO-4 against plant nematode is proof that the genes functions in defense in association with *Gm*-CCA1-1. In *A. thaliana*, TOC1 is a key transcription factor functioning in the clock loop, which in association with GI, activates expression of CCA1 (Dixon et al., 2011; Helfer et al., 2011; Huang et al., 2012). Also, CO has been described as protein homologous to TOC1, having a 43-amino acid region of homology found in *A. thaliana* (Robson et al., 2001).

Further study has characterized the role of *Gm*-CCA1-1 in defense against *H. glycines*. A significant change in expression of *Gm*-CCA1-1 in *Gm*-CCA1-1-OE roots among infected and uninfected plant root has been observed. The amplitude and average expression level of *Gm*-CCA1-1 is reduced in infected plant roots among the OE lines. However, no significant change in amplitude and expression level has been noticed

among the *Gm*-CCA1-1-RNAi lines. These observations reinforce the results in a study on human tumor cells that circadian genes are repressed in tumor cells (Filipski et al., 2005). In plant systems such as *A. thaliana*, as well, altered circadian rhythms and shortened periods of CCA1 expression are observed in pathogenic infection (Zhang et al., 2013). Our findings, notably, demonstrate that clock components are arrested and/or altered in their expression impair the infection process by nematode. As clock components are a global transcript regulator including regulating defense genes, a disrupted circadian rhythm might be a greater consequence in plant cell. Also, the present study has been conducted under light/dark (LD) condition. In order to identify the cross talk between clock component and infection, other conditions of constant light (LL), constant dark (DD) could be performed to determine sole defense role of clock component, but not by light factor. However, clearly, the rhythmic pattern of CCA1-1 expression is happening in the root in the absence of light.

The role of *Gm*-XTH43 in XyG rearrangement as defense mechanism against plant pathogen *H. glycines*

The current study has shown that total XyG amount occurs higher in root samples of *Gm*-XTH43-OE plants and lower amount in *Gm*-XTH43-RNAi lines than their respective control plants. In a complementary study, similar results of increased overall XyG content in XTH-OE in *Populus* sp. has been reported (Nishikubo et al., 2011). In *Gm*-XTH43-OE lines, a statistically significant, higher amount of XyG has been observed in tightly bound sugars than the pRAP15-control (C) samples, (X-OE=11.21%, SD=2.22; C=5.36%, SD=0.13) that has not been observed in the loosely bound sugars analyses (X-OE=1.99%, SD=0.14; C=1.90%, SD=0.38). A significant increase in XyG

amount (X-OE=0.47%, SD=0.09; C=0.23%, SD=0.09) in total dry mass of root sample has also been observed in *Gm*-XTH43-OE lines. However, in XTH43-RNAi lines, although a decrease in total XyG in total dry mass (X-RN=0.16%, SD=0.06; C=0.25%, SD=0.09) and relative decrease of XyG in tightly bound sugars (X-RN=4.70%, SD=0.32; C=7.10%, SD=2.00) while slightly increased in loosely bound sugars (X-RN=1.73%, SD=0.40; C=1.49%, SD=0.57) has been observed, the results are not statistically significant.

In this XyG quantitation study, it has been demonstrated that higher XyG amounts to positively and lower amounts to negatively correlate to how *Gm*-XTH43 gene expression is regulated. Further analyses have shown larger amounts of XyG in tightly bound (24% KOH-extraction) than loosely bound (4% KOH-extraction). The results suggest the role of XTH in generation and developmental rearrangement of XyG in the plant. XyG is reported to change soon after deposition including an increase in size, depolymerization and increment in amount during cell wall expansion (Talbott & Ray, 1992; Thompson et al., 1997; Tokumoto et al., 2002; Kerr & Fry, 2003; Popper & Fry, 2005). Although some previous studies have found a mixed effect of XyG in the transition of loosely bound sugars to tightly bound to cellulose microfibrils network, a definitive role of XTH has been revealed by Nishikubo et al. (2011) in which XTH activity reported to promote XyG incorporation into the cell wall of tightly bound fraction (Herbers et al., 2001; Liu, Lu, Zhang, Liu, & Lu, 2007; Genovesi et al., 2008; Miedes et al., 2011; Zhu et al., 2012; Miedes et al., 2013).

The observation of lower weight average MW of XyG in *Gm*-XTH43-OE and higher MW of XyG in *Gm*-XTH43-RNAi than respective control plants (as shown in

Appendix B) might be associated with cell wall strengthening by XTH-mediated remodeling of the XyG chain. The function of XTH appears more complex regarding chain length and extensibility of cellulose- XyG network (Jan et al., 2004; Shin et al., 2006). In an agreement with our study, Nishikubo et al. (2011) also reported the shift toward lower molecular mass of XyG from the samples of XTH-OE lines in *Populus* species and Herbers et al. (2001) noticed an increase in XyG size by 20% when its XTH gene is suppressed in its expression. However, the chain length estimation of XyG based on MW through GPC must be regarded with caution as they are sensitive to conformation (Park & Cosgrove, 2015). It is plausible that the observation of MW sugars are not all XyG, but also multiple polysaccharide reorganization in the cell wall architecture.

***Gm*-CCA1-1 co-regulates the expression of the cell membrane protein genes *Gm*-NDR1-1 and *Gm*-RIN4-4**

The qPCR analysis of *Gm*-CCA1-1 expression in *Gm*-NDR1-1-OE and *Gm*-NDR1-1-RNAi samples has demonstrated that *Gm*-NDR1-1-OE induces the transcription of *Gm*-CCA1-1. In contrast, *Gm*-NDR1-1-RNAi suppresses *Gm*-CCA1-1 expression. The role of *Gm*-NDR1-1 in plant defense against the plant nematode, *H. glycines,* has already been identified in the feeding site undergoing the process of resistance (Klink et al., 2007, 2010, 2017; Matsye et al., 2012; Pant et al., 2014; Sharma et al., 2016; McNeece et al., 2017). Prior NDR1 results have demonstrated the NDR1-RIN4 interaction on the N-terminal portion of NDR1 is required for activation of ETI following the perception of pathogen (Mackey et al., 2002; Day et al., 2006). While the defense role of NDR1 in association with RIN4 has been established in previous studies, the intrinsic role of

circadian regulating these proteins and possible anticipation of pathogen attack has been addressed by the present study.

The expression pattern of *Gm*-CCA1-1 regulates the expression of *Gm*-MAPKs functioning in defense in *G. max*

The study presented here has demonstrated that *Gm*-CCA1-1 regulates the expression of *Gm*-MAPKs differently, most of them peaking in their expression in the subjective evening/night while few in the subjective morning/day. In *Gm*-CCA1-1-OE lines, the most increased relative transcript level has been found for *Gm*-MAPK4-1 at the 16 hour time point (8:00 PM) of a day. Similarly, in *Gm*-CCA1-1-RNAi lines, the most reduced expression has been noted to *Gm*-MAPK3-1 at the 8 hour time point (12:00 PM). Regardless of abundance at some time point, all *Gm*-MAPKs have shown a rhythmic pattern in their expression. A clock control of MAPK regulation is expected as both are considered evolutionarily conserved, and found to exhibit rhythms in their phosphorylated form of MAPKs in higher eukaryotic model systems (Hayashi et al., 2001, 2003; Coogan & Piggins, 2003; Hasegawa & Cahill, 2004; Vitalini et al., 2007).

A direct transcriptional control of defense genes by *Gm*-MAPKs after pathogen recognition via receptors and phosphorylation cascades has been discovered as biological regulation in plants (McNeece et al., 2019). Some MAPKs are constitutively active during defense response while some MAPKs activate other defense genes resulting in both PTI and ETI branches of defense signaling cascades (Xiong & Yang, 2003; Ren et al., 2006; Wang et al., 2016; Genot et al., 2017) Such observations of rhythmic, but varied patterns of expression of *Gm*-MAPKs along with *Gm*-CCA1-1 in *G. max* reflect clock-MAPKs coexistence in signaling pathway kinases.

***Gm*-CCA1-1 influences the expression of *Gm*-XTH43**

The experiments presented here show that *Gm*-XTH43, a secretory protein transported via vesicle transport machinery into the site of pathogenic attack, is induced in *Gm*-CCA1-1-OE lines while being suppressed in *Gm*-CCA1-1-RNAi lines in *G. max* (Pant et al., 2014; Sharma et al., 2016). Also, *Gm*-RIN4-4-OE has increased the expression of *Gm*-XTH43 while being decreased in *Gm*-RIN4-4-RNAi lines. In *A. thaliana*, RIN4 usually is associated with NDR1, a transmembrane protein, functioning to mediate signaling in pathogenic attack for defense response as ETI (Day et al., 2006). However, RIN4 can negatively regulate disease resistance downstream, independently of NDR1 in the absence of pathogen (Belkhadir et al., 2004). The expression results presented here corroborate the defense role of *Gm*-CCA1-1 in plants, particularly enhancing the defense process involving *Gm*-XTH43 which is transported by vesicle machinery through Golgi apparatus (Albert et al., 2004; Matsye et al., 2011; Pant et al., 2014; Sharma et al., 2016; McNeece et al., 2017). Furthermore, the results presented here indicates the possible involvement of *Gm*-RIN4-4, with or without an association of *Gm*-NDR1, in protein cargo machinery in order to transport secretory protein like *Gm*-XTH43 to the site of infection. The *Gm*-XTH43 protein then would function by remodeling the existing XyG chain or integrating newly synthesized XyG, resulting in physical/chemical barrier in cell wall (Rose et al., 2002; Hardham et al., 2008; Nishikubo et al., 2011).

References

Albert, M., Werner, M., Proksch, P., Fry, S. C., & Kaldenhoff, R. (2004). The cell wall-modifying xyloglucan endotransglycosylase/hydrolase LeKTH1 is expressed during the defence reaction of tomato against the plant parasite *Cuscuta reflexa*. *Plant Biology*, *6*(4), 402–407. https://doi.org/10.1055/s-2004-817959

Belkhadir, Y., Nimchuk, Z., Hubert, D. A., Mackey, D., & Dangl, J. L. (2004). Arabidopsis RIN4 Negatively Regulates Disease Resistance Mediated by RPS2 and RPM1 Downstream or Independent of the NDR1 Signal Modulator and Is Not Required for the Virulence Functions of Bacterial Type III Effectors, *16*(October), 2822–2835. https://doi.org/10.1105/tpc.104.024117.mammalian

Coogan, A. N., & Piggins, H. D. (2003). Circadian and Photic Regulation of Phosphorylation of ERK1/2 and Elk-1 in the Suprachiasmatic Nuclei of the Syrian Hamster. *The Journal of Neuroscience*, *23*(7), 3085–3093. https://doi.org/10.1523/JNEUROSCI.23-07-03085.2003

Day, B., Dahlbeck, D., & Staskawicz, B. J. (2006). NDR1 Interaction with RIN4 Mediates the Differential Activation of Multiple Disease Resistance Pathways in *Arabidopsis*, *18*(October), 2782–2791. https://doi.org/10.1105/tpc.106.044693

Dixon, L. E., Knox, K., Kozma-Bognar, L., Southern, M. M., Pokhilko, A., & Millar, A. J. (2011). Temporal repression of core circadian genes is mediated through EARLY FLOWERING 3 in *Arabidopsis*. *Current Biology*, *21*(2), 120–125. https://doi.org/10.1016/j.cub.2010.12.013

Filipski, E., Innominato, P. F., Wu, M. W., Li, X. M., Iacobelli, S., Xian, L. J., & Lévi, F. (2005). Effects of light and food schedules on liver and tumor molecular clocks in mice. *Journal of the National Cancer Institute*, *97*(7), 507–517. https://doi.org/10.1093/jnci/dji083

Genot, B., Lang, J., Berriri, S., Garmier, M., Gilard, F., & Pateyron, S. (2017). Constitutively Active Arabidopsis MAP Kinase 3 Triggers Defense Responses Involving Salicylic Acid and SUMM2, *174*(June), 1238–1249. https://doi.org/10.1104/pp.17.00378

Genovesi, V., Fornalé, S., Fry, S. C., Ruel, K., Ferrer, P., Encina, A., … Caparrós-Ruiz, D. (2008). ZmXTH1, a new xyloglucan endotransglucosylase/hydrolase in maize, affects cell wall structure and composition in *Arabidopsis thaliana*. *Journal of Experimental Botany*, *59*(4), 875–889. https://doi.org/10.1093/jxb/ern013

Hardham, A. R., Takemoto, D., & White, R. G. (2008). Rapid and dynamic subcellular reorganization following mechanical stimulation of *Arabidopsis* epidermal cells mimics responses to fungal and oomycete attack. *BMC Plant Biology*, *8*, 1–15. https://doi.org/10.1186/1471-2229-8-63

Hasegawa, M., & Cahill, G. M. (2004). Regulation of the circadian oscillator in Xenopus retinal photoreceptors by protein kinases sensitive to the stress-activated protein kinase inhibitor, SB 203580. *Journal of Biological Chemistry*, *279*(21), 22738–22746. https://doi.org/10.1074/jbc.M401389200

Hayashi, Y., Sanada, K., & Fukada, Y. (2001). Circadian and photic regulation of MAP kinase by Ras- and protein phosphatase-dependent pathways in the chick pineal gland. *FEBS Letters*, *491*(1–2), 71–75. https://doi.org/10.1016/S0014-5793(01)02153-6

Hayashi, Y., Sanada, K., Hirota, T., Shimizu, F., & Fukada, Y. (2003). p38 Mitogen-activated Protein Kinase Regulates Oscillation of Chick Pineal Circadian Clock. *Journal of Biological Chemistry*, *278*(27), 25166–25171. https://doi.org/10.1074/jbc.M212726200

Helfer, A., Nusinow, D. A., Chow, B. Y., Gehrke, A. R., Bulyk, M. L., & Kay, S. A. (2011). LUX ARRHYTHMO encodes a nighttime repressor of circadian gene expression in the *Arabidopsis* core clock. *Current Biology*, *21*(2), 126–133. https://doi.org/10.1016/j.cub.2010.12.021

Herbers, K., Lorences, E. P., Barrachina, C., & Sonnewald, U. (2001). Functional characterisation of _*Nicotiana tabacum*_ xyloglucan endotransglycosylase (NtXET-1): generation of transgenic tobacco plants and changes in cell wall xyloglucan. *Planta*, *212*(2), 279–287. https://doi.org/10.1007/s004250000393

Huang, W., Pérez-García, P., Pokhilko, A., Millar, A. J., Antoshechkin, I., Riechmann, J. L., & Mas, P. (2012). Mapping the Core of the Arabidopsis Circadian Clock Defines the Network Structure of the Oscillator. *Science*, *336*(6077), 75 LP-79. Retrieved from http://science.sciencemag.org/content/336/6077/75.abstract

Jan, A., Yang, G., Nakamura, H., Ichikawa, H., Kitano, H., Matsuoka, M., … Komatsu, S. (2004). Characterization of a xyloglucan endotransglucosylase gene that is up-regulated by gibberellin in rice. *Plant Physiology*, *136*(3), 3670–3681. https://doi.org/10.1104/pp.104.052274

Kerr, E. M., & Fry, S. C. (2003). Pre-formed xyloglucans and xylans increase in molecular weight in three distinct compartments of a maize cell-suspension culture. *Planta*, *217*(2), 327–339. https://doi.org/10.1007/s00425-003-1027-2

Klink, V. P., Hosseini, P., Matsye, P. D., Alkharouf, N. W., & Matthews, B. F. (2010). Syncytium gene expression in *Glycine max*[PI 88788]roots undergoing a resistant reaction to the parasitic nematode *Heterodera glycines*. *Plant Physiology and Biochemistry*, *48*(2–3), 176–193. https://doi.org/10.1016/j.plaphy.2009.12.003

Klink, V. P., Overall, C. C., Alkharouf, N. W., MacDonald, M. H., & Matthews, B. F. (2007). Laser capture microdissection (LCM) and comparative microarray expression analysis of syncytial cells isolated from incompatible and compatible soybean (*Glycine max*) roots infected by the soybean cyst nematode (*Heterodera glycines*). *Planta*, *226*(6), 1389–1409. https://doi.org/10.1007/s00425-007-0578-z

Klink, V. P., Sharma, K., Pant, S. R., McNeece, B., Niraula, P., & Lawrence, G. W. (2017). Components of the SNARE-containing regulon are co-regulated in root cells undergoing defense. *Plant Signaling and Behavior*, *12*(2), 1–19. https://doi.org/10.1080/15592324.2016.1274481

Liu, Y. B., Lu, S. M., Zhang, J. F., Liu, S., & Lu, Y. T. (2007). A xyloglucan endotransglucosylase/hydrolase involves in growth of primary root and alters the deposition of cellulose in Arabidopsis. *Planta*, *226*(6), 1547–1560. https://doi.org/10.1007/s00425-007-0591-2

Mackey, D., Iii, B. F. H., Wiig, A., Dangl, J. L., Hill, C., & Carolina, N. (2002). RIN4 Interacts with *Pseudomonas syringae* Type III Effector Molecules and Is Required for RPM1-Mediated Resistance in Arabidopsis, *108*, 743–754.

Matsye, P. D., Kumar, R., Hosseini, P., Jones, C. M., Tremblay, A., Alkharouf, N. W., … Klink, V. P. (2011). Mapping cell fate decisions that occur during soybean defense responses. *Plant Molecular Biology*, *77*(4–5), 513–528. https://doi.org/10.1007/s11103-011-9828-3

Matsye, P. D., Lawrence, G. W., Youssef, R. M., Kim, K. H., Lawrence, K. S., Matthews, B. F., & Klink, V. P. (2012). The expression of a naturally occurring, truncated allele of an α-SNAP gene suppresses plant parasitic nematode infection. *Plant Molecular Biology*, *80*(2), 131–155. https://doi.org/10.1007/s11103-012-9932-z

Matthews, B. F., Beard, H., MacDonald, M. H., Kabir, S., Youssef, R. M., Hosseini, P., & Brewer, E. (2013). Engineered resistance and hypersusceptibility through functional metabolic studies of 100 genes in soybean to its major pathogen, the soybean cyst nematode. *Planta*, *237*(5), 1337–1357. https://doi.org/10.1007/s00425-013-1840-1

McNeece, B., Sharma, K., Lawrence, G. W., Lawrence, K. S., & Klink, V. P. (2019). The mitogen activated protein kinase (MAPK) gene family functions as a cohort during the Glycine max defense response to Heterodera glycines. *Plant Physiology and Biochemistry*, 1–19. https://doi.org/https://doi.org/10.1016/j.plaphy.2019.01.018

McNeece, B. T., Pant, S. R., Sharma, K., Niruala, P., Lawrence, G. W., & Klink, V. P. (2017). A *Glycine max* homolog of NON-RACE SPECIFIC DISEASE RESISTANCE 1 (NDR1) alters defense gene expression while functioning during a resistance response to different root pathogens in different genetic backgrounds. *Plant Physiology and Biochemistry*, *114*, 60–71. https://doi.org/10.1016/j.plaphy.2017.02.022

McNeece, B. T., Sharma, K., Lawrence, G. W., Lawrence, K. S., & Klink, V. P. (2018). Mitogen activated protein kinases function as a cohort during a plant defense response. *BioRxiv*, 396192. https://doi.org/10.1101/396192

Miedes, E., Suslov, D., Vandenbussche, F., Kenobi, K., Ivakov, A., Van Der Straeten, D., … Vissenberg, K. (2013). Xyloglucan endotransglucosylase/hydrolase (XTH) overexpression affects growth and cell wall mechanics in etiolated *Arabidopsis* hypocotyls. *Journal of Experimental Botany*, *64*(8), 2481–2497. https://doi.org/10.1093/jxb/ert107

Miedes, E., Zarra, I., Hoson, T., Herbers, K., Sonnewald, U., & Lorences, E. P. (2011). Xyloglucan endotransglucosylase and cell wall extensibility. *Journal of Plant Physiology*, *168*(3), 196–203. https://doi.org/10.1016/j.jplph.2010.06.029

Nishikubo, N., Takahashi, J., Roos, A. A., Derba-Maceluch, M., Piens, K., Brumer, H., … Mellerowicz, E. J. (2011). Xyloglucan endo-Transglycosylase-Mediated Xyloglucan Rearrangements in Developing Wood of Hybrid Aspen. *Plant Physiology*, *155*(1), 399–413. https://doi.org/10.1104/pp.110.166934

Pant, S. R., Matsye, P. D., McNeece, B. T., Sharma, K., Krishnavajhala, A., Lawrence, G. W., & Klink, V. P. (2014). Syntaxin 31 functions in *Glycine max* resistance to the plant parasitic nematode *Heterodera glycines*. *Plant Molecular Biology*, *85*(1–2), 107–121. https://doi.org/10.1007/s11103-014-0172-2

Park, Y. B., & Cosgrove, D. J. (2015). Xyloglucan and its interactions with other components of the growing cell wall. *Plant and Cell Physiology*, *56*(2), 180–194. https://doi.org/10.1093/pcp/pcu204

Popper, Z. A., & Fry, S. C. (2005). Widespread occurrence of a covalent linkage between xyloglucan and acidic polysaccharides in suspension-cultured angiosperm cells. *Annals of Botany*, *96*(1), 91–99. https://doi.org/10.1093/aob/mci153

Ren, D., Yang, K., Li, G., Liu, Y., Zhang, S., & Nonse-like. (2006). Activation of Ntf4 , a Tobacco Mitogen-Activated Protein Kinase , during Plant Defense Response and Its Involvement in Hypersensitive, *141*(August), 1482–1493. https://doi.org/10.1104/pp.106.080697.addition

Robson, F., Costa, M. M. R., Hepworth, S. R., Vizir, I., Pin, M., Putterill, J., & Coupland, G. (2001). Functional importance of conserved domains in the ¯owering-time gene CONSTANS demonstrated by analysis of mutant alleles and transgenic plants. *The Plant Journal*, *28*.

Rose, J. K. C., Braam, J., Fry, S. C., & Nishitani, K. (2002). The XTH family of enzymes involved in xyloglucan endotransglycosylation and endohyrdolosis: Current perspectives and a new unifying nomenclature. *Plant Cell Physiol.*, *43*(12), 1421–1435. https://doi.org/10.1093/pcp/pcf171

Sharma, K., Pant, S. R., McNeece, B. T., Lawrence, G. W., & Klink, V. P. (2016). Co-regulation of the *Glycine max* soluble N-ethylmaleimide-sensitive fusion protein attachment protein receptor (SNARE)-containing regulon occurs during defense to a root pathogen. *Journal of Plant Interactions*, *11*(1), 74–93. https://doi.org/10.1080/17429145.2016.1195891

Shin, Y. K., Yum, H., Kim, E. S., Cho, H., Gothandam, K. M., Hyun, J., & Chung, Y. Y. (2006). BcXTH1, a *Brassica campestris* homologue of *Arabidopsis* XTH9, is associated with cell expansion. *Planta*, *224*(1), 32–41. https://doi.org/10.1007/s00425-005-0189-5

Talbott, L. D., & Ray, P. M. (1992). Changes in molecular size of previously deposited and newly synthesized pea cell wall matrix polysaccharides : effects of auxin and turgor. *Plant Physiology*, *98*(1), 369–379. https://doi.org/10.1104/pp.98.1.369

Thompson, J. E., Smith, R. C., & Fry, S. C. (1997). Isopycnic Centrifugation in Caesium Trifluoroacetate. *Pharmacia*, *708*, 699–708.

Tokumoto, H., Wakabayadhi, K., Kamisaka, S., & Hoson, T. (2002). Changes in the Sugar Composition and Molecular Mass Distribution of Matrix Polysaccharides during Cotton Fiber Development. *Plant and Cell Physiology*, *43*(4), 411–418. https://doi.org/10.1093/pcp/pcf048

Vitalini, M. W., de Paula, R. M., Goldsmith, C. S., Jones, C. A., Borkovich, K. A., & Bell-Pedersen, D. (2007). Circadian rhythmicity mediated by temporal regulation of the activity of p38 MAPK. *Proceedings of the National Academy of Sciences*, *104*(46), 18223–18228. https://doi.org/10.1073/pnas.0704900104

Wang, F., Wang, C., Yan, Y., Jia, H., & Guo, X. (2016). Overexpression of Cotton GhMPK11 Decreases Disease Resistance through the Gibberellin Signaling Pathway in Transgenic *Nicotiana benthamiana*, *7*(May), 1–16. https://doi.org/10.3389/fpls.2016.00689

Xiong, L., & Yang, Y. (2003). Disease Resistance and Abiotic Stress Tolerance in Rice Are Inversely Modulated by an Abscisic Acid – Inducible Mitogen-Activated Protein Kinase, *15*(March), 745–759. https://doi.org/10.1105/tpc.008714.ported

Zhang, C., Xie, Q., Anderson, R. G., Ng, G., Seitz, N. C., Peterson, T., … Lu, H. (2013). Crosstalk between the Circadian Clock and Innate Immunity in Arabidopsis. *PLoS Pathogens*, *9*(6). https://doi.org/10.1371/journal.ppat.1003370

Zhu, X. F., Shi, Y. Z., Lei, G. J., Fry, S. C., Zhang, B. C., Zhou, Y. H., … Zheng, S. J. (2012). XTH31, Encoding an in Vitro XEH/XET-Active Enzyme, Regulates Aluminum Sensitivity by Modulating in Vivo XET Action, Cell Wall Xyloglucan Content, and Aluminum Binding Capacity in *Arabidopsis*. *The Plant Cell*, *24*(11), 4731–4747. https://doi.org/10.1105/tpc.112.106039

APPENDIX A

SUPPLEMENTARY TABLES AND FIGURES OF CHAPTER II

Table A.1 PCR primers used for cloning of genes (OE).

Gene Name	Accession	Primer Direction	Primer Sequences	GC %	Length	Tmº C
CCA1-1	>Glyma07g05410	Forward	5'CACCTTCCCTCTCTTTTCCGCGTTT3'	52.0	25	66.7
		Reverse	5'TGTGGGGGGATTAAGAAATGACAT3'	41.6	24	61.7
GI-1	>Glyma10g36600	Forward	5'CACCATGGCTGCTTCCAGTGAAAG3'	54.1	24	65.7
		Reverse	5'TCACATGGAAATAGTACAGCCTAACTC3'	40.7	27	61.8
CO-4	>Glyma17g07420	Forward	5'CACCTCGCTGGCAACAACAGCAGTAC3'	57.6	26	69.3
		Reverse	5'TCATGCACTCCATCGTTTCTTCATT3'	40.0	25	62.6
TOC1-1	>Glyma04g33110	Forward	5'CACCATGGAGTCTGGTGATGAGATTAA3'	39.1	27	58.4
		Reverse	5'TCAAGCATCCTCGGGAGAAGAA3'	50.0	22	62.9

Table A.2 PCR primers used in cloning of genes (RNAi).

Gene Name	Accession	Primer Direction	Primer Sequences	GC %	Length	Tmº C
CCA1-1	>Glyma07g05410	Forward	5'CACCTCTCCTGCATCGGTGACTGC3'	62.5	24	68.6
		Reverse	5'CTGATTCTTATTCTTCAAAGCATGAGG3'	37.0	27	59.8
GI-1	>Glyma10g36600	Forward	5'CACCATGGCTGCTTCCAGTGAAAG3'	54.1	24	65.7
		Reverse	5'TGAGAATGAATACTCAGAACAATGGGC 3'	40.7	27	62.7
CO-4	>Glyma17g07420	Forward	5'CACCTCGCTGGCAACAACAGCAGTAC3'	57.6	26	69.3
		Reverse	5'TCATGCACTCCATCGTTTCTTCATT3'	40.0	25	62.6
TOC1-1	>Glyma04g33110	Forward	5'CACCATGGAGTCTGGTGATGAGATTAA3'	39.1	27	58.4
		Reverse	5'TCAAGCATCCTCGGGAGAAGAA3'	50.0	22	62.9

Table A.3 Primes used in qPCR expression studies.

Gene Name	**Accession**	**Type**	**Primer Sequence (5'-3')**
CCA1-1	>Glyma07g05410	qPCR	F-GTTAACCAAGCACTGAACTTGG
			R-AAGAGTAAATACTGCTCCGCG
			P-TTCCAGAGAAACATGATTTAGATGAAGGGAT

F: Forward Primer; R: Reverse Primer; P: Probe

APPENDIX B

DETAIL INFORMATION OF CHEMICAL ANALYSIS

Table B.1 Detail chemical extraction and data analysis of overexpression (OE) and control samples.

Sample name	**Replicates**	**1**	**2**	**3**	**4**	**5**	**6**	**7**	**8**	**9**	**10**	**11**
XTH43-OE	REP1	2.91	2.66	0.11	0.10	4.14	3.76	7.89	8.64	2.08	10.72	0.40
XTH43-OE	REP2	2.71	2.59	0.09	0.04	3.47	1.54	5.02	12.54	1.83	14.38	0.44
XTH43-OE	REP3	3.24	2.22	0.14	0.06	6.31	2.70	9.01	12.45	2.08	14.54	0.58
P15(CONTROL)	REP1	4.41	3.19	0.18	0.08	5.64	2.51	8.15	5.22	1.93	7.15	0.25
P15(CONTROL)	REP2	4.49	2.55	0.16	0.09	6.27	3.53	9.80	5.48	2.27	7.76	0.24
P15(CONTROL)	REP3	4.87	2.44	0.19	0.06	7.79	2.46	10.25	5.38	1.51	6.90	0.23
Average of OE (modified) plants						4.63±0.85	2.66±0.63	7.30±1.18	11.21±1.28	1.99±0.08	13.21±1.24	0.47±0.05
Average of P15 (control) plants						6.56±0.63	2.83±0.34	9.40±0.63	5.36±0.07	1.90±0.21	7.26±0.25	0.24±0.01

1. Dry mass of samples (gram)

2. Dry mass (gram) of Soxhlet-extracted samples

3. Dry mass (gram) of 24% KOH extracted samples

4. Dry mass (gram) of 4% KOH extracted samples

5. Tightly bound sugars (% extracted samples)

6. Loosely bound sugars (% extracted samples)

7. Total sugars (% extracted samples)

8. XG (%) in tightly bound sugars

9. XG (%) in loosely bound sugars

10. XG (%) in total sugar amount

11.XG (%) in total dry mass of root tissues

Table B.2 Detail chemical extraction and data analysis of RNA-interference (RNAi) and control samples.

Sample name	Replicates	1	2	3	4	5	6	7	8	9	10	11
XTH-43-RNAi	REP1	2.87	2.41	0.12	0.07	4.98	2.90	7.88	4.79	1.32	6.11	0.23
XTH-43-RNAi	REP2	3.63	2.48	0.09	0.05	3.63	2.02	5.65	4.97	2.14	7.11	0.15
XTH-43-RNAi	REP3	2.56	1.12	0.05	0.03	4.46	2.68	7.14	4.35	1.73	6.08	0.11
P17(CONTROL)	REP1	3.30	2.26	0.11	0.08	4.87	3.54	8.41	8.41	1.42	9.83	0.31
P17(CONTROL)	REP2	2.94	2.00	0.09	0.07	4.50	3.50	8.00	8.11	1.92	10.03	0.29
P17(CONTROL)	REP3	2.87	1.94	0.05	0.08	2.58	4.12	6.70	4.80	2.22	7.02	0.15
Average of RNAi (modified) plants						4.35±0.39	2.53±0.26	6.89±0.65	4.70±0.18	1.73±0.23	6.43±0.33	0.16±0.03
Average of P17 (control) plants						3.98±0.71	3.72±0.20	7.70±0.51	7.10±1.15	1.49±0.32	8.95±0.97	0.25±0.05

1. Dry mass of samples (gram)

2. Dry mass (gram) of Soxhlet-extracted samples

3. Dry mass (gram) of 24% KOH extracted samples

4. Dry mass (gram) of 4% KOH extracted samples

5. Tightly bound sugars (% extracted samples)

6. Loosely bound sugars (% extracted samples)

7. Total sugars (% extracted samples)

8. XG (%) in tightly bound sugars

9. XG (%) in loosely bound sugars

10. XG (%) in total sugar amount

11.XG (%) in total dry mass of root tissues

B.1 Principal component analysis of chromatograms

B.2.1 GPC spectral analysis of tightly bound sugars

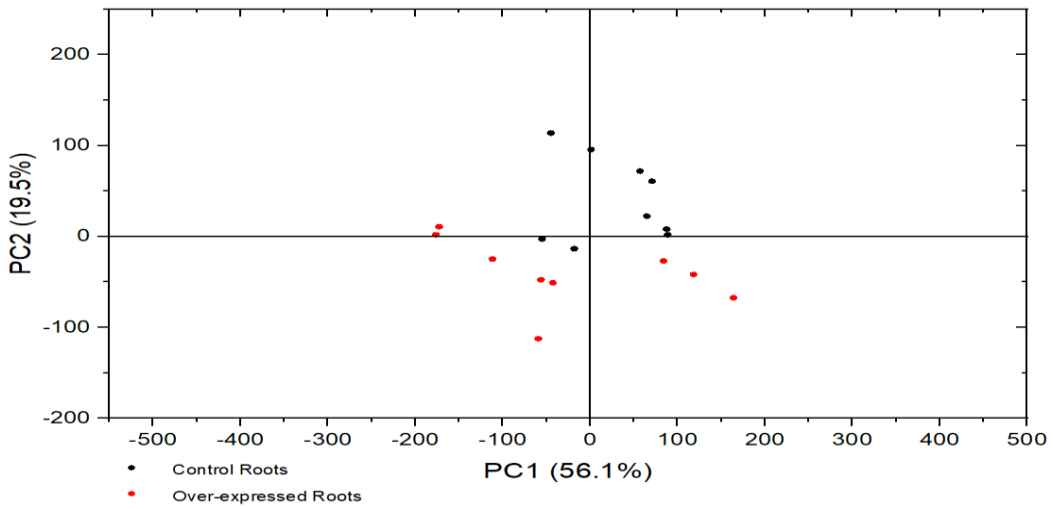

Figure B.01 PC1/PC2 score plot of over-expressed roots (red) and control roots (black) spectra of tightly bound sugars.

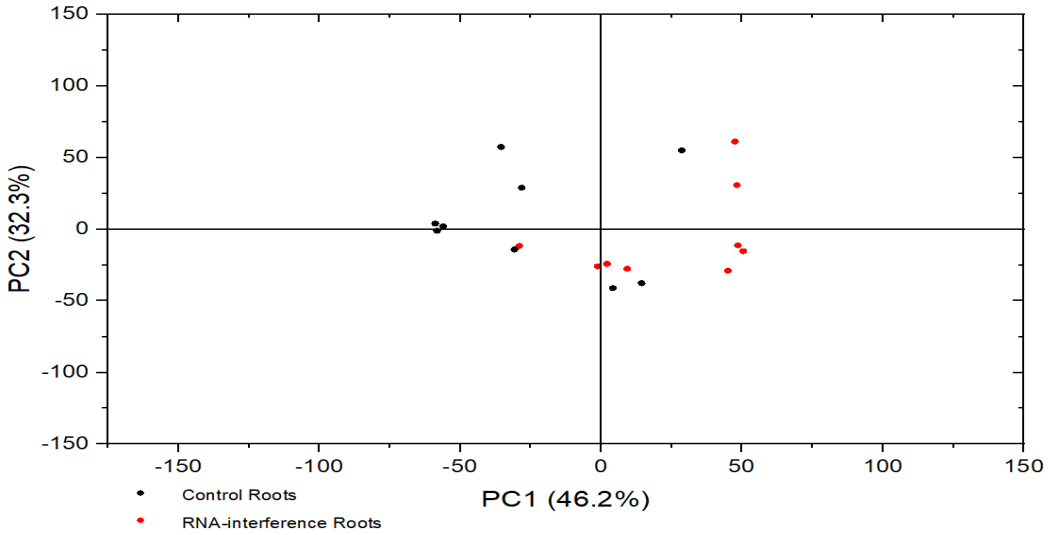

Figure B.02 PC1/PC2 score plot of RNA-interference roots (red) and control roots (black) spectra of tightly bound sugars.

B.1.2 GPC spectral analysis of loosely bound sugars

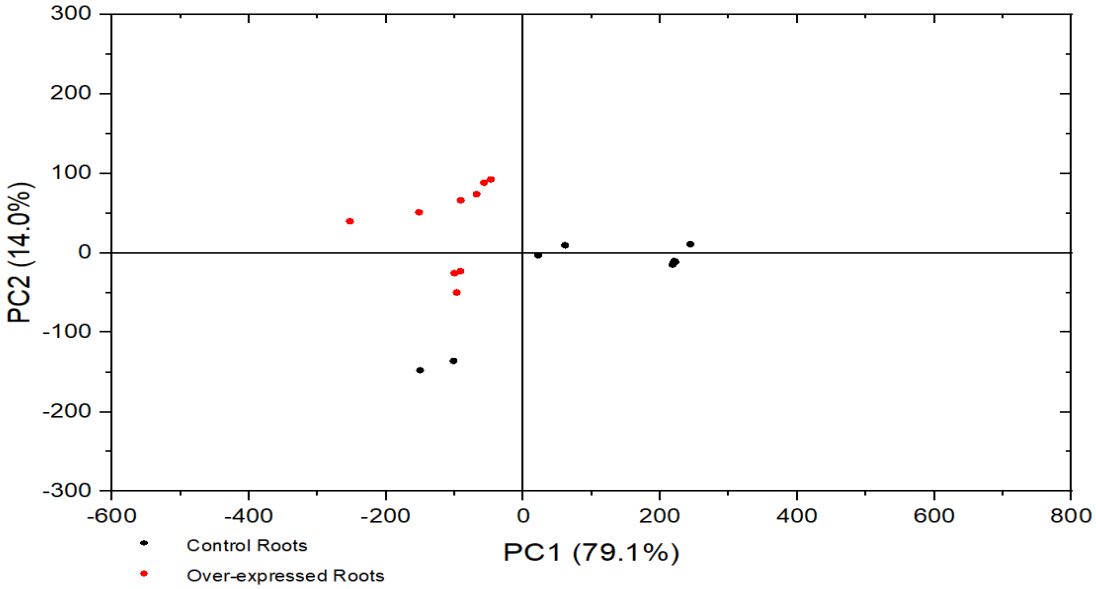

Figure B.03 PC1/PC2 score plot of over-expressed roots (red) and control roots (black) spectra of loosely bound sugars.

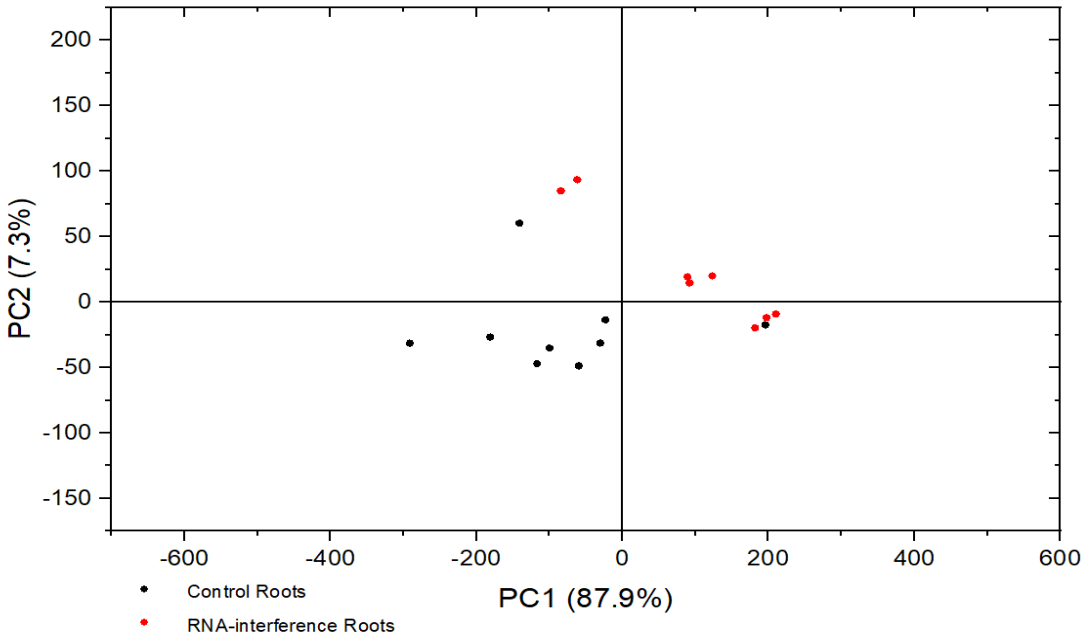

Figure B.04 PC1/PC2 score plot of RNA-interference roots (red) and control roots (black) spectra of loosely bound sugars.

B.2 Weight average molecular weight (WAMW) of extracted sugars

B.2.1 Weight average MW of tightly bound sugars

Table B.3 Characterization of weight average MW of tightly bound sugar in overexpressed (OE) and control roots.

Tightly bound sugars	Molecular Weight (kDa)			Av. MW (kDa)
	REP1	REP2	REP3	
Over-expressed Roots	869.64 ±0.64	839.88 ±3.17	873.28 ±1.75	**860.94 ±10.57**
Control Roots	959.40 ±2.78	927.52 ±0.85	907.08 ±3.46	**931.34 ±15.22**

Table B.4 Characterization of weight average MW of tightly bound sugars in RNA-interference (RNAi) and control roots.

Tightly bound sugars	Molecular Weight (kDa)			Av. MW (kDa)
	REP1	REP2	REP3	
RNA-interference Roots	932.97 ±4.29	907.58 ±4.41	909.69 ±1.98	**916.75 ±8.13**
Control Roots	840.49 ±2.41	841.31 ±1.25	858.59 ±0.70	**846.80 ±5.90**

B.2.2 Weight average MW of loosely bound sugars

Table B.5 Characterization of weight average MW of loosely bound sugars in overexpressed (OE) and control roots.

Loosely bound sugars	Molecular Weight (kDa)			Av. MW (kDa)
	REP1	REP2	REP3	
Over-expressed Roots	745.41 ±5.45	724.39 ±1.75	755.28 ±6.88	**741.69 ±9.10**
Control Roots	808.35 ±3.67	809.03 ±1.59	824.19 ±4.47	**813.86 ±5.17**

Table B.6 Characterization of weight average MW of loosely bound sugars in RNA-interference (RNAi) and control roots.

Loosely bound sugars	Molecular Weight (kDa)			Av. MW (kDa)
	REP1	REP2	REP3	
RNA-interference Roots	769.96 ±1.15	784.60 ±2.85	771.50 ±0.68	**775.35 ±4.64**
Control Roots	765.07 ±1.80	748.66 ±1.74	768.18 ±1.54	**760.63 ±6.05**

APPENDIX C

SUPPLEMENTARY TABLES AND FIGURES OF CHAPTER IV

Table C.1 Primes used in qPCR expression studies.

Gene Name	Accession	Type	Primer Sequence (5'-3')
CCA1-1	Glyma07g05410	qPCR	F-GTTAACCAAGCACTGAACTTGG
			R-AAGAGTAAATACTGCTCCGCG
			P-TTCCAGAGAAACATGATTTAGATGAAGGGAT
XTH43	Glyma17g07250	qPCR	F-GGGAGATGGTCGTGCTAAAATA
			R-TATTCGTTTTTGGATTGGAAGC
			P-CGAAAATCTTCTCACTCTCTCCCTTGACA
RIN4-4	Glyma18g36000	qPCR	F-GTTAGGCAAGAGTGAAGAGAATGT
			R-CCAGCAGAAGAAACTACATCTGA
			P-CCAGAAAGGTCAGCCAGGTTCAAAGATGA
NDR1-1	Glyma12g34210	qPCR	F-CACCACAATACTCTTCGCTCTCAAG
			R-TAGAACCTTTGCACGGTGGC
			P-TTCAGAGTCTTCGAGAGCGTCAACCTCAC
MAPK2	Glyma0g03270	qPCR	F-ACTCCTGTTGAGCCTCCAAAT
			R-TATGCTCCGCGACCAATC
			P-CCCTGTTTGAGATTGACTCAAAATACGTTC
MAPK3-1	Glyma11g15700	qPCR	F-CGTATGGAATCGTTTGCTCG
			R-AAAGCGTTCGCTATCTTCTTAACC
			P-GTTGAATACCGAGACGAATGAGCTGGTG
MAPK3-2	Glyma12g07770	qPCR	F-GATTTTGCGGCGGTTCC
			R-TGAGCAAACGATTCCGTACG
			P-TGGAAACCTCTTCGAGGTTACGACGA
MAPK4-1	Glyma07g07270	qPCR	F-GTCTGTTGTTGAGTCAGGTGAACA
			R-CATAAGCGCCTCTACCCACA
			P-GGCAATCTCTTTGAAGTTTCCAGAAAGTATG
MAPK5-3	Glyma08g0200	qPCR	F-GTTAATTCCGAAACACACGAACA
			R-GGCAATAATATTATCATGGTCCATG
			P-ATCAAGAAGATCGGCAACGCATTTG
MAPK6-2	Glyma02g1590	qPCR	F-TATTCGTTCAAACCAAGGATTATCAG
			R-CACAGTTGGCATTCAGGAGAAG
			P-GCCAATGTTCTGCATAGGGACTTAAAACCT
MAPK13-1	Glyma12g07850	qPCR	F-GACGCTCAGGGAAATCAAGC
			R-TCAACTCGTACACGATATACACGTCA
			P-GACATAATTCGGCCAGCGGAGAGG
MAPK16-4	Glyma07g38510	qPCR	F-GGATAACAAAGGAAGATGTGCG
			R-TTTCTTGAAGTGGTCCACAGC
			P-GAACATCTAGAGGGAGAAGAGCCAACAGG
MAPK20-2	Glyma14g03190	qPCR	F-GGAAAATGGTGGTAAAAGTTATCCAA
			R-TTGTCTGCCGGTTTATGCAG
			P-ATGCATCACTTCCAAGGTCAACAATGG

F: Forward Primer; R: Reverse Primer; P: Probe

Table C.2 MAPKs relative fold change expression in Gm-CCA1-1-OE, Non-infected cDNA samples in 24 hours.

	MK2	MK3-1	MK3-2	MK4-1	MK5-3	MK6-2	MK13-1	MK16-4	MK20-2
4AM(0h)	1.26	1.34	-1.28	-1.45	-1.50	1.18	1.14	-1.29	1.36
8AM(4h)	-2.13	-4.21	-4.28	1.46	-3.80	-3.28	-1.27	-3.90	-1.40
12PM(8h)	-1.22	1.88	1.47	1.20	1.35	1.27	-1.40	1.39	1.86
4PM(12h)	-1.92	1.76	2.51	1.42	1.53	1.39	1.23	1.28	1.54
8PM(16h)	1.95	2.50	1.73	4.18	-1.53	1.12	-4.87	-1.09	-1.22
12AM(20h)	2.19	-4.86	-2.02	-2.52	-4.86	1.64	-1.66	-3.06	-1.20
4AM(24h)	-1.25	-1.58	-1.45	-1.14	-3.14	1.99	-1.27	-1.67	-1.43

Note: Blue filled represents positive fold change; yellow filled represents negative fold change [a cutoff value of ±1.5 is considered as relative fold change difference]

Table C.3 MAPKs relative fold change expression in Gm-CCA1-1-RNAi, Non-infected cDNA samples in 24 hours.

	MK2	MK3-1	MK3-2	MK4-1	MK5-3	MK6-2	MK13-1	MK16-4	MK20-2
4AM(0h)	1.17	-1.29	-1.77	1.63	2.89	1.82	2.73	-1.29	1.10
8AM(4h)	-2.50	-1.35	-1.20	-1.09	-1.42	-3.21	1.65	-1.59	1.29
12PM(8h)	-1.10	-4.27	-3.51	-1.80	-1.49	-1.48	1.13	-1.69	2.59
4PM(12h)	1.56	-1.24	-1.09	1.59	1.63	-1.11	-1.11	-1.21	1.24
8PM(16h)	1.16	1.41	1.46	2.59	-1.62	1.38	-2.14	1.72	1.62
12AM(20h)	1.21	-1.12	-1.23	1.60	-1.85	1.42	-1.16	-1.18	1.15
4AM(24h)	1.19	-1.12	-1.77	1.07	1.54	-3.19	1.61	-1.76	1.42

Note: Blue filled represents positive fold change; yellow filled represents negative fold change [a cutoff value of ±1.5 is considered as relative fold change difference]